

MINISTRY OF EDUCATION AND SCIENCE OF UKRAINE
NATIONAL AVIATION UNIVERSITY
DEPARTMENT OF AIRCRAFT DESIGN

APPROVED BY
Head of department
Professor, Dr. of Sc.
_____ S.R. Ignatovych
«___» _____ 2020

MASTER THESIS

ON SPECIALTY

“AVIATION AND SPACE ROCKET TECHNOLOGY”

Theme: «Comparative study of coating adhesion using scratch test technique»

Prepared by: _____ **R.V. Khailak**

Supervisor: PhD, associate professor _____ **V.I. Zakiev**

Labor protection:

Ph.d., associate professor _____ **O.V. Konovalova**

Environmental protection:

Ph.d., associate professor _____ **L.I. Pavliukh**

Examined:

Ph.d., associate professor _____ **S.V. Khiznyak**

Kyiv 2020

NATIONAL AVIATION UNIVERSITY

Faculty aerospace

Department of aircraft design

Specialty 134 «Aviation and space rocket technology»

Educational professional program «Aircraft equipment»

APPROVED BY

Head of department

D. Sc., professor

_____ S.R. Ignatovych

«___» _____ 2020.

TASK

For the master thesis

Khailak Roman

1. Topic: «Comparative study of coating adhesion using scratch test technique», approved by Rector's order № 1906/CT_from 5 october 2020 year.
2. Period of work execution: from 5.10.2020 year to 13.12.2020 year.
3. Initial data: diamond indenter having a cone shape with a tip radius of 10 μm . Maximum load – 130 g. Loading rate – 13 g/s. Scanning path length – 455 microns. Steel X12M with CrC and VC sublayers and AlN coatings on MA8.
4. Content (list of topics to be developed): analysis of metals and coatings, influence of protective coatings adhesion strength on functional performance, methods and instruments of experimental study, experimental investigation of coating adhesion strength, labor protection, environmental protection.
5. Required material: The list of obligatory graphic (illustrative) material: Drawings by Micron-Gamma device.
6. Thesis schedule

№	Task	Execution period	Done
1	Task receiving, processing of statistical data.	5.10.2020–8.10.2020	
2	Analysis of metals and coatings.	13.10.2020–18.10.2020	
3	Analysis of the basic principles of sclerometer test application.	18.10.2020–25.10.2020	

4	Experiments and data collection.	26.10.2020–5.11.2020	
5	Preparation of the graphic component.	6.11.2020–15.11.2020	
6	Analysis of harmful and dangerous production factors	16.11.2020–17.11.2020	
7	Analysis of the harmful effects of the aircraft on the environment	18.11.2020–20.11.2020	
8	Completion of the explanation note.	21.11.2020–05.12.2020	

7. Special chapter consultants

Chapter	Consultants	Date, signature	
		Task Issued	Task Received
Labor protection	O.V. Konovalova		
Environmental protection	L.I. Pavliukh		

8. Date of issuance of the task:

Supervisor _____ V.I. Zakiev

Student _____ R.V.Khailak

ABSTRACT

Master degree thesis «Comparative study of coating adhesion using scratch test technique»

102 pages, 53 pictures, 4 tables, 20 references.

Object of study – magnetron coatings n-TiC / a-C on samples of steel X12M with CrC and VC sublayers and AlN coatings on MA8.

Subject of study – the scratch test technique adhesion measurements.

Aim of master thesis - Comparative study of magnetron coatings n-TiC/a-C and AlN adhesion using scratch test technique.

Research and development methods – scratch test for assessment coating adhesion

Novelty of the results – Proposed new methodology of coating adhesion measurement using scratch test.

The practical value of the work - is determined by the possibility to use the data received by the tests for the development of the new coatings concept and optimizing existed ones.

COATINGS, THIN FILMS, ADHESION STRENGTH, SCRATCH TEST, INDENTERS

ABBREVIATIONS

TiN – titanium nitride

TiC – titanium carbide

PVD – physical vapor deposition

CVD – chemical vapor deposition

MOCVD – metallo-organic chemical vapor deposition

PECVD – plasma enhanced chemical vapor deposition

SEM – scanning electron microscope

VOC – volatile organic compounds

MEMS – micro electromechanical systems

MSC – Micro Spark Coating

DAC – digital-to-analog converter

ADC – analog digital converter

CONTENT

INTRODUCTION	11
PART 1. INFLUENCE OF PROTECTIVE COATINGS ADHESION STRENGTH ON FUNCTIONAL PERFORMANCE	13
1.1 Coatings and their application in aviation	13
1.2 Thin film deposition processes	19
1.3 Adhesion between substrate and thin films, its influence on functional performance and measurement techniques	26
Conclusion to part 1	36
PART 2. METHODS AND INSTRUMENTS OF EXPERIMENTAL STUDY	37
2.1 Basic Principles and application of scratch test	37
2.2 Indenter types	44
2.3 Description and principle of operation of the nanoindentation tester "Micron-Gamma"	47
2.4 Structure of nanoindentation tester "Micron-Gamma"	51
2.4.1 Software description	57
Conclusion to part 2	64
PART 3. EXPERIMENTAL INVESTIGATION OF COATING ADHESION STRENGTH	65
3.1 Experimental procedure	65
3.2 Results and discussion	67
Conclusion to part 3	83
PART 4. LABOR PROTECTION	84
Introduction	84
4.1 Organizing of working space	85
4.2 The list of harmful and hazardous factors	86
4.3 To carry out methods of decreasing influence of harmful and dangerous factors	86
4.4 Analysis of harmful and hazardous factors	86
4.5 Calculation of fan performance for normal ventilation	87

	7
4.6 Fire safety	89
4.6.1 Category room	89
4.6.2 The type and number of fire extinguishers	89
4.6.3 Sensor and fire alarm system	90
4.6.4 Exits	90
Conclusion to part 4	91
PART 5. ENVIRONMENT PROTECTION	92
5.1 Evaluation of the aircraft as a source of environment pollution	93
5.2 Atmospheric emissions impact	94
5.3 Recommendations to reduce environmental impact	97
Conclusion to part 5	100
GENERAL CONCLUSION	101
REFERENCE	102

INTRODUCTION

The field of material science and engineering community's ability to conceive the novel materials with extraordinary combination of chemical, physical and mechanical, properties has changed the modern society. There is an increasing technological progress. Modern technology requires thin films for different application. Thin film technology is the basic of astounding development in solid state electronics. The usefulness of the optical properties of metal films, and scientific curiosity about the behavior of two-dimensional solids has been responsible for the immense interest in the study science and technology of the thin films. Thin film studies have directly or indirectly advanced many new areas of research in solid state physics and chemistry which are based on phenomena uniquely characteristic of the thickness, geometry, and structure of the film.

When we consider a very thin film of some substance, we have a situation in which the two surfaces are so close to each other that they can have a decisive influence on the internal physical properties and processes of the substance, which differ, therefore, in a profound way from those of a bulk material. The decrease in distance between the surfaces and their mutual interaction can result in the rise of completely new phenomena. Here the one dimension of the material is reduced to an order of several atomic layers which creates an intermediate system between macro systems and molecular systems, thus it provides us a method of investigation of the microphysical nature of various processes. Thin films are especially appropriate for applications in microelectronics and integrated optics. However, the physical properties of the films like electrical resistivity do not substantially differ from the properties of the bulk material. For a thin film the limit of thickness is considered between tenths of nanometer and several micrometers.

Thin film materials are the key elements of continued technological advances made in the fields of optoelectronic, photonic, and magnetic devices. The processing of materials into thin films allows easy integration into various types of devices. The properties of material significantly differ when analyzed in the form of thin films. Most of

the functional materials are rather applied in thin film form due to their specific electrical, magnetic, optical properties or wear resistance. Thin film technologies make use of the fact that the properties can particularly be controlled by the thickness parameter. Thin films are formed mostly by deposition, either physical or chemical methods. Thin films, both crystalline and amorphous, have immense importance in the age of high technology. Few of them are: microelectronic devices, magnetic thin films in recording devices, magnetic sensors, gas sensor, A. R. coating, photoconductors, IR detectors, interference filters, solar cells, polarizer's, temperature controller in satellite, superconducting films, anticorrosive and decorative coatings.

Thin film materials have already been used in semiconductor devices, wireless communications, telecommunications, integrated circuits, rectifiers, transistors, solar cells, light-emitting diodes, photoconductors, light crystal displays, magneto-optic memories, audio and video systems, compact discs, electro-optic coatings, memories, multilayer capacitors, flat-panel displays, smart windows, computer chips, magneto-optic discs, lithography, micro electromechanical systems (MEMS), and multifunctional emerging coatings, as well as other emerging cutting technologies [1].

PART 1

INFLUENCE OF ADHESION STRENGTH ON PROTECTIVE COATINGS FUNCTIONAL PERFORMANCE

1.1 Coatings and their application in aviation

Most materials used in high technology applications are composites, i.e., they have a near-surface region with properties differing from those of the bulk materials. This is caused by the requirement that the material exhibit a combination of various, and sometimes conflicting, properties. For example, a particular engineering component may be required to have high hardness and toughness (i.e., resistance to brittle crack propagation). This combination of properties can be obtained by having a composite material with high surface hardness and a tough core. Alternately, the need may be for a high temperature, corrosion-resistant material with high elevated-temperature strength as is the case with the hot stage blades and vanes in a gas turbine. The solution again is to provide the strength requirement from the bulk and the corrosion requirement from the surface. [2]

In general, coatings are desirable, or even necessary, for a variety of reasons including economics, materials conservation, unique properties, or the engineering and design flexibility which can be obtained by separating the surface properties from the bulk properties.

This near-surface region is produced by depositing a coating onto it (i.e., overlay coating) by processes such as physical or chemical vapor deposition, electrodeposition, and thermal spraying, or by altering the surface material by the in-diffusion of materials (i.e., diffusion coating or chemical conversion coating), or by ion implantation of new material so that the surface layer now consists of both the parent and added materials.

“Coatings” may also be formed by other processes such as melt/solidification (e.g., laser glazing technique), by mechanical bonding of a surface layer (e.g., roll bonding), by mechanical deformation (e.g., shot peening), or other processes which change the properties without changing the composition.

As stated above, the coating/substrate combination is a composite materials system. The behavior of this composite system depends not only on the properties of the two components (i.e., the coating material and the substrate material), but also on the interaction between the two (i.e., the structure and properties of the coating/substrate interface) which is integral to the very important factor of adhesion of coatings. In some cases, such as for overlay coatings, this is a distinct region. For others, such as ion implantation or diffusion coatings, it is not a discrete region.

Historically, most solid metallic and some ceramic materials were produced by melting/solidification technology. Since the advent of deposition technologies (i.e., production of solid materials from the vapor), the diversity of materials that can be produced has more than doubled because the properties of solid materials produced from the vapor phase can be varied over a much wider range than the same material produced from the liquid phase. This is because melt techniques produce solid materials with properties close to equilibrium properties whereas the deposition conditions may be so chosen as to produce materials from the vapor phase with properties close to equilibrium (similar to their melt-produced counterparts), or properties far removed from equilibrium properties (non-equilibrium properties). Moreover, a much greater variation in microstructure is possible with vapor source materials. For example, a copper-nickel alloy produced by solidification from the melt will always consist of a single phase solid solution, whereas the same alloy produced by alternate deposition from two sources may consist of alternate layers of nickel and copper, i.e., a laminate composite or a solid solution depending on the deposition temperature.

A large number of materials are used for coatings today. These may range from the naturally occurring oxide layer which protects the surfaces of many metals such as aluminum, titanium, and stainless steel, to those with very deliberate and controlled alloying additions to the surface to produce specific properties, as exemplified by techniques such as molecular beam epitaxy or ion implantation. Other examples with increasing degree of criticality range from paint coatings applied to wood and metals, electrostatically painted golf balls, the print in the daily newspaper, optical coatings on lenses and other elements, vapor deposited microcircuit elements such as resistors,

diffusion or overlay coatings on superalloys used in gas turbines for high temperature corrosion protection, hard overlay coatings of engineering components and machine tools, etc. [3].

Coating application has next advantages:

1. Modern solution for increase of reliability and lifetime of mechanical components;
2. Environmentally friendly alternative to other coating technologies (e.g. electroplating);
3. Ability to boost performance while reducing weight, use of less expensive materials;
4. Indirect impact: Improving efficiency of manufacturing technology – cutting, forming, casting.

Erosion of compressor blades:

1. Leads to:
 - power loss,
 - higher fuel consumption and emission of pollutants;



Figure 1.1 – Erosion wear mechanism

2. Manifests as:
 - leading and trailing edges chord loss;
 - profile change;
 - tip loss;
3. Caused by ingestion of sand, fly ash, salt, ice

Thin film coatings are applied for protection jet engines against:

1. Erosion;
2. HT Oxidation and hot corrosion;
3. Fretting;
4. Galling/seizure;
5. Surface fatigue;
6. (Sand) sticking;
7. Thermal impact (TBC);
8. General corrosion.

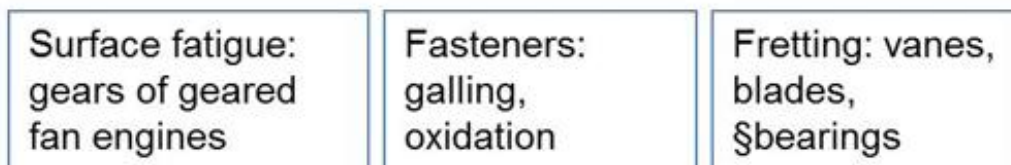
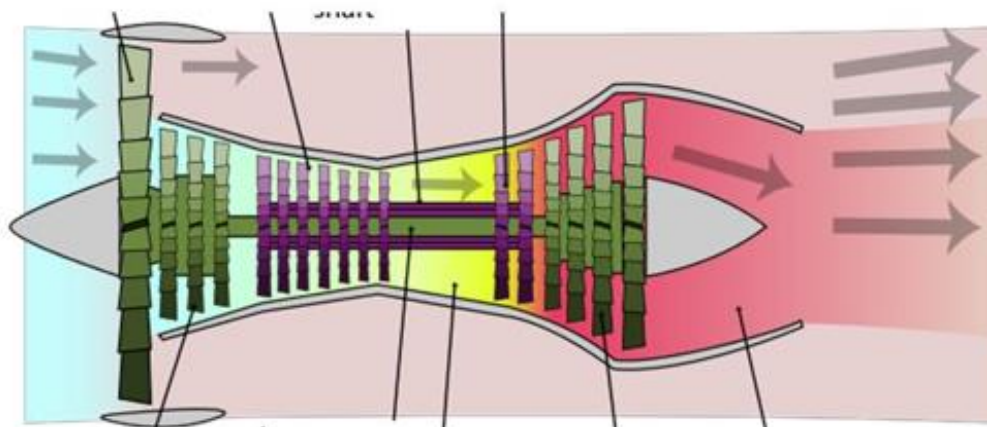
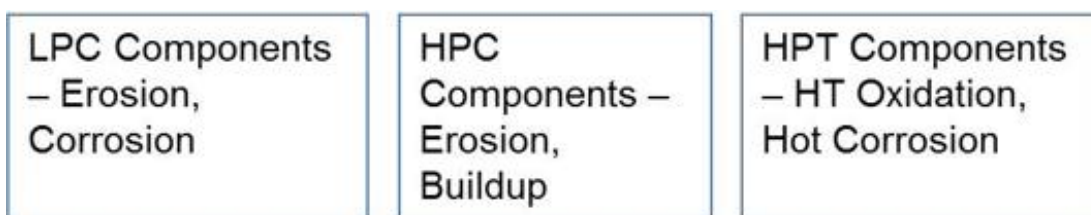


Figure 1.2 – Engine components which need film coatings the most



Figure 1.3 – Types of blade damage

PVD coatings are applied on blades for protection against erosion in LPC and HPC

Jet Engine: Fretting Wear Protection

1. Fretting motion occurs between dovetail joint (root) of a blade and disk;
2. Fretting: adhesive transfer of material between contacting surfaces: leads to pits, abrasive wear, crack formation;

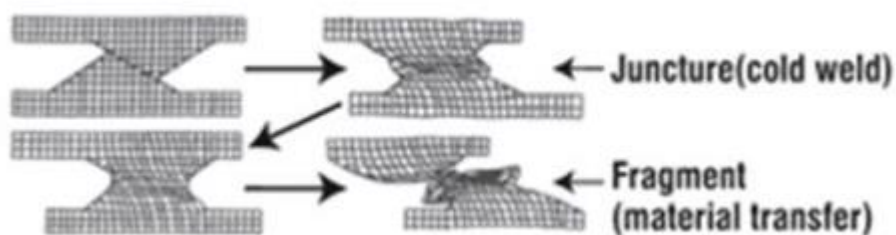


Figure 1.4 – Adhesive wear occurrence in highly-loaded, poorly lubricated sliding machine contacts

3. Remedies:

- High hardness – PVD coatings;
- Low friction – PVD coatings;
- Material selection – PVD coatings;
- Compressive stress – PVD coatings.

Jet Engine: Micro Spark Coating

1. Micro Spark Coating (MSC) is a variant of electro spark deposition;
2. Protects against wear and fretting at normal and elevated temperatures;

3. Wide range of deposited materials, including application-specific compositions;
4. Thickness of more than 50 μm ; repair applications are possible;
5. Applications: shrouds, blade tips, cladding repair, labyrinth seals.



Figure 1.5 – Low pressure turbine shroud: welding and MSC coating

Applications on Aerospace Fasteners

1. Function:
 - Protection against galling and seizure;
 - Corrosion protection;
2. Working temperatures from -60 of up to 800°C;
3. Traditional coating: Ag electroplating; Cd plating (not permitted for the engine use);
4. Potential replacement: TiN, CrN, CrON;
5. DLC (for temperatures < 350 C);

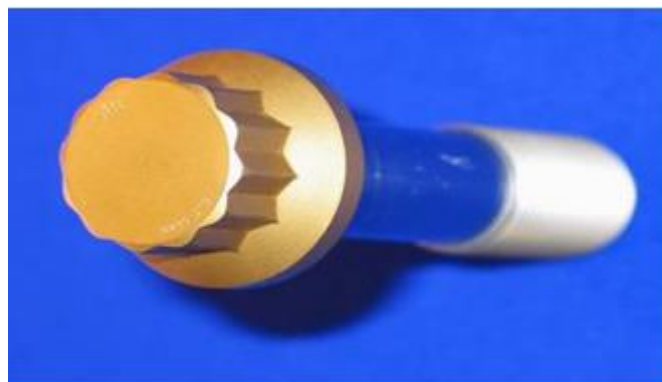


Figure 1.6 – Fastener with TiN coating

CVD Aluminizing (CVA)

1. Diffusion bond coating for turbine components; Ni_xAl_y intermetallide based;
2. Provides protection against HT oxidation and hot corrosion; forms alumina (TGO) for reliable bonding of TBC layer;

3. Halide CVD process for aluminizing;
4. Alternative to powder-based techniques (pack, out-of-pack, slurry);

Applications for Airframe Components

1. Protection against fretting is one of the most common coating applications;
2. Use of fretting-prone materials (Ti, Al, SS) in combination with vibrations accentuates fretting issues;
3. Spherical bearings, mounts, knuckle joints are among typical components benefiting from thin film coatings;
4. Typical coatings are nitrides and carbon-based films;



Figure 1.7 – Different airframe components with coating

1.2 Thin film deposition processes

The methods by which TiN thin films are applied to the cutting tools include chemical vapor deposition (CVD), physical vapor deposition (PVD) and metallo-organic chemical vapor deposition (MOCVD). The basic reaction in the CVD coating of TiN is between titanium tetrachloride, nitrogen and hydrogen: $2\text{TiCl}_4 + \text{N}_2 + 4\text{H}_2 \rightarrow 2\text{TiN} + 8\text{HCl}$, which takes place at a temperature typically between 850°C and 1100°C. Since this temperature range is comparable with that used in the original hardening treatment of many tool steels, the CVD process is not suitable for tool steels because post-coating treatments (hardening and tempering) may be required to re-harden the substrate material, which, in turn, may affect the dimensional tolerance of the tool as well as coating adhesion. PVD processes, on the other hand, operate at much lower temperatures (between

400°C and 600°C) and are thus used widely for tool steels.

Friction and wear in different engine components have crucial effects on the engine performance, combustion efficiency, oil consumption and lifetime of the internal combustion (IC) engine. Under certain loads, speeds, and temperatures, the metallic components of the IC engine, especially the piston and valve system suffer from a higher friction. Thin film coating is one of the novel techniques to reduce the frictional forces and improve the mechanical properties of engine components. Due to some versatile tribological properties, increasing attention has been paid to the physical vapor deposition (PVD) technology in the recent decade to deposit thin film coating on engine components. This article presents a comprehensive literature review on thin film coatings for IC engine components deposited by PVD technique. Issues related to tribological properties (wear and coefficient of friction) and mechanical properties (hardness and roughness) are also highlighted. Scientific improvements are presented in the light of literature. It is revealed that PVD coating is significantly effective on wear resistance, scuffing resistance, surface roughness, and friction of the components in IC engine.

Laboratory test and data from actual service so far suggest that the plasma-activated electron beam evaporation coating is perhaps one of the best choices for smooth surface finishing with improved mechanical and tribological properties. However, there are still some problems in its practical usage. This compressive review paper presents the major shortcomings of PVD coatings on IC engine components and the possible solutions if any. Finally, a number of issues have been reported which need to be encountered for further studies.

PVD technology dates back to 1938 but has been available widely only in the last two decades [2]. PVD coating of tools started in Europe in early 1977 with the successful coating of cold-forming tools followed by twist drills and hobs in 1980 and fine-blanking tools in 1981. PVD coating of TiN was introduced in the United States in the early 1980s. Since then TiN-coated tools have gained rapid acceptance in the automotive, off-the-road vehicle and tractor, and gear and bearings industries. Being TiN-coated, expensive gear-cutting tools, such as hobs, shaper cutters, selected broaches, and circular form tools, provided excellent performance and immediate return of the coating cost many times over.

PVD processes rely on ion bombardment instead of high temperatures as the driving force (as is the case of CVD). The substrate to be coated is contained in a vacuum chamber and is heated to a temperature between 400°C and 600°C; the coating material, Ti, is vaporized and the reactive gas, N₂, is introduced and ionized; the vaporized titanium atoms then react with the ionized nitrogen to form TiN compound that deposits on the substrate to form the coating. For coating tools, at least, there are three major PVD processes: evaporating, sputtering and reactive ion plating, differing in the way the reacting metal is vaporized and the electrical configuration.

Evaporation of the source material (Ti) can be accomplished through heating by direct resistance, radiation, laser beam, arc discharge or an electron beam in a vacuum chamber. In an arc-evaporation system, the coating thickness is greatest directly above the center line of the source and decreases away from it, thus creating a uniformity problem, which can be overcome by using a multi-arc system, as illustrated in figure 1.8.

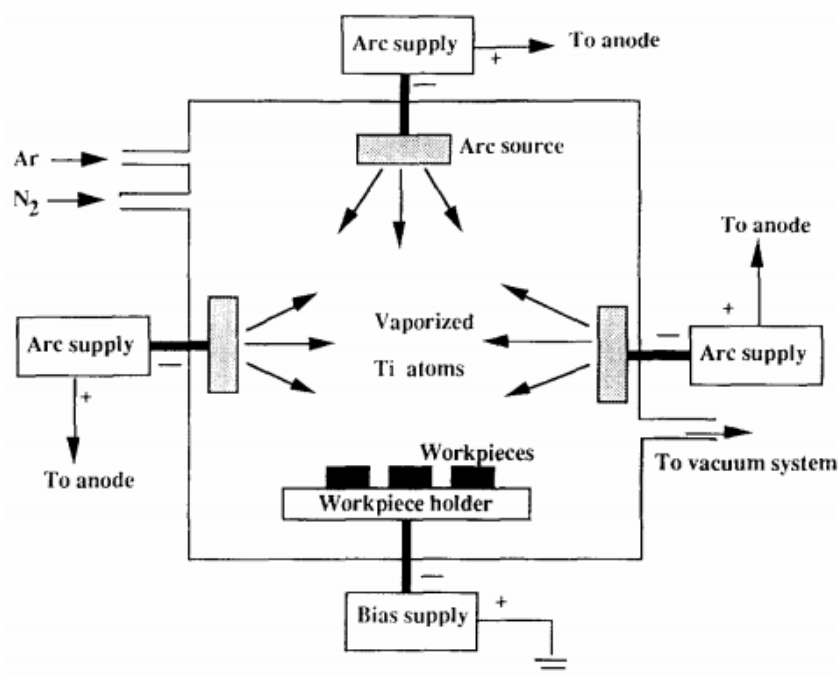


Figure 1.8 – Principles of the multi-arc evaporation system for TiN coating

Sputtering is an old technique, more widely used in electronics, that applies a high voltage (500-5000 V, generally direct current for metals and radio frequency for non-conductive targets), between an anode (the substrate) and a cathode that supplies coating ions liberated by the bombardment of inert gas ions. For coating TiN, solid titanium is

used at the cathode, and nitrogen is introduced as the reactive gas (figure 1.9). The inert gas atmosphere (such as Ar at a pressure of $10^{-3} - 10^{-1}$ Torr) is used to avoid chemical reactions at the target and substrate. This process is termed "reactive sputtering" since reactive gas is involved. The disadvantages of the sputtering process are a low deposition rate and a high thermal load on the substrates due to bombardment by secondary electrons. Addition of a properly shaped magnetic field can speed up the deposition [3], in which case the technique becomes "reactive magnetron sputtering". The essential disadvantage of magnetron sputtering is the strong decrease of the substrate ion current with increasing distance of substrates from the magnetron target: this can be corrected by additional gas ionization or magnetic confinement of the plasma [4].

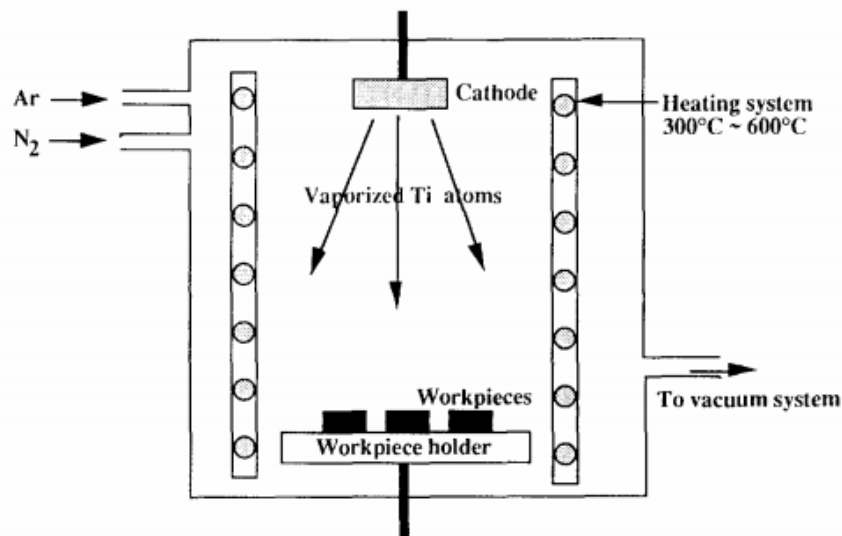


Figure 1.9 – Principles of the reactive sputtering of TiN coating

The vast varieties of thin film materials, their deposition processing and fabrication techniques, spectroscopic characterization and optical characterization probes that are used to produce the devices. It is possible to classify these techniques in two ways [5]:

- Physical process
- Chemical process

Physical method covers the deposition techniques which depends on the evaporation or ejection of the material from a source, i.e. evaporation or sputtering, whereas chemical methods depend on physical properties. Structure-property relationships are the key

features of such devices and basis of thin film technologies. Underlying the performance and economics of thin film components are the manufacturing techniques on a specific chemical reaction. Thus chemical reactions may depend on thermal effects, as in vapour phase deposition and thermal growth. However, in all these cases a definite chemical reaction is required to obtain the final thin film[6].

When one seeks to classify deposition of films by chemical methods, one finds that they can be classified into two classes. The first of these classes is concerned with the chemical formation of the film from medium, and typical methods involved are electroplating, chemical reduction plating and vapour phase deposition. A second class is that of formation of this film from the precursor ingredients e.g. iodization, gaseous iodization, thermal growth, sputtering ion beam implantation, CVD, MOCVD and vacuum evaporation.

The methods summarized in table 1.1 are often capable of producing films defined as thin films, i.e. 1 μm or less and films defined as thick films, i.e. 1 μm or more. However, there are certain techniques which are only capable of producing thick films and these include screen printing, glazing, electrophoretic deposition, flame spraying and painting.

Table 1.1 – Classification of Thin Film Deposition Techniques

Sputtering	Evaporation	Gas Phase	Liquid Phase
Glow discharge DC Sputtering	Vacuum Evaporation	Chemical vapour Deposition	Electro-deposition
Triode Sputtering	Resistive heating Evaporation	Laser Chemical vapour deposition	Chemical bath deposition (CBD)/ Arrested Precipitation Techniques (APT)
Getter Sputtering	Flash Evaporation	Photo-chemical vapour deposition	Electro less deposition
Radio Frequency	Electron beam	Plasma enhanced	Anodisation

sputtering	Evaporation	vapour deposition	Liquid phase Epitaxy
Magnetron Sputtering	Laser Evaporation	Metal-Organo Chemical Vapour Deposition (MOCVD)	Sol- gel
Ion Beam sputtering			Spin Coating
			Spray-pyrolysis technique (SPT)
A.C. Sputtering	Arc		Ultrasonic (SPT)
	R.F. Heating		Polymer assisted deposition (PAD)

Generally, the PVD processes are performed under vacuum circumstances, and it is involved four steps. Firstly, evaporation, over this stage the target is evaporated by high energy source such as resistive heating or electrons beam. Secondly, transportation, the vaporized atoms move from target to the surface of substrate through this phase. The third step is reaction, in some cases deposition, if there is a gas such as nitrogen or oxygen in the system, the atoms of materials reacts with the gas. If, however, in cases where the coating does not contain of gas, but it only consists of the target material, this phase does not be part of the process. Finally, deposition, through this stage the surface of substrate will be built. This technique is classified into two sorts, thermal evaporation and sputtering [7].

Advantages and disadvantages of PVD process

Nothing is ever perfect; everything has negative and positive effects. It is undoubtedly true to say that although PVD process plays an important role in many fields, it has some obvious drawbacks. One of the significant advantages of using PVD process is that this process makes it possible for materials to deposit with developed properties compared to the substrate material. For instance, these techniques are commonly used to increase oxidation resistance, hardness and resistance of wear. As a result, it uses in a several of applications such as automotive, aerospace, surgical/medical, dies and shapes for all types of material processing, cutting tools and fire arms. Moreover, the PVD

process enables approximately any type of inorganic material to use as well as certain categories of organic materials. In addition, it is environmentally approachable further than processes such as electroplating.

Also the advantages of PVD include a lower deposition temperature, thus post-coating treatment is avoided, no dimensional change in precision tooling, the possibility of tailoring the coating properties by careful control of deposition conditions, excellent adhesion due to the high arrival energy of the coating material and the ability to clean the surface prior to coating very thoroughly by a sputtering stage in the cycle, a good surface finish that in some systems equals that of the substrate, the elimination of finish machining, no effluents or pollutants as a result of the process, no hydrogen embrittlement, dense structures, controllable and repeatable stoichiometry and crystallographic structure, a wide range of coatings and substrate materials, including metals, alloys and ceramics, the possibility of multiple coatings, and greater productivity and major cost savings. The limitations of PVD processes arise because in a PVD process it is necessary to rotate the substrate in order to achieve uniformity, the deposition temperatures are still not low enough for some applications, holes in a substrate should not be more than twice as deep as their diameter if coating is needed to the full depth, although holes can be 4–5 times the diameter in depth.

On the other hand, one of the important disadvantages is that the PVD technique requires appropriate cooling system for some processes operate at high vacuums and temperatures such as evaporate materials that has high melting point, and this system not only need skilled operators, but also demands high capital cost. In addition, frequently the rate of coating deposition is fairly slow; it is enormously difficult to coat similar surface and undercuts.

In conclusion, it is important to note that even though there are some drawbacks associated with PVD process, particularly, slowing of rate of coating deposition and cost of existence of appropriate cooling systems, the benefits probably outweigh the disadvantages, especially as regards with increasing oxidation resistance, hardness and resistance of wear. As a consequence, the PVD is more preferable method than CVD, which will be focused in the next part, for depositing thin film for many materials as well

as useful in wide range of applications such as automotive, aerospace and surgical/medical.

Secondly, as far as temperature is concerned, the most remarkable similarity between PVD and CVD techniques is that the temperature of deposition in both systems is generally more than 150°C. In contrast, PVD coating is deposited between 250°C and 450°C, whereas, CVD coating is deposited at high temperatures in the range of almost 450°C to roughly 1050°C.

Finally, in CVD, the material introduces in gaseous form onto the substrate, but it introduces in solid form in PVD. On the other hand, the gaseous molecules react with substrate in CVD, whereas the atoms are moving and depositing on the substrate in PVD.

Overall, it would appear that PVD and CVD systems are quite different in terms of temperature and degree of vacuum [8].

So, which method of these two is most suitable. Definitely PVD one. As its undoubted advantages are lower temperature of deposition and degree of vacuum.

But which physical definition let us know about how coating and detail surfaces interact with each other? For sure adhesion.

1.3 Adhesion between substrate and thin films and its influence on functional performance

Adhesion is the tendency of dissimilar particles or surfaces to cling to one another (cohesion refers to the tendency of similar or identical particles/surfaces to cling to one another). The forces that cause adhesion and cohesion can be divided into several types. The intermolecular forces responsible for the function of various kinds of stickers and sticky tape fall into the categories of chemical adhesion, dispersive adhesion, and diffusive adhesion. In addition to the cumulative magnitudes of these intermolecular forces, there are also certain emergent mechanical effects.

Recent advances in the number of variety of technological applications of thin films, have to varying degrees, been limited by their adherent qualities. While adhesion enhancement may be demonstrated qualitatively, no reliable method of quantifying these forces exists. In part, this is due to the fact that the test method must be appropriate to the

proposed application. For example, the production of reliable ohmic contacts without any significant interdiffusion represents a very different problem to that of producing abrasion resistant coatings of thin films able to withstand chemical attack.

In addition, the adhesion of thin films (typically 100 nm) is an area which is not amenable to direct study, since the films are too weak to exist without being supported by a substrate and the adhesive forces are frequently centered around an interfacial layer which may be only a few atoms thick.

The first case provides an interesting model for thin film adhesion, particularly where the film and substrate show no chemical affinity towards one another-as in the case of gold on silica. In such situations the adhesive forces must be ascribed to purely physical phenomena. These physical forces are determined by the degree of intimacy of contact between film and substrate. In the ideal case of perfect physical contact the adhesive force is normally quoted as 10^8 Nm^{-2} . Since the ultimate tensile strengths of most common materials lie within a factor of 10 of this value, it must be stressed that this represents the upper limit for purely physical adhesive forces.

In reality, vacuum deposited thin films frequently exhibit considerably worse adhesion than this theoretical limit. The measured value of the adhesive force of evaporated films can be as little as 10^4 Nm^{-2} . Thus, thin film adhesion concerns itself more with the problems of surface contaminants than with genuine differences between physical and chemical bonding phenomena. For example, at 10^{-5} mbar a monolayer of gas is absorbed onto the surface in a few seconds.

In cases where the adhesive force approaches 10^8 Nm^{-2} the film and substrate behave as a single solid entity, and no reliable method of quantifying the adhesion exists. In such cases techniques which involve abrasion or penetration of the film give information about the mechanical properties of the film, rather than the adhesive qualities of the interface. For good adhesion of gold on silicon, for example, the majority of the gold will be removed easily, as it is a relatively soft material, but a well adhered thinner layer may remain on the silicon surface.

Whatever their intended use may be, the properties, structure, functional characteristics, and performance all depend, inter alia, on adhesion between the coating

and the substrate. Below are cataloged some of the prime reasons emphasizing the importance of adhesion of thin films.

1) Adhesion is very important in thin film technology because the thin films (usually $1\ \mu\text{m}$ and in some applications of the order of $50\ \text{nm}$) are so fragile that these must be supported by more substantial substrates and the degree to which the film can share the strength of the substrate depends upon the adhesion between the two.

2) Adhesion is very important in determining the durability of thin film devices, for example, in microelectronic circuits.

3) Adhesion plays an important role in governing the kinetics of the growth and structure of the films (formed by vacuum deposition, for example), with the result that performance of thin films is dictated by adhesion forces. Film structure will be aggregated whenever the cohesive energy exceeds the energy of adhesion. This dependence of film integrity upon adhesion forces is not only important from the viewpoint of performance of such films but it also has a basic scientific import.

4) The durability and longevity of thin films are largely dependent upon their adhesion to the substrate since this determines the ease of removal.

5) It is highly desirable that films should be capable of being cleaned and polished, particularly where these are used for front surface reflectors and it means they should have good adhesion in addition to other factors like resistance to corrosion.

6) Wear is intimately related to the extent of adhesion of thin film to the substrates; if the adhesion is poor, the film will wear off quite rapidly.

7) Adhesion is a fundamental parameter in surface chemistry and physics because it depends directly on interatomic and intermolecular forces. Thin films should provide an ideal situation because it is in such systems that conditions of true interfacial contact can most nearly be attained. For example, a film deposited on a clean substrate under high vacuum conditions faithfully contours all surface irregularities and imperfections and almost perfect contact between the film and the substrate should be readily obtained.

8) Good adhesion of thin films, used as protective overcoats, is very vital for the environmental protection (e.g., protection from corrosion) of the substrates. If the adhesion is poor, the extent of deterioration of the substrates by environmental factors (humidity,

corrosive gases, etc.) is greatly accelerated [9].

Industrial techniques adhesion control based on such techniques as brushing, bending, stretching, applying a grid of scratches, etc. However, these methods do not provide quantitative values of adhesion strength. To quantify strength clutches use the direct break method films from the substrate or shear relative to the latter. To this end, to the surface of the film is glued or soldered metal rods, to which then tensile reinforcement is applied. The disadvantage of this method is the probability of material penetration. solder or glue on the film-to-lining interface and changes in grip characteristics. In the case of a direct break, the gap is usually starts at the point where local stress exceeds local strength. In that case, naturally, the measurement results separation effort can not be attributed to a specific area. However, to assess the performance of the coating, it is sufficient to relate the tearing forces to the projection of the separation area onto a plane perpendicular to the acting force. In determining the strength the shear grip force is directed to the coating layer on the substrate surface.

To determine the adhesive strength of coatings by the method of separation without the use of adhesive bonding and soldering use pin method. The essence of this method is as follows. In the cone-shaped hole of the matrix freely put the pin of the cone-shaped form

The first and second scratch marks are typical of plastic materials. and the third is for fragile ones such as transition metal nitrides and carbides.

Depending on the degree of contamination, such cleaning methods are used as chemical etching, grinding, polishing, washing in solutions to remove contamination organic origin (subject to such), washing in alcohol, or a combination of such methods.

Immediately before Coating deposition is also used to clean the substrate by bombarding with high-energy ions. The most widely used methods for producing coatings include galvanic, chemical, deposition from powders of metals in plasma jets, method of gas transport reactions, magnetron and vacuum-arc.

Before embarking on the techniques per se, two points should be made clear:

- a) The practical adhesion may not be a direct measure of the basic adhesion as defined above;

- b) The values of experimental adhesion obtained by different methods may not be directly comparable.

The methods of measurement of adhesion of thin films can be categorized in a number of ways:

- 1) Qualitative and quantitative methods;
- 2) Destructive and non-destructive methods;
- 3) Mechanical and non-mechanical methods;
- 4) Fully developed, partly developed and the methods in inchoate stage;
- 5) Practical methods and the methods of academic interest;
- 6) Routine and non-routine methods.

However, the methods have been classified into three categories: (a) nucleation methods, (b) mechanical methods, and (c) miscellaneous techniques. Mechanical methods are further divided depending upon the mode of application of forces to detach the film from the substrate. Miscellaneous methods comprise the following: Thermal method, X-ray technique, ESR, capacitance method, cathodic treatment, and pulsed laser or electron-beam technique.

A few comments regarding nucleation methods are in order: (a) These are not the tests for measuring adhesion; the information from this type of work has led to a better understanding of thin film formation and structures (b) The techniques are not applicable to completed films, (c) Unlike mechanical tests, nucleation studies yield the adsorption energy of a single atom, and the validity of using such adsorption energy to calculate adhesion energy per unit area is questionable on the grounds that the bond energy in a continuous film will not in general be the same as that for a single atom. But more common methods are mechanical ones. We will analyze them in more detail.

Mechanical Methods

All mechanical methods use some means of removing the film from the substrate. These methods can be broadly classified into two categories depending upon the mode of detachment of the film: (a) methods involving detachment normal to the interface, and (b) methods involving the lateral detachment of the film from the interface. Methods involving detachment normal to the interface a force of increasing magnitude is applied to

the film-substrate interface until the interface is disrupted. Either the maximum force applied is measured, or some other criterion such as area of detachment is used to designate adhesion. In these methods, an attempt is made to detach the film in a direction normal to the interface, so that the whole area of the film is detached simultaneously when the interface is broken. If the whole area is not detached simultaneously, then the analysis of the forces is more complex. The most common mechanical methods are scratch, peel and pull one.

The peel test is a sophistication of the qualitative tape test devised by Strong [10], which provides a quantitative measure of peel force. Several methods have been reported for measuring the peel force, Chapman [11], used a load cell and synchronous motor, while more recently Baglin [12] avoided the use of adhesive tape by coating the film under test with a 10 μm copper film, applying the peel force directly to the unattached end of the copper film.

The peel test described here is a simple, reliable method of quantifying the adhesion of poorly adherent thin films. The apparatus (figure 1.10) consists of a modified analytical balance in which the force applied to the tape may be smoothly and continuously increased by filling the measuring cylinder with water. The tape, readily available pressure sensitive tape, cut into strips 2 mm wide is applied with firm pressure to the film. The balance arm is raised from its rest position, and the peel force is gradually increased by filling the measuring cylinder. Provided that the film is removed by the tape, the peel force (in g) may be directly read from the measuring cylinder (calibrated in cm^3).

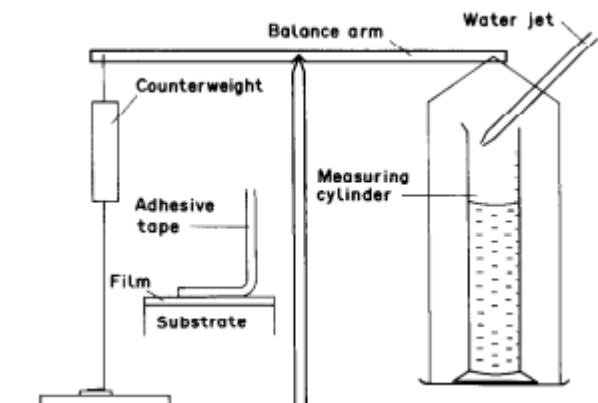


Figure 1.10 – The peel test

The advantages of the test are the simplicity, minimal cost, suitability for both hard and soft substrates, and its independence of the adhesive quality of the tape (except that this will affect the useable range of the test). The principal limitations are that the test is only suitable for films whose adhesion to the substrate is worse than that for the film to tape interface, the measured data is subject to considerable random fluctuation and, once peeling starts, the momentum of the water is usually enough to allow it to continue.

For most vacuum deposited thin films, the surface temperature increases during deposition, resulting in considerable internal stresses. The net effect of these stresses will result in a tendency for the top of the film to contract relative to the bottom. In the peel test, these stresses will manifest themselves in terms of a reduced peeling force.

The two forms of pull test for measuring thin film adhesion are show in figure 1.11. The direct pull method [13] measures the perpendicularly applied force required to remove the film, whereas the topple test [14] measures the force applied parallel to the surface to remove a rod attached to the film. The direct pull test described here is suitable for quantitative measurement of thin film adhesion over a wide range. The perpendicular force required to remove a stud glued to the thin film is measured using an electronic force gauge. Short cylindrical steel studs (4×4 mm dia), freshly cleaned and abraded with a fine file, are attached to the film with either cyanoacrylate adhesive and aerosol activator, or epoxy resin adhesives. When the adhesive has set, the sample is carefully mounted directly below a Salter EFG2-200 force gauge mounted on a test stand. The sample stand is mechanically lowered, removing the stud and film from the substrate, and the maximum force immediately prior to failure is displayed on the gauge.

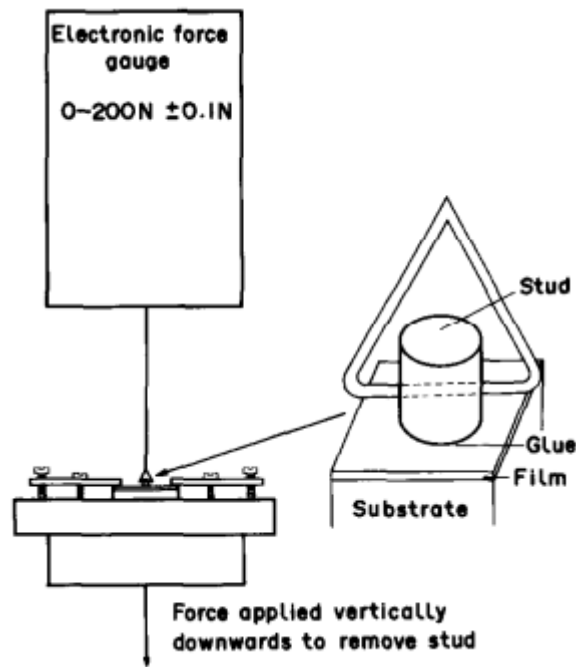


Figure 1.11 – The pull test

The maximum value of measurable adhesion is determined by removing the stud from a piece of pure gold. In designing the steel studs, it was found that statistical fluctuations could be reduced by increasing the ratio of base diameter to height. The pivoted link allows maximization of the base area to effective height ratio. Extreme care must be taken to align the stud accurately on the axis of the force tester, to eliminate any component of the force acting in the horizontal plane.

In contrast with the peel test, the film is supported on a rigid stud, and, thus, the method is independent of the internal forces acting on the film. Since internal force is not itself an adhesive force, but acts in competition with it, it is useful, by comparative use of both peel and pull testing to assess the significance of this parameter.

The data obtained from the pull test may readily be converted into units of adhesion (Nm^{-2}) since the area of the film removed can be measured directly and can thus be related to the upper limit for van der Waals' bonding. For cyanoacrylate adhesive, used with the activator on pure gold, the adhesion was measured as 10^7 Nm^{-2} corresponding to 10 % of the theoretical maximum for perfect physical contact. For epoxy resin adhesives, the measured adhesion was 6 % of the theoretical maximum. The pull test is quite susceptible to random fluctuation, though this is somewhat less than for the peel test [15].

Scratch test. The first quantitative use of the scratch test was reported by Heavens [16] and later developed by Weaver [17]. A recent claim that it may be used to calculate adhesion energies has been reported by Langier [18]. The test has been extensively used as a measure of thin film adhesion, probably due to the simplicity and high degree of reproducibility offered by the method. However, considerable controversy still surrounds both the use and the interpretation of the data from the scratch test.

The apparatus consists of a hemispherical diamond stylus mounted on a pivoted beam above a coordinate table on which the sample is mounted. An optical microscope is mounted directly above the coordinate table, so that the scratch produced may readily be examined. In order to test the thin film adhesion, the stylus is moved relative to the film, with a load mounted on the beam, directly above the stylus. The load on the stylus is progressively increased until the film is removed from the substrate, the minimum load required to achieve this being termed the critical load. The scratch may then be examined by optical and electron microscopy. Figure 1.12 shows the relative sizes of the stylus and film.

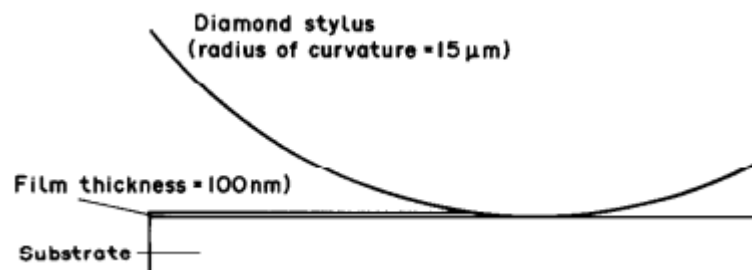


Figure 1.12 – Scratch test

The difficulty in interpretation arises from the degree of significance that may be attached to the value of the critical load. Since the adhesive force to be measured acts on the stylus in the horizontal plane, and the load on the stylus acts in the vertical plane, the critical load cannot be described as a direct measure of the adhesive force. The critical load is highly dependent on the thickness and hardness of the film and its major component will be a function of these two parameters. Some useful information can be obtained from microscopic examination of the scratches. In cases of poor adhesion large areas of the film can be seen to have been detached and creased by the stylus whereas, in

cases of good adhesion of a relatively soft film, interpretation is more difficult since it is uncertain whether all the film has been removed, or a very thin layer, perhaps 1–2 nm remains at the bottom of the track. In cases where the adhesion mechanism involves a diffuse interface, an intermediate layer, or, mechanical interlocking, the problem is considerably more complicated. The scratch test offers no correlation between one film substrate combination and another, and is unsuitable for systems where the substrate is softer than the film, for example, a gold film on a PTFE substrate. However, in comparison to most other methods of adhesion testing it is the least susceptible to random fluctuation [19].

Reproducibility of peel, pull and scratch tests

In order to establish the experimental reproducibility of the tests described above, gold (60 nm) was evaporated onto silicon, cleaned in Decon 90 in an ultrasonic bath, and rinsed thoroughly in de-ionized water. The adhesive properties of the films were then tested in identical groups of six, in order to assess the degree of significance that could be attached to a set of results. The measured values are presented (figure 1.13) as bar charts, and the average value as a horizontal line. The standard deviation is illustrated and presented as a percentage.

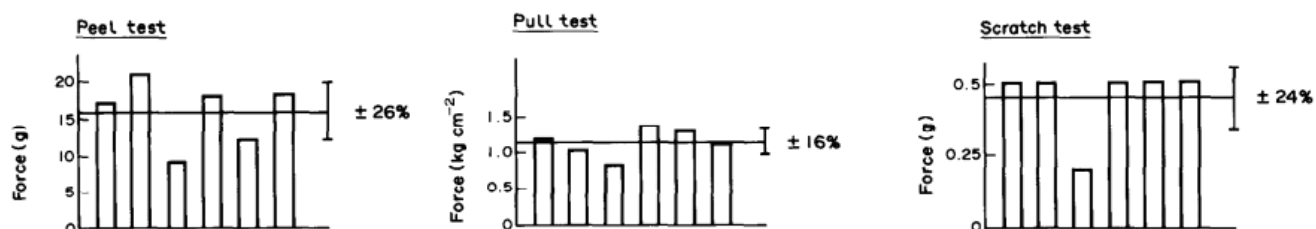


Figure 1.13 – Reproducibility of peel, pull and scratch tests

The results indicate a high degree of random fluctuation for the peel test, and significant random fluctuation for the pull test. The scratch test exhibits an unrealistically high degree of reproducibility offset by one very low value [20].

In most scratching devices diamond cone-shaped indenters with a radius of apex ranging from $\sim 13 \mu\text{m}$ to $400 \mu\text{m}$ were used. The speed of movement of the indenter was, as a rule, several mm per minute. The moment of scratching of the film was determined microscopically, as well as by registering an acoustic emission signal that appears when

scratching films from fragile materials. Scratch method is the easiest and fastest way to assess the adhesive characteristics. However, despite its widespread use, there are difficulties in quantifying adhesion strength assessment. Usually, adhesion strength is characterized by the magnitude of the vertical (critical) load on the point at which the film is scratched. When testing adhesion by scratching, the thinnest groove that forms (depending on from factors like material hardness coatings and substrates, film thickness, vertical load on the tip and from some parameters related to the test conditions) can be obtained by:

- plastic deformation of the coating material without destruction (plastically crumpled, extruded scratch);
- plastic deformation followed by cutting the finest chips;
- brittle fracture, practically without plastic deformation with cleaving of the thinnest areas (chipped scratch).

Conclusion to Part 1

Surface engineering will remain a growth industry in the next decade, because surface-engineered products increase performance, reduce costs, and control surface properties independently of the substrate, thus offering enormous potential due to the following:

- Creation of entirely new products;
- Solution of previously unsolved engineering problems;
- Improved functionality of existing products—engineering or decorative;
- Conservation of scarce materials;
- Ecological considerations—reduction of effluent output and power consumption

Thin film coatings are commonly utilized to prevent wear, modify surface properties, and manipulate the frictional behavior of various mechanical systems. The behavior of a coating has a direct effect on the life as well as performance of the system.

Analysis has shown that thin film coatings use in aerospace industry increases. In certain aerospace applications, thin films are ‘designed-in’ solutions for wear and corrosion protection. However, the coating itself is subject to damage, and the quality of the coating is related to the adhesion characteristics between the coating and the substrate. The level of performance of such layers depends on their composition and structure, the deposition parameters and also the reliability of the technologies associated with measurement of characteristics commonly represented by the hardness, modulus of elasticity and adhesion of thin films.

The adhesion between coatings and substrates is a complex phenomenon, and depends on different factor, so it becomes quite difficult to study. Coating is only effective when it adheres to the substrate. In practice, it is necessary to characterise the adhesion of a coating according to the industrial applications that it is predestined for.

Therefore, a quantitative assessment of the adhesion properties of thin film is important to guarantee the reliability of not only the thin film but also will help in development of new materials, deposition processes etc.

PART 2

METHODS AND INSTRUMENTS OF EXPERIMENTAL STUDY

2.1 Basic principles and application of scratch test

The scratch resistance of thin films and protective coatings is usually expressed in terms of their ability to withstand abrasion without fracturing. Scratch testing on a large scale enables films and coatings to be ranked according to the results of a particular test method. A typical scratch test involves a ramped load and the measure of performance is the critical load at which the surface fails. However, various modes of failure can be generated at different loads with different shapes of indenter.

Many nanoindentation instruments can be configured to operate in a scratch testing mode. As shown in figure 2.1, in this mode of operation, a normal force F_N is applied to the indenter, while at the same time, the specimen is moved sideways. In some instruments. An optional force transducer can be used to measure the friction, or tangential force F_T . In some cases, a lateral force F_L , normal to F_T can also be applied.

Scratch tests on a micron scale were initially performed inside the chamber of an SEM. The stylus or indenter in these tests was typically electro-polished tungsten tips with a radius of about 1 μm . The “scratch hardness” was defined as the track width of the scratch divided by the diameter of the scratch tip [16].

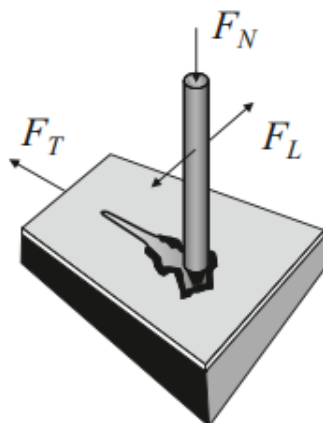


Figure 2.1 – Configuration of an indentation scratch test.

The normal force F_N can be held at a constant value or ramped up or down while the specimen is moved sideways by a tangential force F_T . In addition, a lateral force F_L can sometimes also be applied

The physical meaning of the results of such a scratch test are fairly open to interpretation. In modern methods, the applied normal force is ramped up in value while the specimen is moved in a sideways direction and the minimum force F_C at which failure occurs is an indication of scratch resistance. The detection of this critical load can be determined using a variety of techniques such as optical microscopy, acoustic emission, and an analysis of the coefficient of friction, the latter method requiring a measurement of the tangential force F_T as well as the applied normal force F_N . The coefficient of friction μ can be readily calculated from:

$$\mu = \frac{F_T}{F_N} \quad (2.1)$$

A diamond sphero-conical indenter with a tip radius of between 10–200 μm is usually used as the stylus. The use of the critical load as a measure of scratch resistance is complicated by its dependence on scratching speed, loading rate, tip radius, substrate hardness, film thickness, film and substrate roughness, friction coefficient, and friction force. Despite these difficulties, the method allows comparative tests to be performed with some degree of confidence to mechanical performance. Figures 2.3 and 2.4 show the results of a scratch test on multilayer Al/TiN/SiO film on a silicon substrate for a constant applied normal load of 30 mN using a 20 μm scratch tip. The circled areas in both figures are an indication of an area of poor adhesion of the film. In a ramped load scratch test, there is usually observed a transition from elastic to plastic deformation in the surface, and if the surface is a thin film, delamination eventually occurs. For scratches made on very soft materials, the shape of the indenter often affects the visibility of the scratch owing to an increase in piling-up along the length of the scratch. Jardret and Oliver demonstrate the differences in piling-up with a Berkovich indenter with the blunt face of the indenter facing forward, and the edge facing forward, on an automotive paint film.

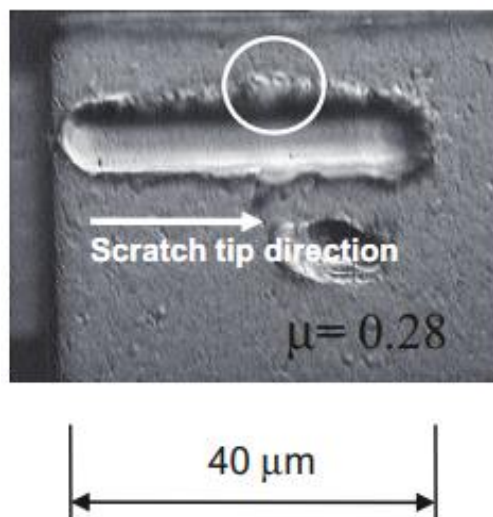


Figure 2.2 – Scratch test on a multilayer Al/TiN/SiO film on a silicon substrates. The tip moved in a left to right direction as shown in the figure. The coefficient of friction is shown. The *circled* area indicates an area of poor adhesion of the film. (Courtesy Fischer-Cripps Laboratories)

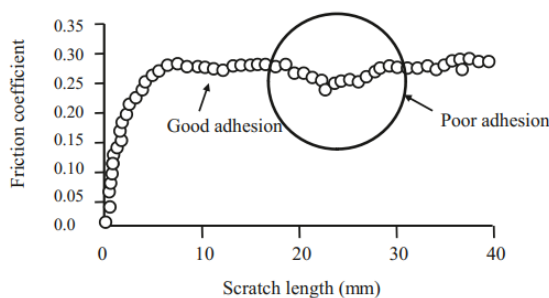


Figure 2.3 – Plot of coefficient of friction vs scratch length for specimen

Similar results obtained by Enders, Grau, and Berg with sol-gel films on fused silica were interpreted in terms of an analytical model incorporating both sliding and ploughing friction terms. Interestingly, this latter work treated the contact at very low loads as a single asperity contact in which surface adhesive forces were included. The sliding part of the friction coefficient is given as:

$$\mu_s = \pi \left(\frac{3}{4E^*} \right)^{2/3} TR^{2/3} F_N^{-1/3} \left[1 + \frac{F_A}{F_N} + \sqrt{\left(1 + \frac{F_A}{F_N} \right)^2 - 1} \right]^{2/3} \quad (2.2)$$

where T is the interfacial shear strength found from the tangential force F_T divided by the contact area, R is the radius of the indenter, F_A and F_N are the adhesive and normal forces respectively. The ploughing part as:

$$\mu_p = KP^*F_N^{(2-n)/n} \quad (2.3)$$

where n and K are constants that depend upon the shape of the indenter. The total friction coefficient is the sum of these:

$$\mu = \mu_s + \mu_p \quad (2.4)$$

Both the sliding and ploughing parts of the friction are functions of the normal force F_N . The sliding part of the friction coefficient dominates the process at low values of F_N and decreases with increasing load. The ploughing part of the friction is shown to dominate the process where, during the transition, the total friction coefficient passes through a minimum at a critical value of normal force F_N .

Scratch testing is of course closely related to the field of tribology. Tribological testing usually involves techniques such as pin-on-disk, ball-on-disk, and pins, rings, or disks on disks leading to measurements of friction force and friction coefficient, adhesion force of films, wear rate, contact resistance and acoustic emission of fracture events. While conventional nanoindentation instruments do not generally offer these capabilities, there is considerable overlap with some tribology instruments offering a nanoindentation mode of operation.

The scratch test has been used for many years to provide a measure of coating/substrate adhesion. In the normal configuration of the test a diamond stylus is drawn across the coated surface under an increasing load until some well-defined failure occurs at a load which is often termed the critical load, L_C . Many different failures are observed which include coating detachment, through-thickness cracking and plastic deformation or cracking in the coating or substrate. In fact, it is usual that several different failure modes occur at the same time and this can make the results of the test difficult to interpret.

The failure modes observed in the scratch test depend on many factors and are most easily characterized in terms of the hardness of both substrate and coating. In the case of a

typical Rockwell 'C' diamond indenter (120° cone with 200 mm hemispherical tip), for soft coatings and soft substrates the test is dominated by plastic deformation and groove formation and little or no cracking is observed except at very high loads. For hard coatings on soft substrates deformation of the substrate is predominantly plastic whilst the coating may plastically deform or fracture as it is bent into the track created by plastic deformation of the substrate. Soft coatings on a harder substrate tend to deform by plastic deformation and some extrusion of the coating from between the stylus and the substrate may occur. Considerable thinning of the coating by plastic deformation will occur before plastic deformation and fracture of the substrate becomes significant. For hard coatings on hard substrates plastic deformation is minimal and fracture dominates the scratch response.

As the indenter becomes sharper, plastic deformation becomes more localized to the surface and it is easier to prevent plastic deformation of the substrate. In such cases the results of the test are easier to analyze and quantify, particularly for more modern depth sensing indentation and scratch systems. However, damage to the diamond stylus during the test becomes much more significant as its sharpness increases. The choice of stylus thus represents a compromise between damage and ease of data analysis – for industrial hard coatings of reasonable thickness (0.1 mm) the Rockwell 'C' stylus has proved very successful whilst for sub-micron coatings a conical indenter with a tip radius of a few microns is more suitable.

The scratch test is not well-suited to measure the adhesion of soft coatings but can give some information if the interfacial shear strength is less than the shear strength of either the coating or substrate. In general, the scratch test is most effective if the substrate does not plastically deform to any great extent. In such cases the coating is effectively scraped from it and the uncovering of the substrate itself can be used as a guide to adhesion. However, it is difficult for this to be quantified. Detection of the uncovered substrate may be a problem unless post facto chemical analysis methods can be employed. However, some success is possible by measuring the change in friction during the scratch if the coating and substrate behave differently. For instance, an increase in friction may be observed if a high friction coefficient substrate is uncovered during the test.

The scratch adhesion test is much more useful for hard coatings, particularly when

these are deposited on softer substrates. For a harder coating on a soft substrate the spallation and buckling failure modes arise from interfacial detachment and can thus be used as the basis for an adhesion test. Both may be quantified in some circumstances and are discussed in this paper.

The technique of scratch test. Scratch hardness testing has a very long history. As early as 1640, gems were classified by hardness by scratching with a rasp. In 1822, Moos proposed a scale of hardness consisting of 10 reference minerals, which still retains its value in mineralogy. The first device for assessing hardness by scratching – the sclerometer was created by Seebeck in 1833. The principle of representing hardness as a load on a diamond cone with an angle of 90° when it forms a scratch $10\ \mu\text{m}$ wide was proposed by Martens in 1890, and for a long time (until 1936) was the only method for quantifying microhardness.

Depending on the combination of certain factors: the material properties, the type and position of the indenter during scratching, the depth of its introduction, the scanning speed, four scratch forming mechanisms are implemented:

- 1) plastic deformation by displacing the material from under the indenter;
- 2) cutting with chip separation;
- 3) dispersion with the separation of the crushed material;
- 4) brittle chipping.

There are intermediate forms and mixed mechanisms for the formation of scratches.

For sclerometer tests, diamond cones with corners at the apex of 90 and 120 , the trihedral Berkovich pyramid and the tetrahedral Vickers are used as indenters.

Depending on the purpose of the research and the size level of the test, the load on the indenter can vary widely – from 200 to 10^{-5} H, and the scan rate from 0.4 to 600 mm/min (table 2.1).

There are three types of presentation of test results while scratching:

- according to the load on the indenter required to obtain a scratch due to the width (or depth);
- according to the size of the scratch width obtained when the indenter load is caused;

• the largest tangential force T required to form a scratch at a given normal load on the indenter (this tangential force is often called the friction force, and in foreign sources the lateral force is lateral force).

Table 2.1 – Working parameters of modern sclerometers

Parameters	Dimensional test level		
	Macroscopic	Microscopic	Nanometric
Indentation force, H	1 – 200	0.05 – 30	10^{-5} – 1.0
Maximum friction force, H	200	30	$6 \cdot 10^{-5}$ – 1.0
Scanning trace length, mm	70	120	120
Scan speed, mm/min	0.4 – 600	0.4 – 600	0.4 – 600

The first type of presentation of the results was proposed by Martens. Hardness is estimated by the load at which a scratch is formed with a width of 10 microns. The method of selecting such a load is rather laborious.

The method of assessing the hardness of the scratch width δ when $P = const$ widespread.

Mayer proposed to measure the hardness when scratching with a cone indicator $8P/\pi\delta^2$, which corresponds to the specific pressure on the projection of the contact surface. For the Vickers pyramid, the analogous indicator is equal to $4P/\delta^2$, and the same result was obtained by interpreting the hardness as the specific pressure on the projection of the contact surface, and in the form of the specific work expended on scratching.

According to the Birbaum method, scratching is carried out with a regular triangular pyramid with an angle of 90 between the ribs edge forward with a fixed load of $P = 0.03 H$. The hardness number is defined as $K = 10^4/\delta^2$ where δ is measured in microns.

Methods for assessing hardness when scratching by measuring tangential force (K. Savitsky, M. Tenenbaum) did not receive due development due to the technical difficulties of recording this force on instruments of the time when these methods were proposed.

This, however, relates generally to the sclerometer test methodology, which, unlike the methods of local indentation, did not develop intensively enough. However, in the last decade, scratch testing has become popular in the study of the physical and mechanical properties of various materials, the adhesion of thin films and coatings, and the corresponding methodology has begun to be widely implemented in modern instrumentation [22].

The possibility of registering tangential force when scratching opens up the wide possibilities of this method for research and control of materials and products. This is an assessment of adhesion of thin films and coatings, modeling of friction and wear processes, determination of hardness along the scanning route, study of the micromechanical characteristics of the processes of deformation and fracture, evaluation of the anisotropy of the physical and mechanical properties in micro and nano-scales.

2.2 Indenter types

Nanoindentation hardness tests are generally made with either spherical or pyramidal indenters. Consider a Vickers indenter with opposing faces at a semi-angle of $\theta=68^\circ$ and therefore making an angle $\beta=22^\circ$ with the flat specimen surface. For a particular contact radius a , the radius R of a spherical indenter whose edges are at a tangent to the point of contact with the specimen is given by $\sin \beta=a/R$, which for $\beta=22^\circ$ gives $a/R=0.375$. It is interesting to note that this is precisely the indentation strain¹ at which Brinell hardness tests, using a spherical indenter, are generally performed, and the angle $\theta=68^\circ$ for the Vickers indenter was chosen for this reason.

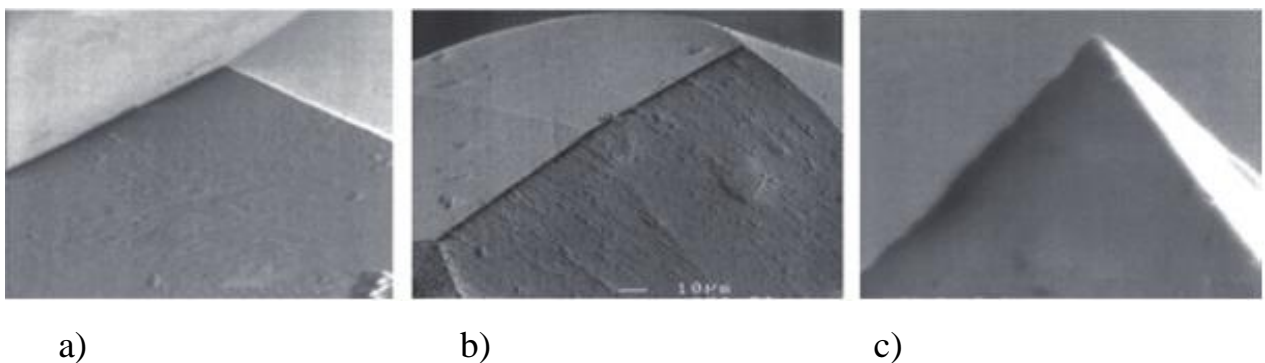


Figure 2.4 – SEM images of the tips of (a) Berkovich, (b) Knoop, and (c) cube-corner indenters used for nanoindentation testing [21]

The tip radius of a typical diamond pyramidal indenter is in the order of 100 nm.

The Berkovich indenter, (a) in figure 2.4, is generally used in small-scale indentation studies and has the advantage that the edges of the pyramid are more easily constructed to meet at a single point, rather than the inevitable line that occurs in the four-sided Vickers pyramid. The face angle of the Berkovich indenter normally used for nanoindentation testing is 65.27° , which gives the same projected area-to-depth ratio as the Vickers indenter. Originally, the Berkovich indenter was constructed with a face angle of 65.03° , which gives the same actual surface area to depth ratio as a Vickers indenter. The tip radius for a typical new Berkovich indenter is on the order of 50–100 nm. This usually increases to about 200 nm with use. The Knoop indenter, (b) in figure 2.4, is a four-sided pyramidal indenter with two different face angles. Measurement of the unequal lengths of the diagonals of the residual impression is very useful for investigating anisotropy of the surface of the specimen. The indenter was originally developed to allow the testing of very hard materials where a longer diagonal line could be more easily measured for shallower depths of residual impression. The cube corner indenter, (c) in figure 2.4, is finding increasing popularity in nanoindentation testing. It is similar to the Berkovich indenter but has a semi-angle at the faces of 35.26° .

Conical indenters have the advantage of possessing axial symmetry, and, with reference to figure 2.5, equivalent projected areas of contact between conical and pyramidal indenters are obtained when:

$$A = \pi h_c^2 \tan^2 \alpha \quad (2.5)$$

where h_c is depth of penetration measured from the edge of the circle or area of contact.

For a Vickers or Berkovich indenter, the projected area of contact is $A=24.5h^2$ and thus the semi-angle for an equivalent conical indenter is 70.3° . It is convenient when analyzing nanoindentation test data taken with pyramidal indenters to treat the indentation as involving an axial-symmetric conical indenter with an apex semiangle that can be determined gives expressions for the contact area for different types of pyramidal indenters in terms of the penetration depth h_c for the geometries shown in figure 2.5.

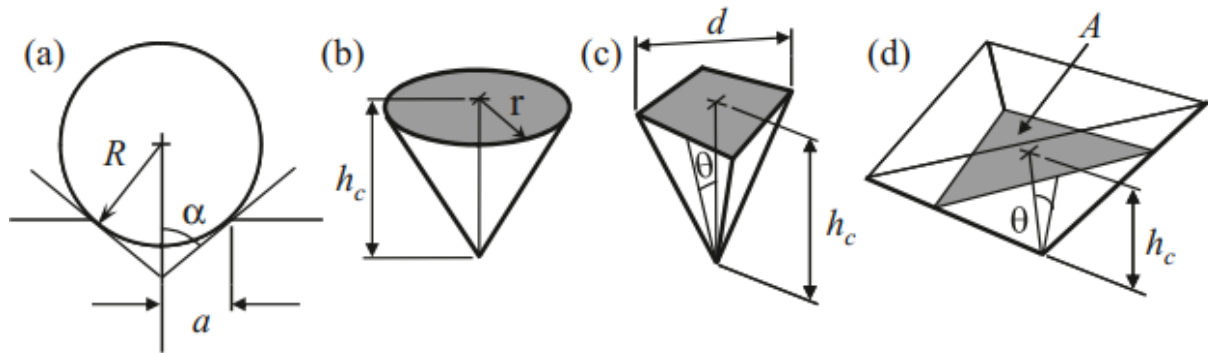


Figure 2.5 – Indentation parameters for (a) spherical, (b) conical, (c) Vickers, and (d) Berkovich indenters (not to scale)

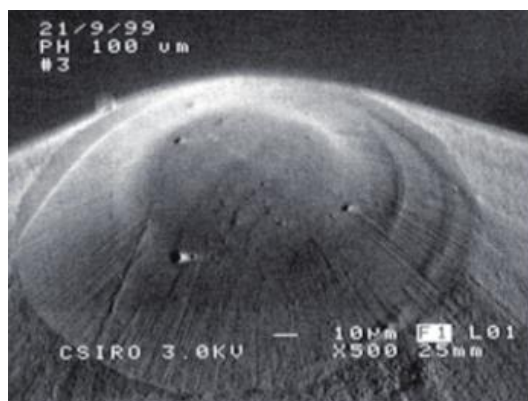


Figure 2.6 – Tip of a spheroconical indenter used for nanoindentation and scratch testing

Spherical indenters are finding increasing popularity, as this type of indenter provides a smooth transition from elastic to elastic–plastic contact. It is particularly suitable for measuring soft materials and for replicating contact damage in in-service conditions. As shown in figure 2.6, the indenter is typically made as a spherocone for ease of mounting. Only the very tip of the indenter is used to penetrate the specimen surface in indentation testing. Diamond spherical indenters with a radius of less than 1 micron can be routinely fashioned. Indenters can generally be classified into two categories – sharp or blunt. The criteria upon which a particular indenter is classified, however, are the subject of opinion. For example, some authors classify sharp indenters as those resulting in permanent deformation in the specimen upon the removal of load. A Vickers diamond pyramid is such an example in this scheme. However, others prefer to classify a conical or pyramidal indenter with a cone semi-angle $\alpha > 70^\circ$ as being blunt.

Thus, a Vickers diamond pyramid with $\theta=68^\circ$ would in this case be considered blunt. A spherical indenter may be classified as sharp or blunt depending on the applied load according to the angle of the tangent at the point of contact. The latter classification is based upon the response of the specimen material in which it is observed that plastic flow according to the slip-line theory occurs for sharp indenters and the specimen behaves as a rigid-plastic solid. For blunt indenters, the response of the specimen material follows that predicted by the expanding cavity model or the elastic constraint model, depending on the type of specimen material and magnitude of the load. Generally speaking, spherical indenters are termed blunt, and cones and pyramids are sharp.

2.3 Description and principle of operation of the nanoindentation tester "Micron-Gamma"

The multifunctional device, “Micron-Gamma” (figure 2.7), is designed to study the physicomaterial properties of the surface layers of materials using the methods of continuous indentation of the indenter, scanning, metallography and topography [23].

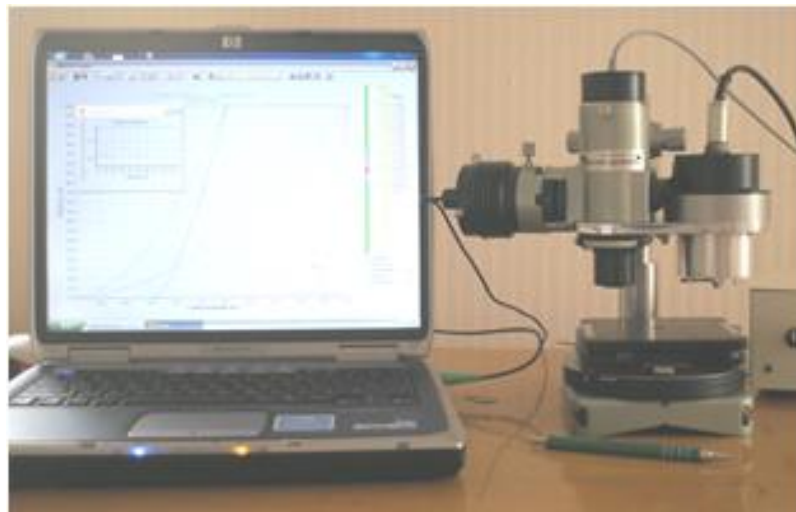


Figure 2.7 – “Micron-Gamma” appearance

Main technical specifications:

Maximum load is.....500,

Loading resolution:

at range of 150g.....0.001;

at range of 500g.....0.01

Range of measured premises, mkm.....	0.01 – 200
Indenter loading rate, gps.....	0.01 – 100
Number of logged values:	
in micro indentation mode.....	2000;
in scan mode.....	unlimited
Table positioning accuracy, mkm.....	10
Maximum microscope magnification.....	×400
The possibility of drawing an aiming injection	

This method is based on automatic registration in the process of load testing (P) on the indenter and depth (h) of its introduction into the surface of the test material in the form of a loading diagram $P = f(h)$ (see figure 2.8). The decoding of such a diagram allows obtaining not only more extensive, but also fundamentally new, as compared with the standard microhardness test method, information. The method allows you to capture valuable information about the process of indentation of the indenter, taking into account the processes occurring as a result of stress relaxation, material change under the indenter in the process of indentation, during exposure under load, during loading, etc.

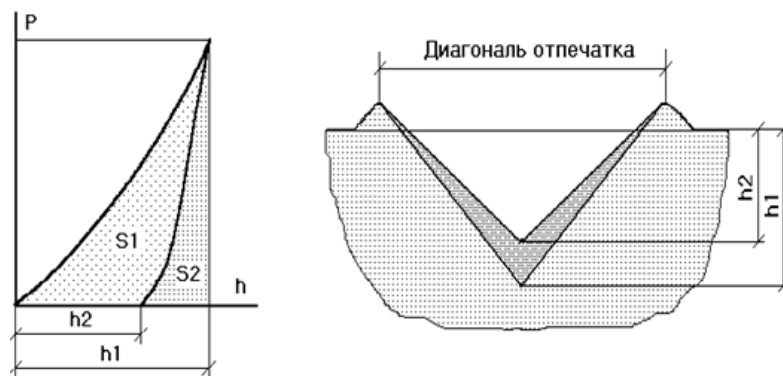


Figure 2.8 – Load diagram and footprint cross section

The continuous indentation method allows you to:

- to carry out tests for microhardness in the range of low and ultra-low loads;
- to study the features of the micro strain of materials on the kinetics of the introduction of the indenter;
- register micro creep of materials;

- measure the gradient of properties over the depth of implementation;
- to test materials with poor reflectivity (in particular polymeric materials), as well as materials whose imprint greatly changes the size after removing the load;
- measure the fragility of materials according to the implementation diagram;
- measure the elasticity of materials.

Indenter Scan Method (Scratch Test)

The scanning method is based on the continuous recording of the resistance of the movement of the indenter over the surface with a given load. Determining the statistical relationships between the resistances of local microvolumes of the material to contact deformation using the methods of the theory of random processes makes it possible to make a comprehensive assessment of the state of the surface layer on the scanning path and, in particular, makes it possible to:

- to evaluate the average strength of the surface layer on the scanning route;
- assess the variation and heterogeneity of the strength properties;
- to simulate the elementary acts of the processes of friction and wear (micro-cutting, micro-slipping, brittle fracture, adhesion of coatings, etc.).

In figure 2.10 a model is presented which explains the essence of the scanning method. If the investigated surface along the indenter scan path consists of solid (and shallow L2) and soft (and large L1) fragments, treating the tribogram (the interpolation depth versus time t) as a random process and plotting the spectral density, you can get a strength portrait of the surface. The spectral density can be judged on the size, quantity and strength of fragments on the scan path.

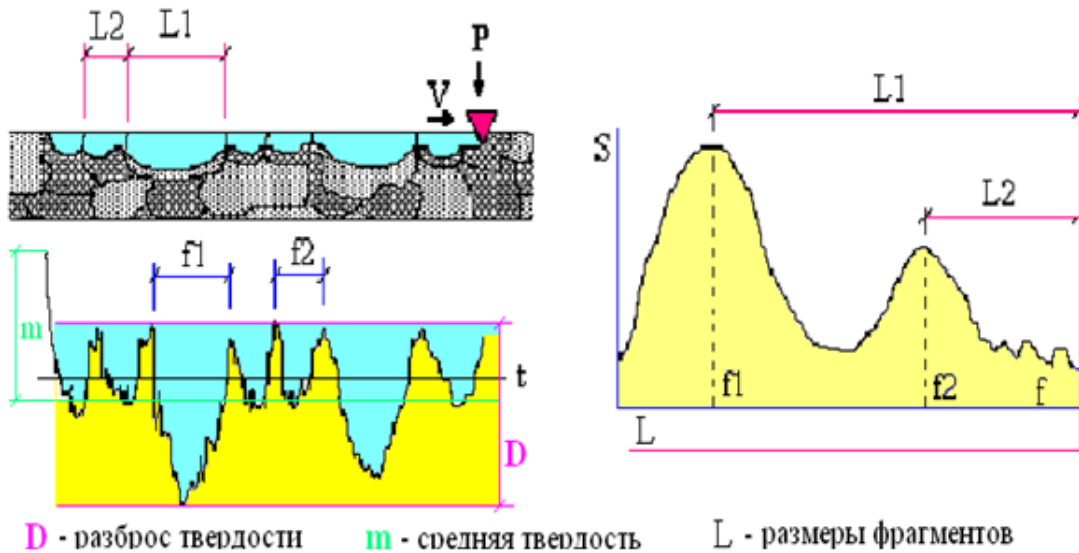


Figure 2.10 – Model explaining the principle of the scanning method

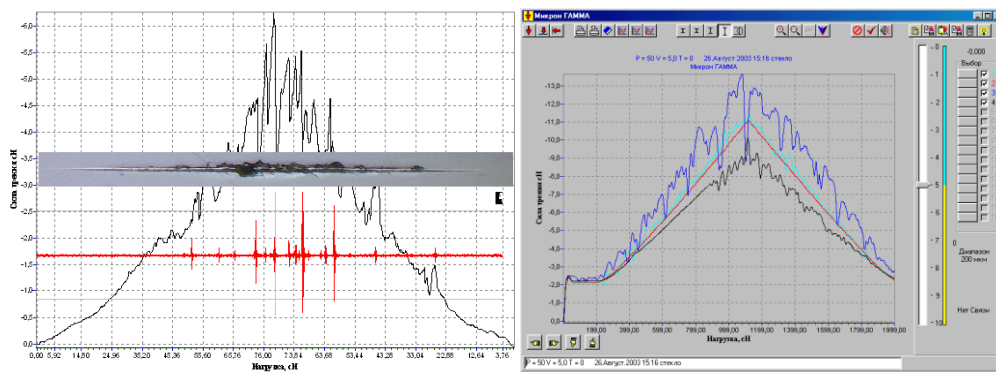


Figure 2.11 – a) tangential force, micrograph of the scratch and acoustic signal (with an additional sensor); b) tangential force for various materials. With a gradually increasing and decreasing load on the indenter.

Metallography method is based on the registration of the image by means of an optical microscope with an integrated digital video camera and subsequent statistical processing of the image.

The method allows you to:

- quantitative image analysis;
- analysis of non-metallic inclusions;
- analysis of porosity;
- analysis of the grain structure;
- phase analysis;

- registration in the dynamics of the processes of destruction, cracking;
- build a three-dimensional brightness model of the surface.

In addition, it allows to conduct an aiming “injection” in the required place of the surface, while observing the image on the monitor screen (figure 2.12).

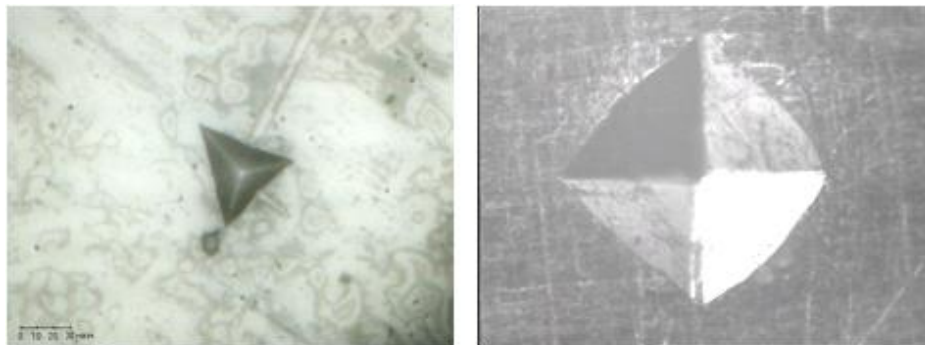


Figure 2.12 – Prints of different indenters

The topography method is based on scanning the surface with an indenter with a minimum load on the indenter (0.01–0.1 g) Followed by processing of the profilograms and, in particular, allows the construction of the surface profile.

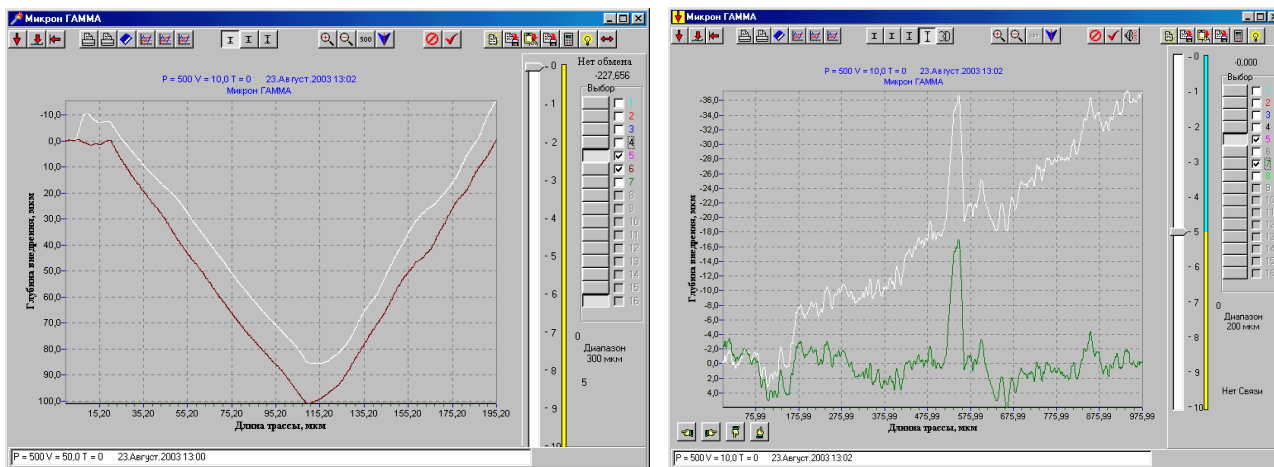


Figure 2.13 – Profilograms of holes of prints and rough surface (before and after the removal of the trend)

2.4 Structure of nanoindentation tester "Micron-Gamma"

The device works as follows (see figure 2.14 block diagram of the device). The rod 4 with the indenter 5 and the probe 9 are fixed to the body of the loading unit 3 using flat springs 6 and 10, respectively. The springs allow the rod 4 and the probe 9 to move in a strictly vertical direction within 0.5 mm.

Smoothly lowering the body of the loading unit 3, install the indenter 5 and the probe 9 on the surface of the sample 11.

By running the software and selecting the required load and loading rate, the indenter is loaded by means of an electromagnetic loader 1, by means of a digital-to-analog converter (DAC) 2.

In the process of loading the indenter 5, the depth of its insertion relative to the probe 9 (relative to the sample surface) is recorded.

The insertion depth is recorded by a small displacement sensor 7 by means of an analog digital converter (ADC) 8. Sensor body 7 is fixed to probe 9, and an anchor (movable part) to rod 4 with indenter 5. Thus, sensor 7 always measures movement of rod 4 with indenter 5 with respect to the probe 9.

The microprocessor 13 serves to control the ADC, DAC, two-coordinate subject table 12 and generates communication protocols with a computer.

The use of a probe (differential measurement method) allows tens of times to reduce the effect of vibrations and rigidity of the device on the readings, since the depth of the indenter's insertion is measured relative to the probe, i.e. – the surface, and not the deflections of the object table and the instrument stand.

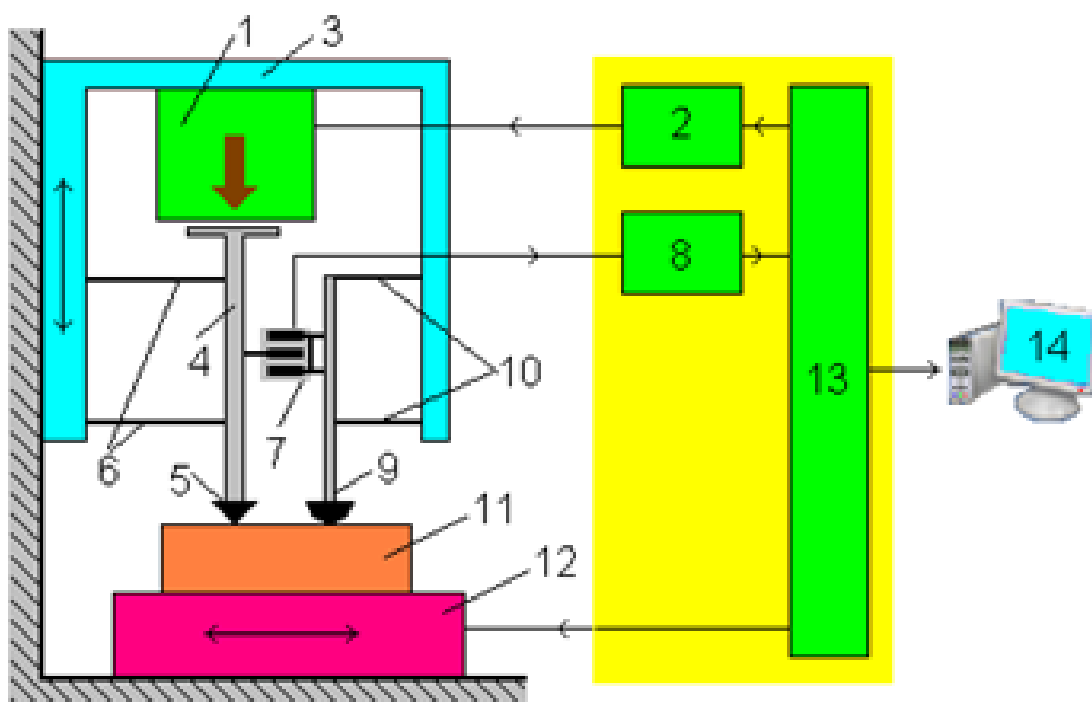


Figure 2.14 – Block diagram of the device:

1 – electromagnetic loader, 2 – D/A converter, 3 – loading unit body, 4 – rod, 5 – indenter, 6 – flat springs of the indenter, 7 – small displacement sensor, 8 – ADC, 9 – probe, 10 – flat spring of the probe, 11 – sample, 12 – subject table, 13 – microprocessor, 14 – computer

The mechanical unit (figure 2.15) consists of a frame with a stand 1, a two-coordinate mechanized table 10, an optical microscope with an interchangeable lens 9 and a video camera 5, a loading head 14 with an integrated inductive small displacement sensor, an electromagnetic loader and a diamond indenter 15.

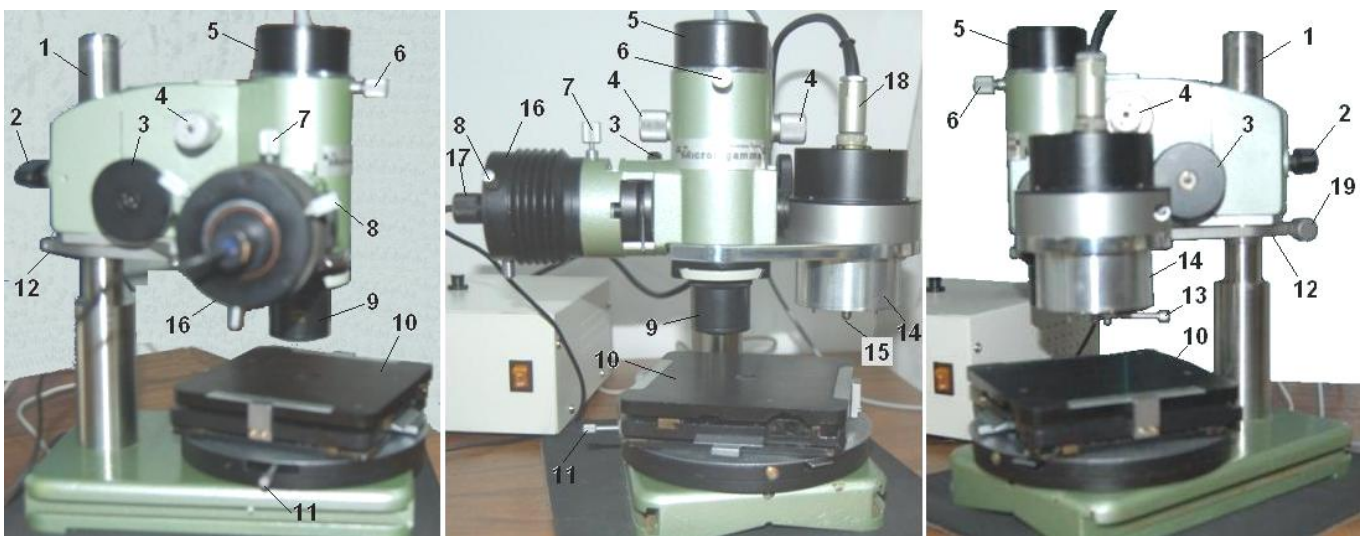


Figure 2.15 – The appearance of the mechanical unit of the device.

1 - stand, 2 - microscope fixing handle on the stand, 3 - coarse movement handle of the microscope and the indenter, 4 - precise movement handle of the microscope, 5 - video camera, 6 - camera mounting screw, 7 - illuminator mounting screw, 8 - illuminator centering screws, 9 - lens, 10 - two-coordinate table, 11 - screw for fixing the rotation of the table, 12 - aiming needle stop, 13 - probe handle, 14 - loading unit, 15 - indenter, 16 - microscope illuminator, 17 - lampholder, 18 - connector heads, 19 - the screw of fixing of the limiter

The loading unit 14 and the microscope are rigidly connected. The optical axis of the microscope and the indenter 15 are located on the same radius relative to the axis of the rack 1.

A microscope with a loading unit 14 is rotated around pillar 1 at an angle

proportional to the distance between the optical axis and the indenter for the application of an aiming injection. The angle of rotation is limited by the limiter 12. The limiter 12 is fixed on the rack 1 with a screw. Limiter 12 also supports the microscope. Handle 2 serves to fix the microscope while carrying. With a slight tightening of the handle 2, the backlash is eliminated when the microscope turns. The tightening force of the handle 2 is selected so that the microscope can be turned relative to the rack 1 with a slight friction.

The two-coordinate table 10 can be rotated around its own axis, and the screw 11 serves to fix the selected position, for example, during scanning. Movement along the X and Y coordinates is carried out by built-in micromotors with gearboxes.

To adjust the microscope for sharpness and smooth movement of the indenter up or down, use the coarse 3 and precise 4 handles. It should be remembered that the course of the exact movement of the handle 4 is limited to 2 millimeters. If the sample is large and there is not enough progress in height, then you can raise the microscope along the rack 1. To prevent damage caused by the falling of the microscope with the loading unit 14 down the rack, you need to lift it in the following sequence:

1. Release the handle 2 and manually raise the microscope with the load unit 14 on the rack 1;
2. Clamp knob 2 and fix the microscope on the stand 1;
3. To release the screw 19 and bring the limiter 12 close to the microscope;
4. Firmly tighten the screw 19 and fix the limiter 12 on the rack 1;
5. Release the handle 2 so that the microscope with the loading unit 14 can be turned relative to the support 1 with a slight friction, without any backlash.
6. In order to lower the microscope with the loading unit 14 in a stand downward, it is necessary to perform the following actions and in strict sequence:
 7. Tighten the handle 2 and fix the microscope on the rack 1;
 8. Loosen the screw 19 and lower the stopper 12 down the rack 1 by the required amount;
 9. Firmly clamp the screw 19 and fix the stop 12 on the rack 1;
 10. Release the handle 2 and hold the microscope with the loading unit 14 on a rack 1 up to the stop with the limiter 12;

11. Tighten the handle 2 so that the microscope with the loading unit can be turned relative to the rack 1 with a slight friction and no backlash.

The handle of the probe 13 is used to adjust the height of the probe. Spinning (turning around the axis of the probe) shorten the probe and vice versa.

Camera 5 can be rotated around the optical axis of the microscope and fixed with screw 6. By turning the camera, you can change the position of the image on the screen.

Load block design

Indenter 2 (see figure 2.16) with a rod 3 and a coil weighs about 10-20 g., And is fixed to the body in the form of a glass by means of springs 4. The small displacement sensor 6 with a stylus 8 is fixed by means of springs 7. The probe 8 is threaded a spherical tip 10 with a handle 9 is screwed in. By turning the handle 9 you can change the length (height) of the probe. The load on the indenter is set by an electromagnetic loader 5 with a linear characteristic and with a minimum sampling step of 0.001 grams. The indenter 2 and probe 10 are mounted on sample 1, and the small displacement sensor 6 measures the position of the indenter relative to the probe.

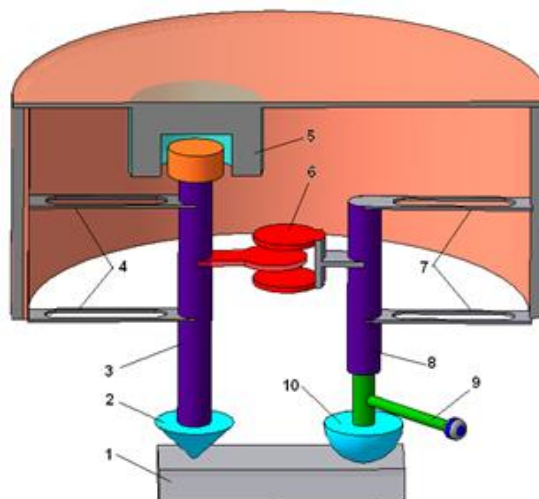


Figure 2.16 – Load head model in section

The electronic unit

It is a box with an electronic board located inside. The board contains the AT8958253 microprocessor, table motor control drivers, interface port driver, ADC and DAC with current amplifier. On the back of the electronic unit there is a power connector, a fuse holder, a docking port connector with an IBM-compatible computer, and a loader

connector. The program, recorded in the microprocessor, controls the periphery, which allows the release of computer resources, and prepares data for transmission. ADC 24-bit sigma delta. DAC 16-bit.

2.4.1 Software description

It is impossible to give a complete description of the program, because of the large occupied volume, and besides, they are made in the same familiar Windows style. Therefore, I will give only a brief description and principle of action.

After launching the “Micron-gamma.exe” program, a dialog box in the form of an interface is displayed on the screen (figure 2.18).

The interface consists of toolbar 1 (in the upper part of the screen), graphic field 2 (in the center), indenter position indicator 3 in the selected range (slider on the background of a multi-colored bar), loading status indicator 4 (vertical yellow bar), 16 buttons graph selection 5, comment line 6, status line 7 (at the bottom of the screen) and service information field 8.

The toolbar includes the following set of buttons:



- Injection: start-up of the process of continuous indentation for registration of loading diagrams in the coordinates “load-depth of penetration”.



- Scanning: start of the scanning process for registration of profilograms and tribograms (depending on the selected conditions) in the coordinates “Depth Depth — Scan Length”.



- Friction: start of the scanning process to register the friction force in the coordinates “friction force-load”.



- 500 gram range: button for selecting the “larger” load range.



- The range of 150 grams: the button select the "smaller" range of load.



- 300 micron range: low sensitivity button for low displacement sensor.



- Range 20 μm : high sensitivity button for low displacement sensor.



- 1/8 Range: button to enable the multiplier 1/4 of the selected sensitivity range of the small displacement sensor.

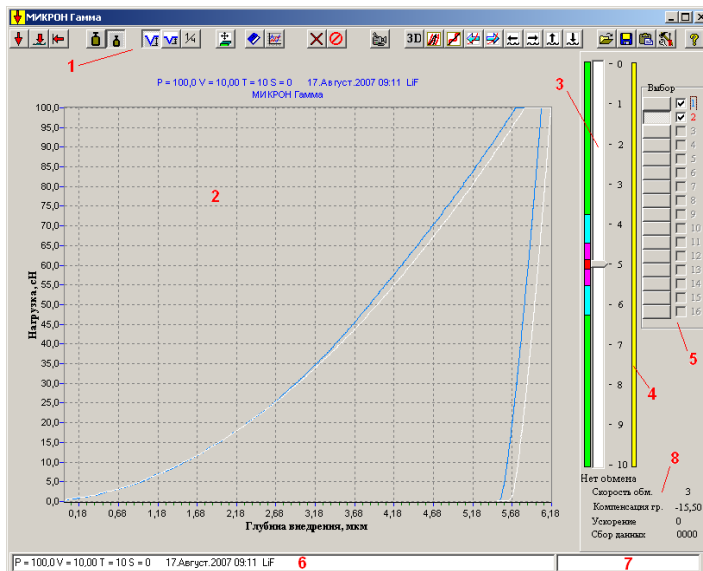

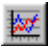




Figure 2.17 – The appearance of the Micron-Gamma software interface

 - Table management: a button for calling the control window and editing the position of a two-coordinate table.


 - calculation table: displaying the calculation table.

 - graphs: display of exposure graphs on the screen (in the coordinates “embedding depth - exposure time”), hardness (in the coordinates “hardness unrestored — load”), h2-P dependences (in the coordinates “load – depth in square”), hardening (in the coordinates "the number of repeated injections - the depth of introduction after each repetition").


 - Clear: button to clear the graph field.


 - Store: emergency stop button of the entire system.

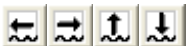
 - Camera: call the video surveillance window.

 - Three-dimensional graph: output window of three-dimensional graphics.

 - Averaging: averaging the two selected charts.

 - Approximation: displays the window for approximation of the selected plot of the diagram by the method of least squares.

 - Shift of the curve: the shift buttons of the theoretical curve relative to the selected loading diagram (fitting the diagram to the theoretical curve).

 - Shift of the graph: buttons for editing the position of the selected profilogram (tribogram) relative to each other.



- Read file: display the saved file.



- Save file: save the experiment results in the format * .mkm (own) or * .txt (for subsequent processing in other applications).







- Paste from clipboard: display graphics from clipboard.



- Settings: display the settings window (by password).

The graphical field is designed to display the results of the experiment in the form of diagrams (graphs of the dependence “load - depth of penetration”), profilograms and tribograms (graphs of the dependence “depth of insertion - length of the scan path” and “friction force - load”) with automatic scaling to the whole field, moreover, as the results of the current experiment, and saved for the purpose of subsequent comparison and editing. Simultaneously displayed graphs can be 16 with different colors. It is possible to select a part of the chart by highlighting it, while pressing the left mouse button down - from above, and by reverse movement - to restore it. You can move the graph while pressing the right mouse button.

The position of indicator, (indicator) in the form of a slider on a white background with a scale (0–10) and a vertical multi-colored column, is intended for visual observation of the position of the indenter relative to the probe. The indicator functions during the whole time the program is running, i.e. the slider all the time tracks the position of the indenter relative to the probe. The coarsest range is colored green and is about 200 μm (depending on the sample of the device, the values may differ), and each following sensitivity varies by blue ($\approx 50 \mu\text{m}$), pink ($\approx 20 \mu\text{m}$) and red ($\approx 5 \mu\text{m}$, respectively). Moreover, each color has its own range of sensitivity of the small displacement sensor switchable by means of buttons  (figure 2.18). Buttons  and  are made with dependent fixation, and  is a multiplier and acts together. The indicator also allows you to monitor the implementation process of the indenter.

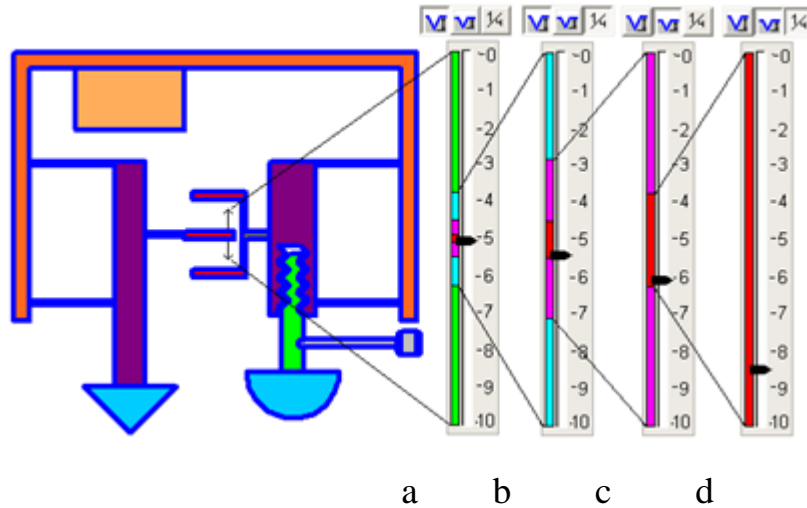





Figure 2.18 – Indicator indications (position of the indenter relative to the probe) depending on the included sensitivity mode: a \approx 200 μ m; b \approx 50 microns; c \approx 20 microns; d \approx 5 microns

Management of a two-coordinate subject table

When you call  - “Table management”, the “Table position” control window appears (figure 2.19), which is used to adjust the table position, autonomous table control, and offset by a specified distance. In the window, you can start the engines of the corresponding X and Y coordinates with buttons in the form of arrows ( )

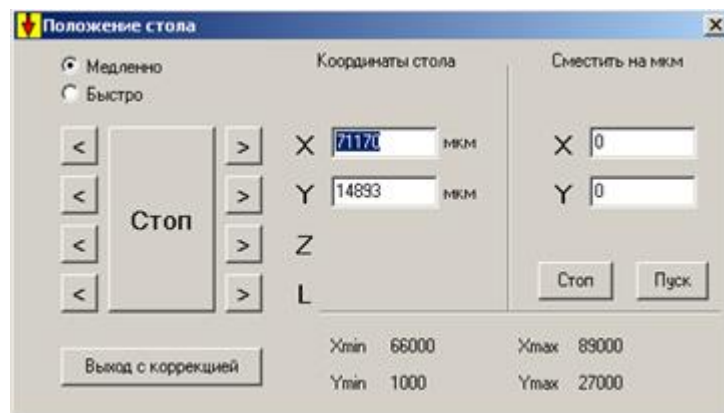


Figure 2.19 – Table management window


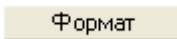
To move the table to the specified value, you must type the corresponding number in microns (with a “-” sign in the opposite direction) in the field under the word “Move to μm ” and press the “Start” button (Пуск). By pressing “Stop” (Стоп) - the process can be interrupted at any time. The speeds are selected by the corresponding switching “Slow” and “Fast” (the speed values can be found in the settings of clause 7.3.). For all table movements, the current coordinate values are automatically taken into account (calculated). The calculation algorithm is simple, knowing the speed of movement, the time of movement in that or the opposite direction is recorded. However, in case of system failures and errors, it is necessary to check and correct the table coordinates from time to time, comparing with the true values on the micrometric rulers located on the table. For this, the true values read from the table rulers in μm (in μm , not mm) are entered into the appropriate fields under the word “Table coordinates”. To save the changed values, you must click the “Exit with correction” button (Выход с коррекцией), otherwise close the window by clicking on the cross in the upper right corner of the “Table position” window.

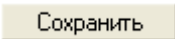
The inscriptions Xmin 66000 and Xmax 89000 (Ymin 1000 and Ymax 27000) indicate the extreme values of the coordinates in microns beyond which the table should not go. These values are individual for a particular instrument sample. In case of going beyond the limits of scanning, a corresponding message will be displayed, and the movement of the table will stop. To get out of this state, it is necessary to push the arrow in the opposite direction (maybe several times) to bring the table out of its extreme position and return to the origin.


To avoid confusion, the coordinates (rulers) are specially divided into ranges, X – 60/85 mm, Y – 0/25 mm, which must also be taken into account when adjusting the position of the table.

Video registration system


To apply an aiming prick and photograph a print, you must click “Video”, and a “Video Sight” window will appear with a print image, the quality of which depends on the camera settings (brightness, contrast, resolution, etc.), backlight brightness, position iris diaphragm, focusing and reflectivity of the surface.

Access to the camera settings is carried out using the  and  buttons.


To save microphotographs, click the button  (remove the tag beforehand) and specify the path and format.

The window  is used to display or delete a target mark from the video image (dotted circle). The aiming mark is used to see the location of the injection when the specimen is displaced, and to put it by pressing the left mouse button at the point where the indenter hits.

Using the F1, F2 and F3, F4 keys including the table motors according to the coordinates X and Y, respectively, you can move the sample under the microscope objective. When performing other operations (“prick”, scanning, etc.), the “Video Sight” window should be minimized, otherwise the exchange rate of the computer with the electronic unit may fall.

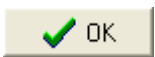
During video surveillance, you can also move the table with a mouse from the “Table position” window called by the  “Table management” button (see Section 3.6, Figure 16).

Preparation of loading conditions with continuous implementation

To prepare the loading conditions it is necessary to press the Prick -  button. In the “Conditions” window that appears, you can select the load, the loading rate, the exposure time under load and shift the sample by a specified microns value.

By default, the loading rate is automatically set to 10 times less than the selected load.

To avoid overheating, the exposure time for large loads is not desirable to set more than 10 seconds.

At the touch of a  button, a loading process takes place, followed by unloading with the selected parameters and registration of the loading diagram from the point of tangency of the surface, i.e. the point of tangency of the surface by the indenter will be assigned 0, the origin.

If there is a tick in front of the inscription "Loading/10", respectively, the selected load value is divided by 10, for example, 10 grams. will correspond to 1 gram. This is done for convenience when working with loads less than 1 gram.

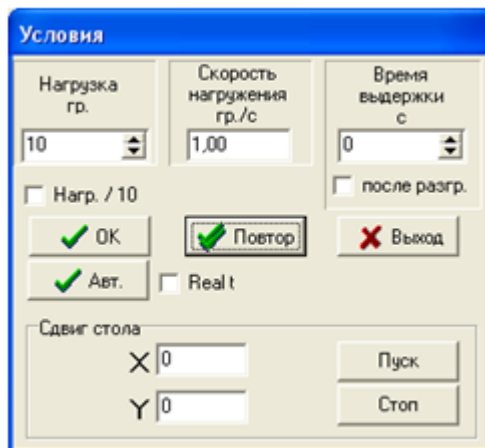
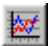





Figure 2.21 – Window loading conditions selection

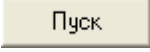

If there is a tick in front of the inscription “after unloading”, then the exposure time will be equally distributed before loading and after removal of the load. For example, with a dwell time of 20 seconds, 10 of them will stand on the surface of the indenter, then the loading-unloading process will proceed at the selected speed, and after removing the load, the indenter will be sustained for 10 seconds on the surface of the well with a minimum load (0.1 g) to register the recovery process. The relaxation recovery graph can be observed instead of the exposure graph (press the  button).

If there is a tick opposite “Real t”, the loading diagram will be displayed on the screen in real time, however, the screen redraws a lot of processor resources, especially when redrawing several diagrams on the screen, which in turn leads to a decrease in the exchange rate with the device . To increase the speed in this mode, it is desirable to extinguish all the present graphs (diagrams) on the screen or leave one.

At the touch of a  button, it is reintroduced into the previous point at the origin from the same point, and not from scratch. In this case, you can change the load and other parameters.

At the touch of a  button, the device will smoothly raise the indenter to the edge of the range (by a few microns), then shift the table along the X-Y coordinates by a



set distance and smoothly lowering to the surface will begin to penetrate with the specified parameters. This, the automatic mode is faster and most convenient to use, especially with smooth surfaces, it remains only to install the indenter on the surface for the first time, and to set the step of displacement of the table (sample) to press the  button.

The  button serves to shift the table to the specified values of the corresponding coordinates, while the indenter will not rise. You can interrupt the bias process at any time by pressing a  button.

In all modes, 2000 points of each chart are recorded.

It must be remembered that in all modes only the indenter rises automatically or from the keyboard, not the probe. The probe remains always on the surface and can only be lifted mechanically by hand.

Preparation of loading conditions during scanning

To prepare the scanning conditions, you must click the Scan button -  the “Conditions” window will appear in which most of the functions coincide with the previous window. At the touch of a  button, a scan with the specified conditions will occur.

If you put a tick in front of the inscription “No table movement”, then scanning will occur without moving the table, i.e false. This mode is useful for registering external oscillations with the indenter raised.

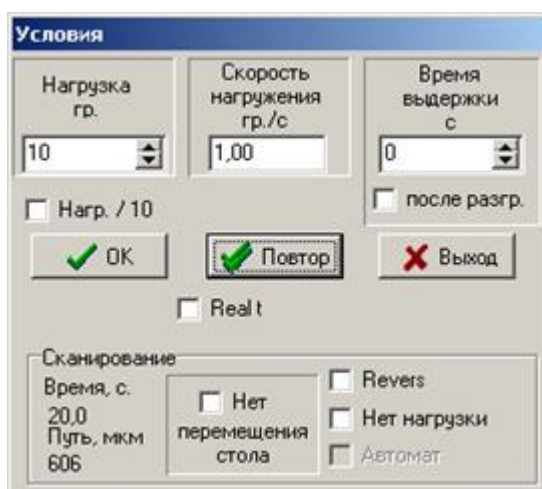


Figure 2.22 – Scanning selection window

If you put a tick in front of the inscription "No load", then the scan will occur without loading, i.e. false loading. The mode is used to register a profile with a minimum load.

If you put a tick in front of the inscription "Revers", then the scan will occur in the opposite direction with all selected conditions. Typically, this mode is used to return the table to its original position with the "No load" enabled.

If you tick the box next to the "Automat" inscription, then the minimum load on the indenter is automatically maintained during scanning to prevent hanging over deep holes on the surface when registering a profile. This mode is a rough analogue of an atomic force microscope and has not been fully developed.

The scan time is displayed under the "Scanning" label and let the scans be automatically calculated based on the load, loading speed, holding time and table moving speed. You can change the scan path by changing these parameters, and the loading rate is the last, since its value is automatically set as a load / 10.

Difficult at first glance conditions make it possible to use the scanning mode more flexibly, for example, scan with increasing and decreasing load, with exposure, without loading return to the initial position and repeat scanning without load, register external oscillations and sensor drift.

Conclusion to Part 2

Scratch testing, an important technique for the assessment of the mechanical failure behaviour and adhesion strength of different coatings and a simulation tool of single asperity contact in tribological experiments, is increasingly becoming an established nanomechanical characterization method.

Nanoindentation tester, allows simulation of many real-life failures in thin coatings. By applying loads in a controlled and closely monitored fashion, the instrument allows to identify at what load failure in the scratch occurs. This can then be as a quantitative value for comparing scratch resistance and adhesive strength between samples. A clear difference in the force required to fail is observed between the two samples. The very small standard deviations also show the reproducibility of the technique and of the instrument. This type of information can help manufactures improved the quality of their thin films and provide quality control during manufacturing.

Spherical indenters are finding increasing popularity, as this type of indenter provides a smooth transition from elastic to elastic–plastic contact. It is particularly suitable for measuring soft materials and for replicating contact damage in in-service conditions.

PART 3

EXPERIMENTAL INVESTIGATION OF COATING ADHESION STRENGTH

3.1 Experimental procedure

The scanning method is based on the continuous recording of the resistance to the movement of the indenter over the surface with a given loading. In figure 3.1 it is shown a model explaining the essence of the dynamic scanning method.



Figure 3.1 – Scheme of scratch testing of coating adhesion

An indenter, with a tangential sensor (force sensor “friction”) and a piezo acoustic emission sensor, scans the surface at a constant speed V . At the same time, the load on the indenter increases smoothly and evenly, half the way, and then gradually decreases.

At the moment of reaching the critical load of brittle fracture of the surface or spalling of the coating, there is a sharp jump in the friction force, accompanied by an increase in the amplitude of the acoustic emission signal. The critical load corresponding to the destruction of the coating characterizes the adhesive strength of the coating and the “brittleness” of the surface.

Experimental conditions: The adhesion strength of the coatings provided was measured using a Micron-Gamma instrument in the dynamic scanning mode (sclerometry). In this case, the load F_{cr} was fixed at which the coating was destroyed. The critical load (F_{cr}) of destruction is determined by the graphs of friction force, acoustic emission and micrographs of scratches. Micrographs of scratches were recorded after scanning the surface with the help of an integrated microscope instrument with a digital camera.

The scanning was performed with a diamond indenter having a cone shape with a tip radius of 10 μm (figure 3.2). Maximum load – 130 g. Loading rate – 13 g/s. Scanning path length – 455 microns. Each sample produced 3 scratches.

Scan results are presented for each scratch separately on one page in the following sequence:

- the top shows a graph of the friction force (tangential force) on the load on the indenter during scanning;
- under the graph of friction force is an oscillogram of the acoustic signal recorded during the scanning process;
- the micrograph of the scratch is shown below.

Moreover, these results are presented on the same scale, i.e. The scratch length (455 microns) is proportional to the plots. In the figures, the beginning of the scratch coincides with the moment of the start of registration of the acoustic signal and the friction force, and the end - with the moment of the end of the scanning and registration process.

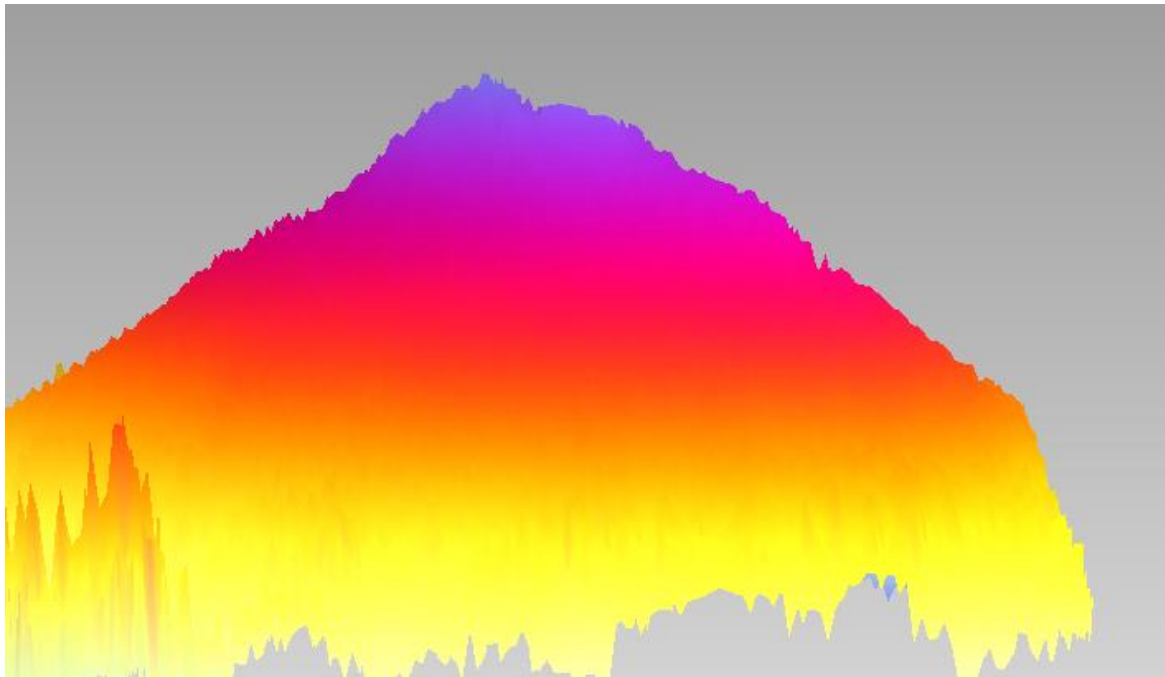


Figure 3.2 – Three-dimensional indenter topography

3.2 Results and discussion

To obtain reliable results, each sample was scanned three times. As a result of the tests, the critical load F_{cr} was determined at which the destruction of the coating occurs. Table 2 shows the values of the critical load F_{cr} for each scratch, as well as the average value of the critical load for three scratches applied to the surface of magnetron coatings n-TiC / a-C on samples of steel X12M with CrC and VC sublayers.

Analysis of the tests performed showed that sample № 6 has the highest adhesive strength. The average critical load is 97 g, which is confirmed by graphs of friction, which clearly show jumps of friction caused by brittle fracture of the coating, as well as graphs of the acoustic emission signal (figures 3.11, 3.12, 3.13). The brittle destruction of the coating is accompanied by small petals of chipped coating along the edges of the scratches. The area of chips is the smallest among this group of samples, which also confirms the best adhesion of this coating.

Sample №3 has the lowest adhesion strength. The average critical load is 48 g. As the scan continues with increasing load, the coating repeatedly peels off, as evidenced by numerous bursts of the amplitude of the acoustic signal (figures 3.5, 3.6, 3.7). Chipped petals have the largest area. The smallest adhesion strength of this coating is also

confirmed by the “ball-cut” method, after which the coating broke off (peeled off) from the substrate. This is the only sample out of all that has a peeling of the coating from the substrate after the “ball-grinding” test.

The sample №2 coating has an average critical load of 50 g. With further scanning, the coating repeatedly peels off, as evidenced by the numerous bursts of the amplitude of the acoustic emission signal. The area of the petals of the coating chips is somewhat smaller than that of sample №3 (figures 3.3, 3.4, 3.5).

The sample №5 coating has an average critical load of 81 g. Then, with an increase in load, the brittle destruction of the coating is accompanied by the shearing of the coating from the substrate, which is confirmed by bursts of amplitude of the acoustic emission signal (figures 3.8, 3.9, 3.10). The area of the petals of chips is insignificant, which confirms the relatively high adhesion strength of this coating compared to the other coatings of this group.

The coating of sample №7 has an average critical load of 78 g. The destruction of the coating is accompanied by chipping of large coating petals (figures 3.14, 3.15, 3.16). Chips have a large area, which indicates poor adhesion of this coating.

Table 3.1 – The values of the critical load at which the destruction of n-TiC / a – C coatings on X12M steel specimens with CrC and VC sublayers occurs

Number of sample	Scratch 1 F_{cr} (g)	Scratch 2 F_{cr} (g)	Scratch 3 F_{cr} (g)	Average value F_{cr} (g)
2	49	51	50	50
3	49	47	40	48
4	78	91	74	81
6	100	100	91	97
7	78	78	78	78

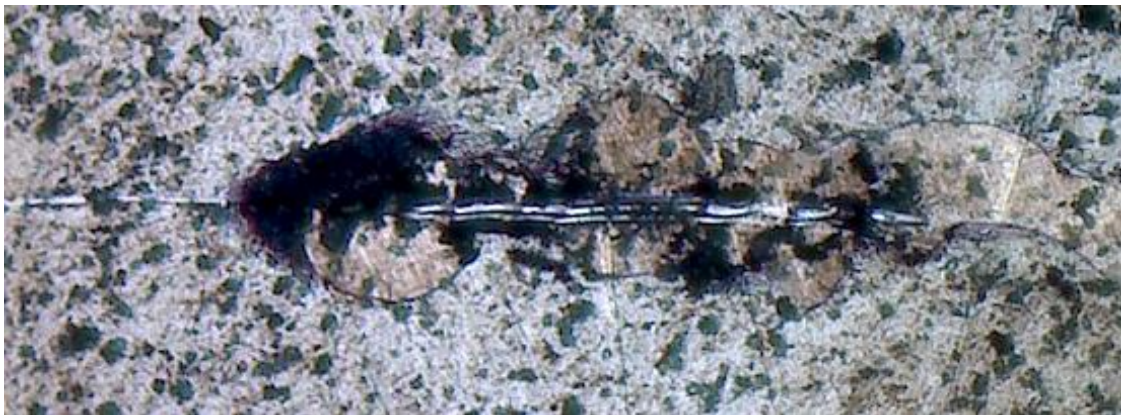
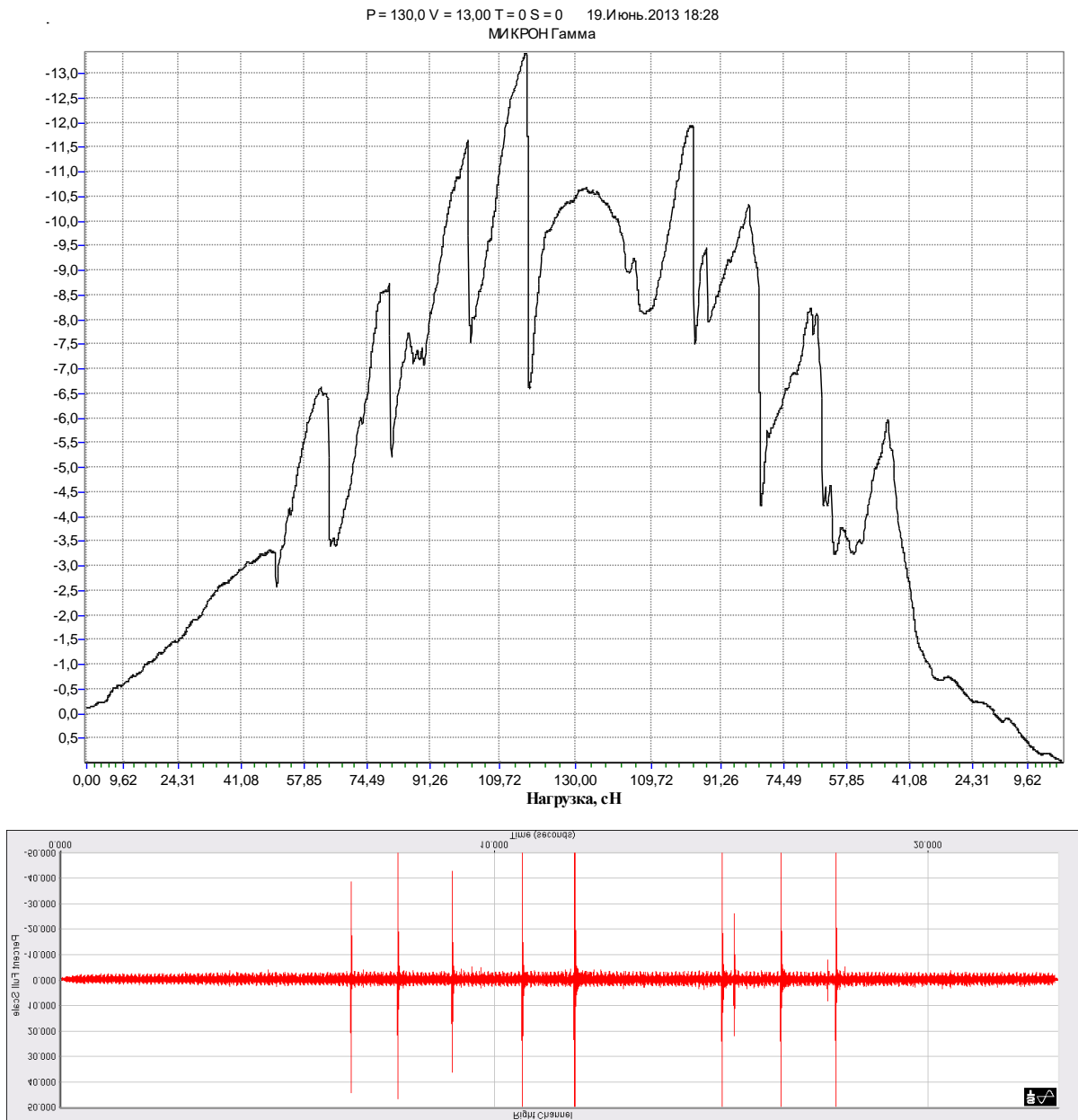


Figure 3.3 – Sample №2 (Scratch №1)

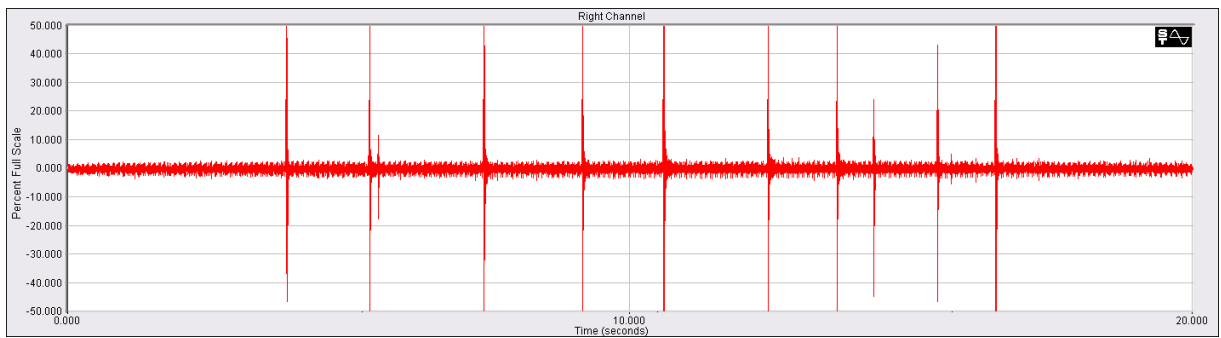
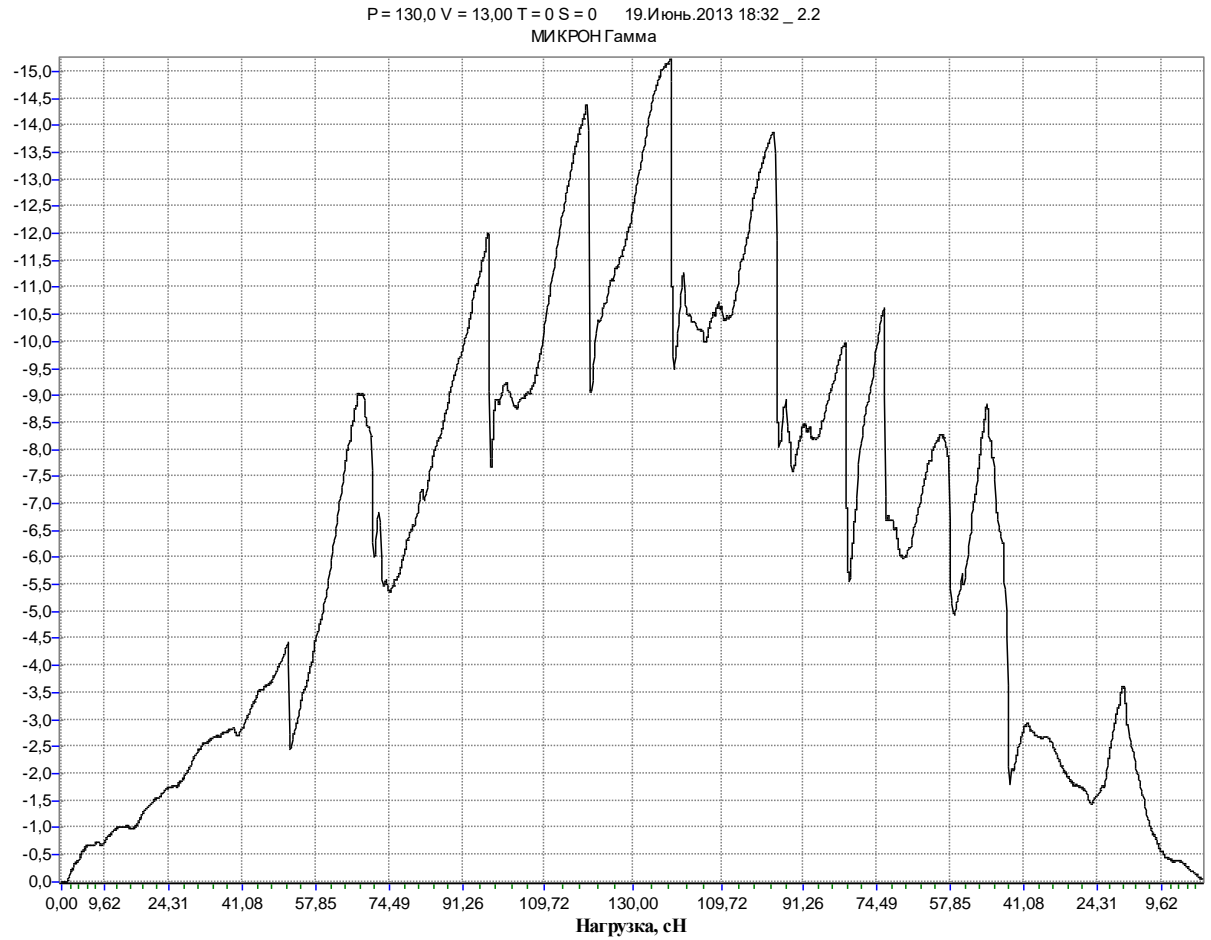


Figure 3.4 – Sample №2 (Scratch №2)

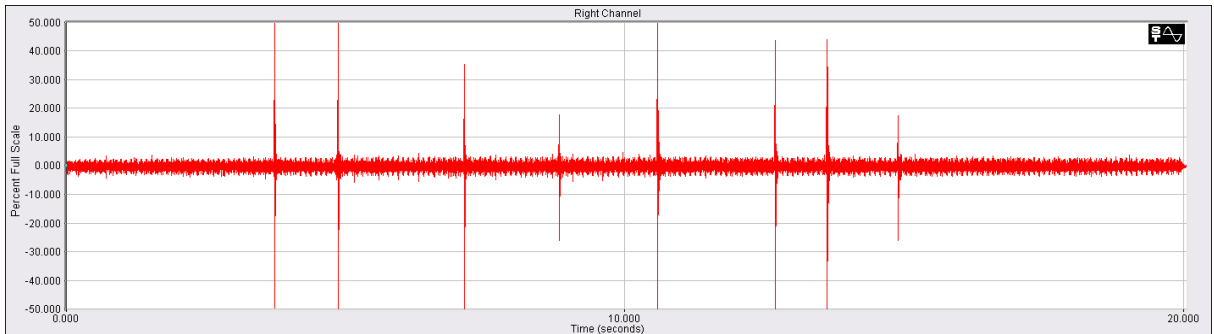
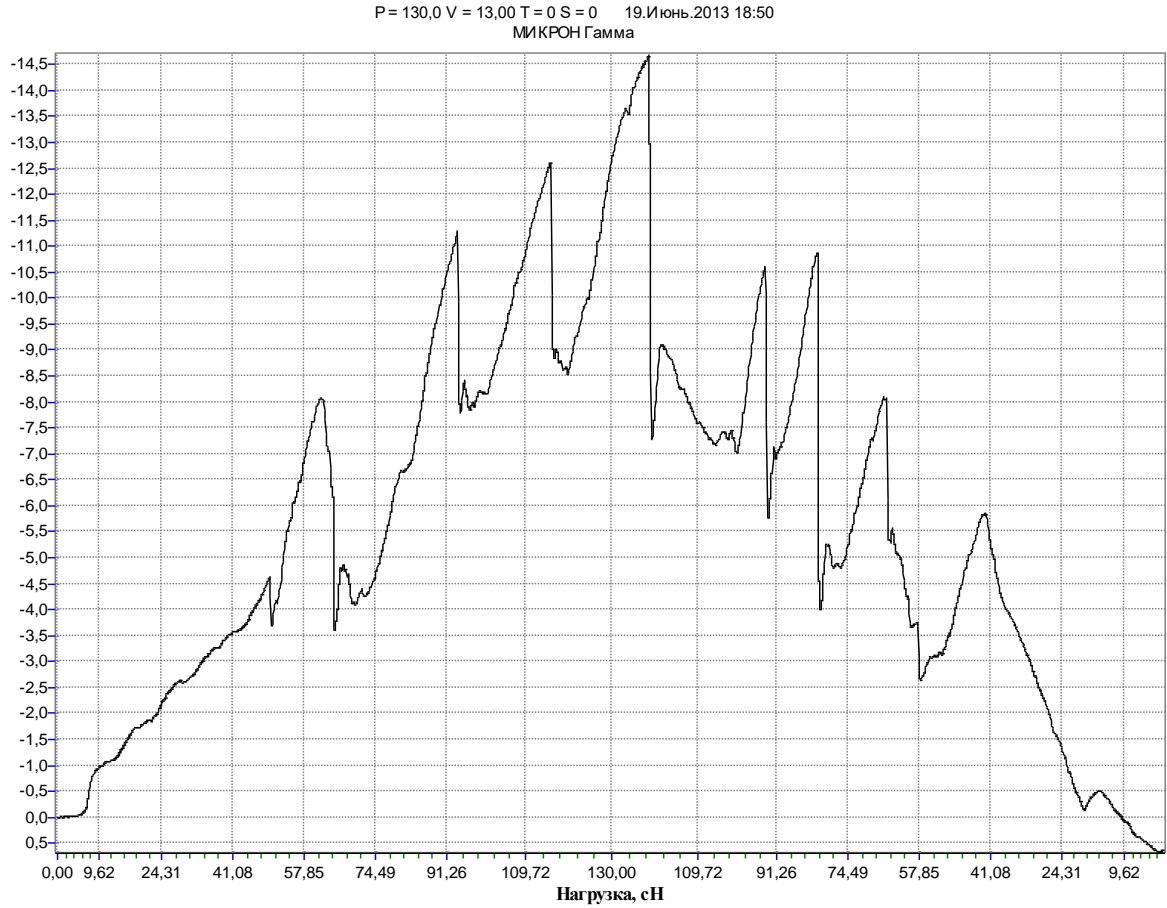


Figure 3.5 – Sample №3 (Scratch №1)

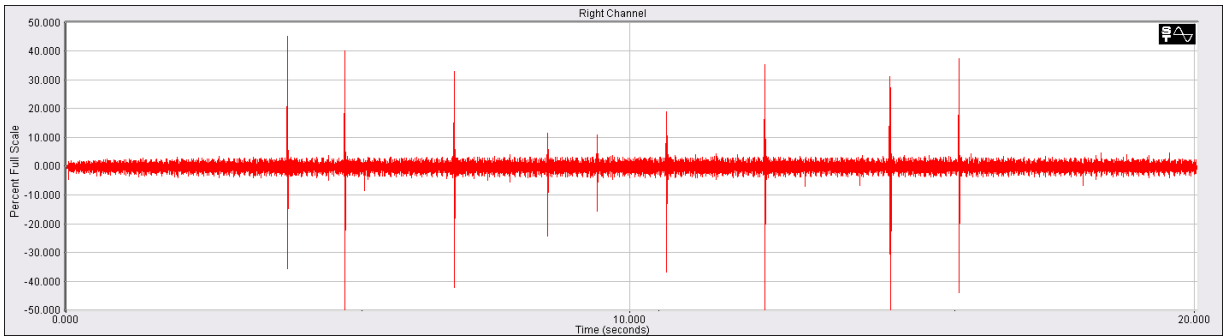
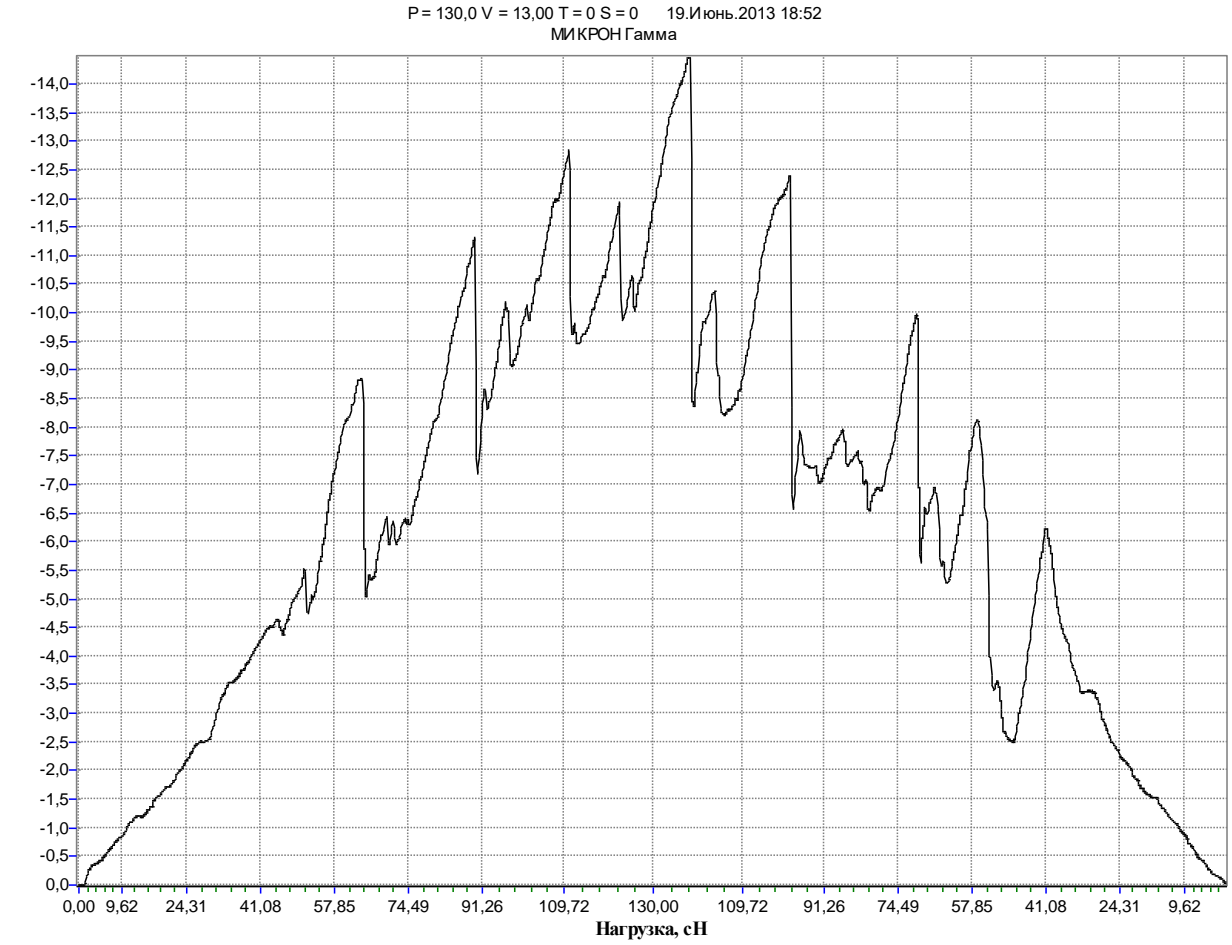


Figure 3.6 – Sample №3 (Scratch №2)

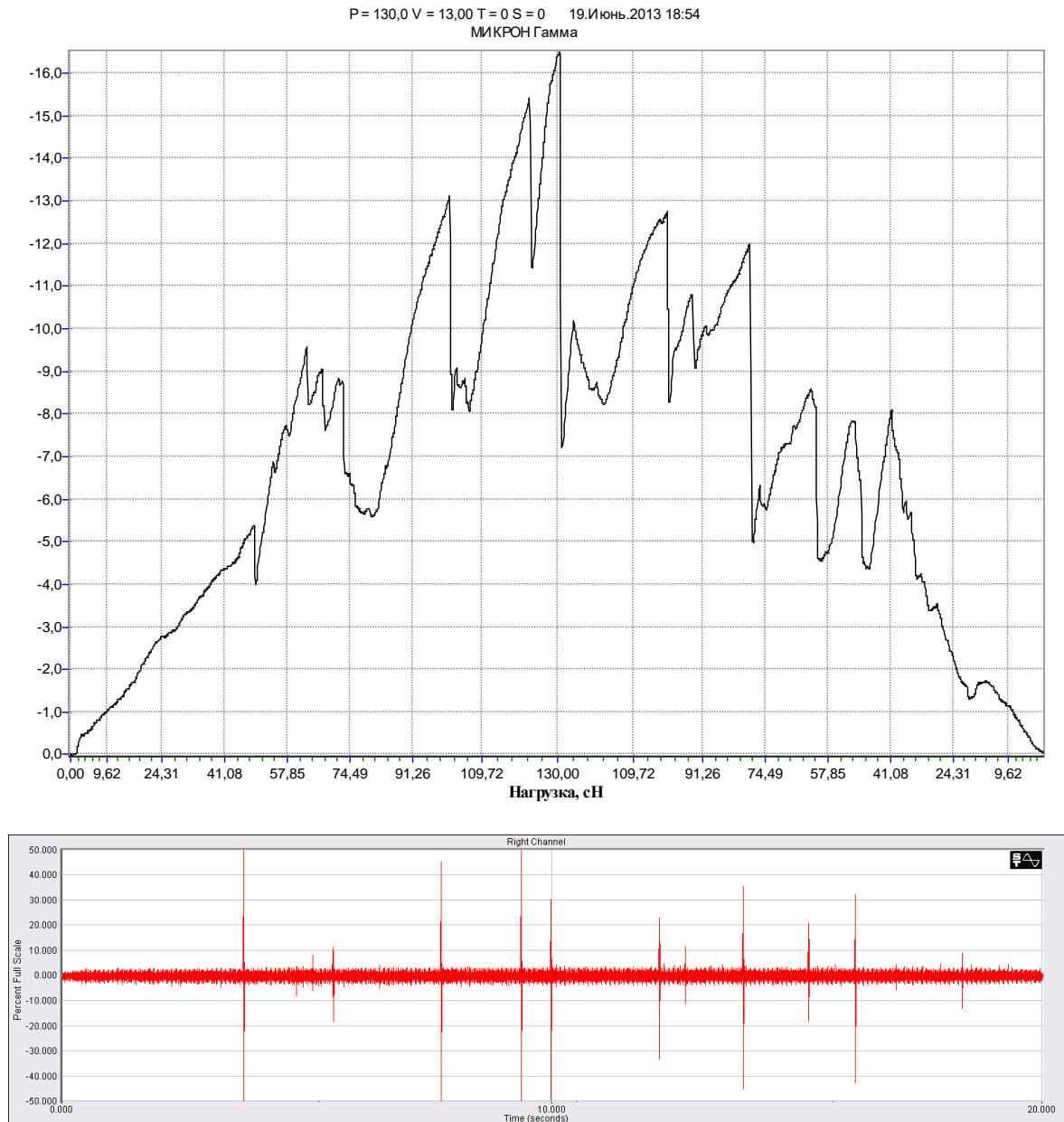


Figure 3.7 – Sample №3 (Scratch №3)

P = 130,0 V = 13,00 T = 0 S = 0 19.Июнь.2013 19:28
МИКРОН Гамма

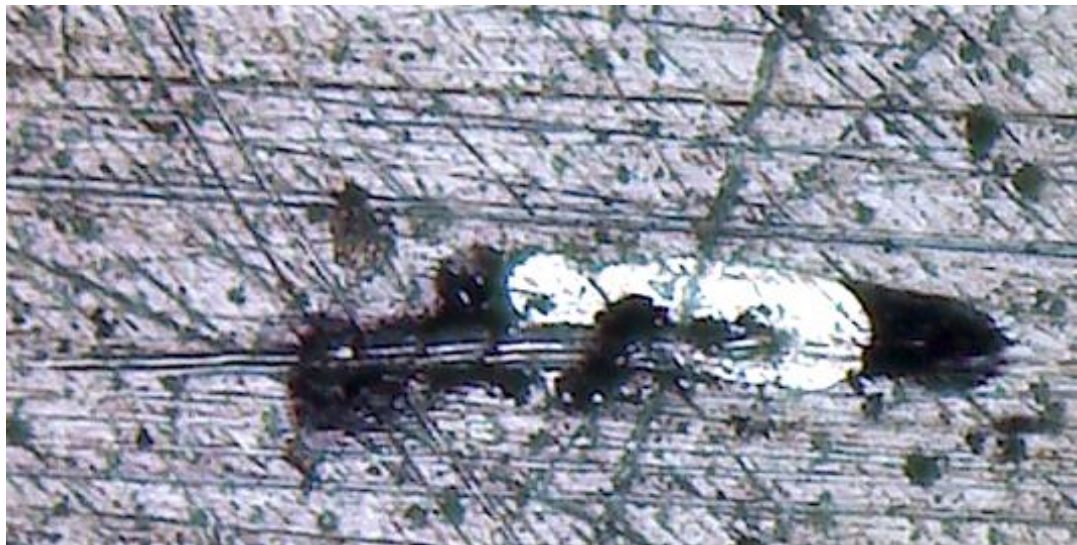
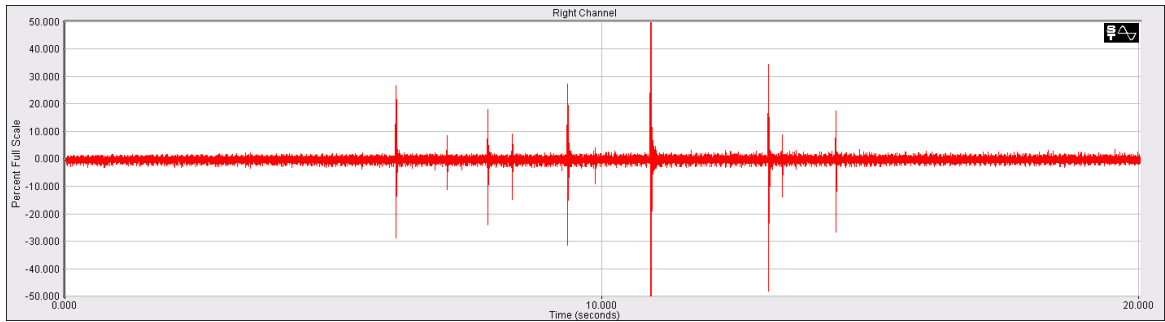
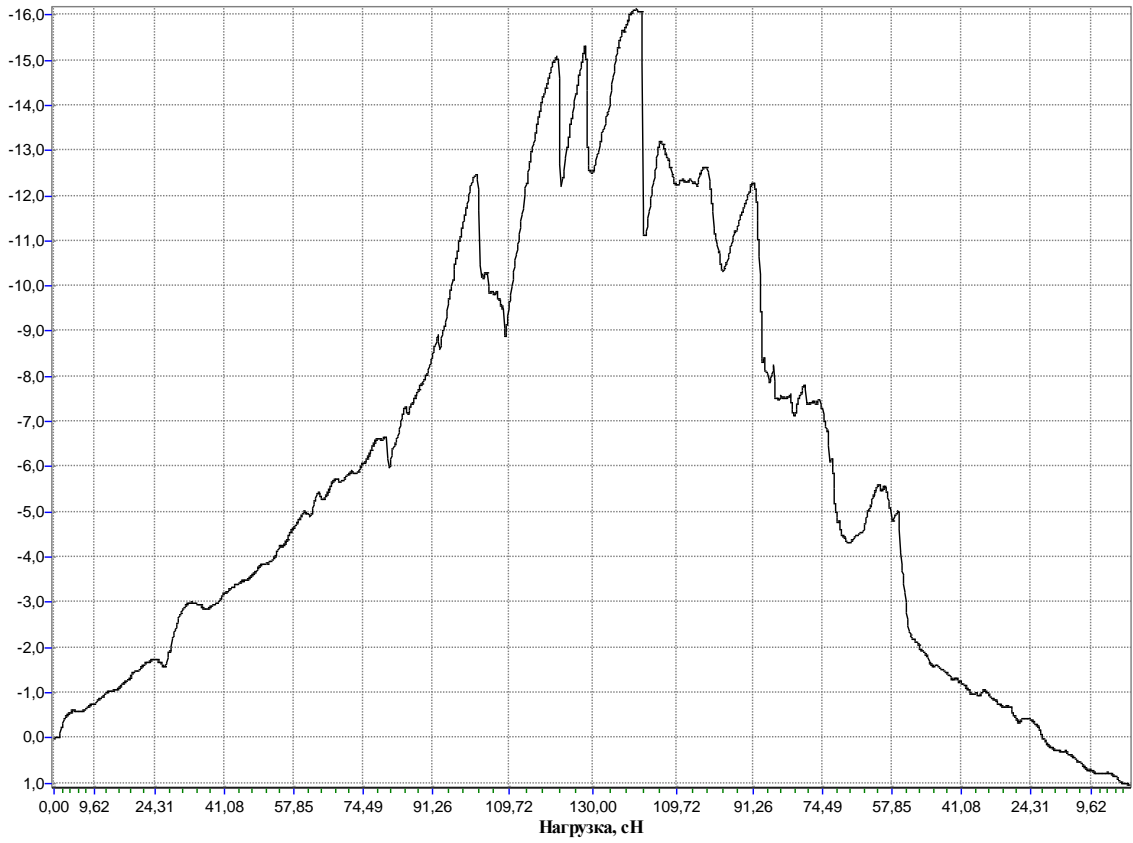


Figure 3.8 – Sample №5 (Scratch №1)

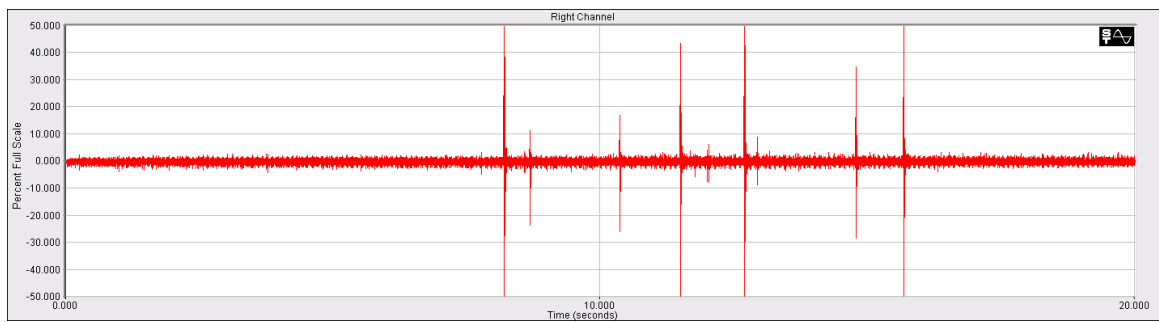
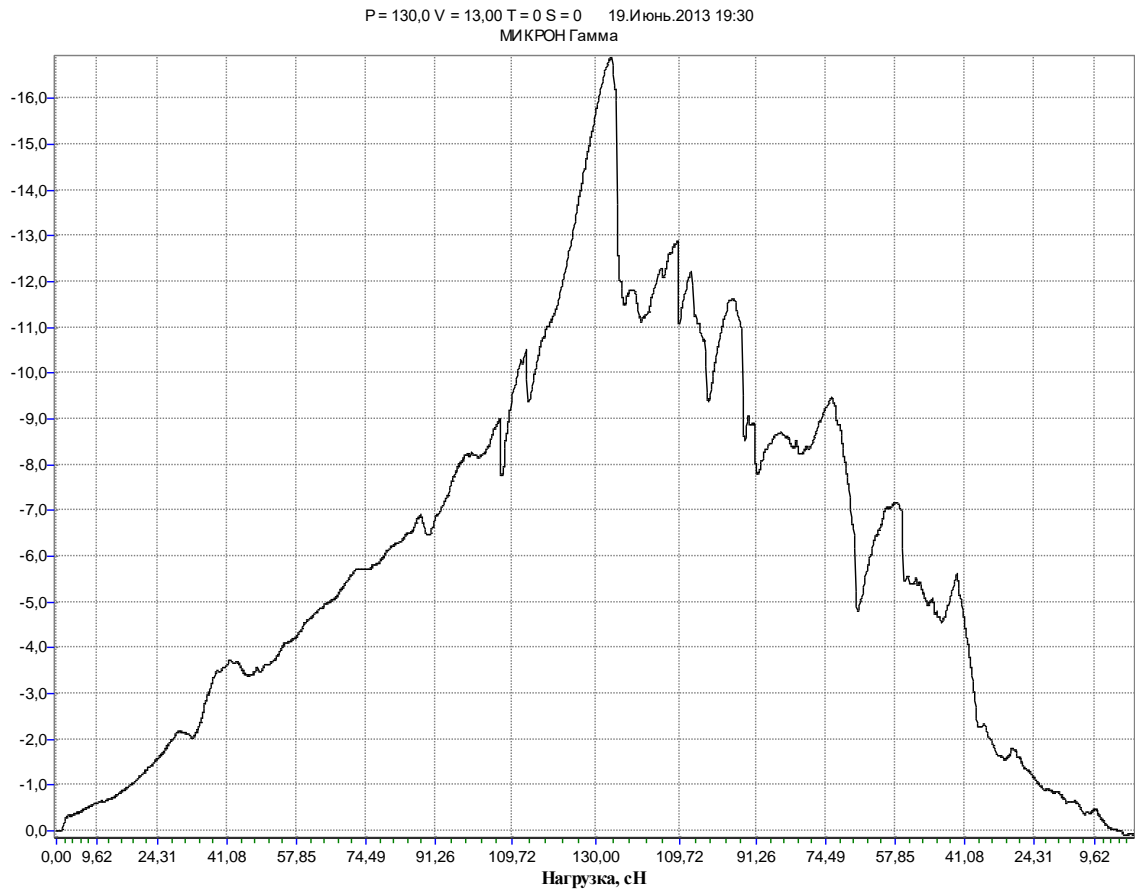


Figure 3.9 – Sample №5 (Scratch №2)

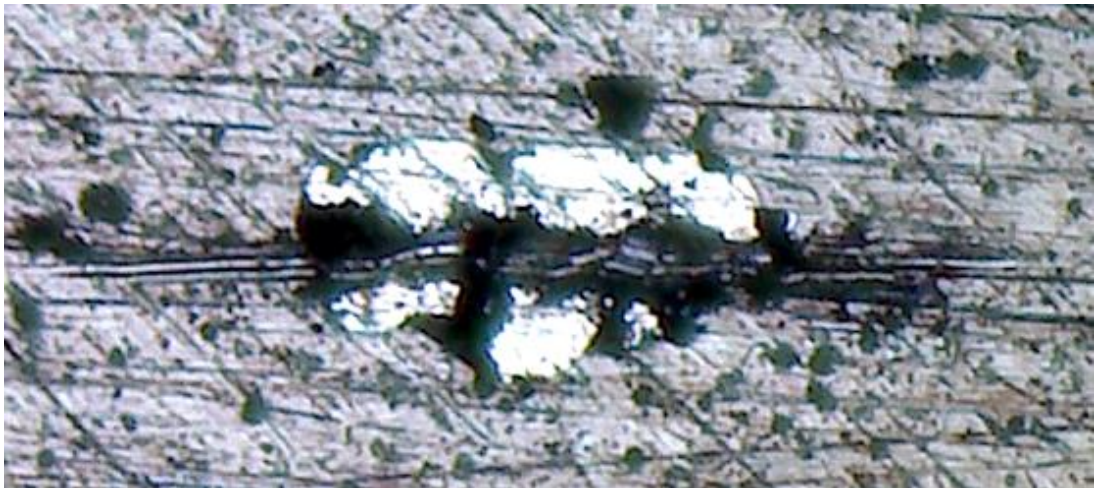
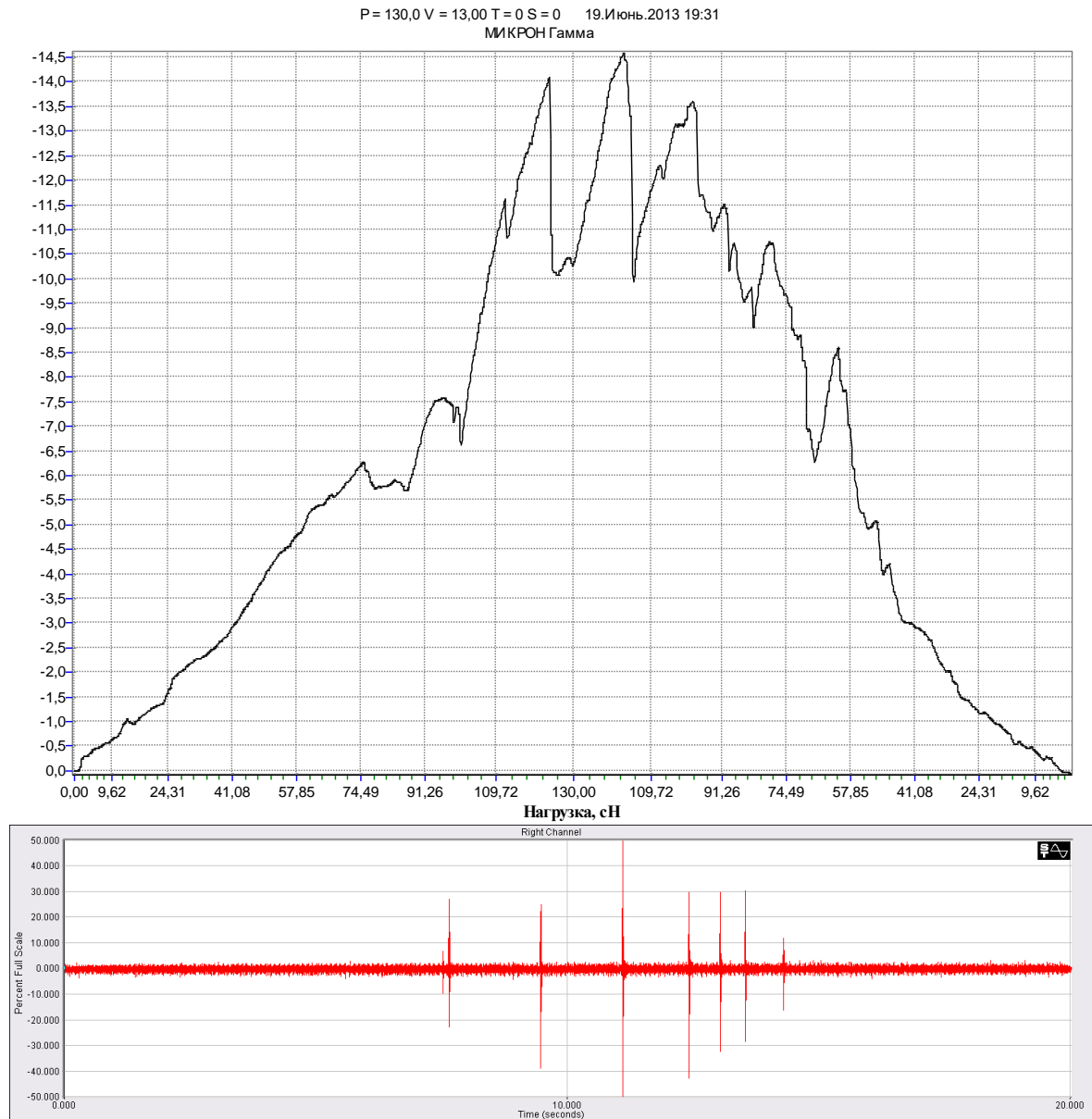


Figure 3.10 – Sample №5 (Scratch №3)

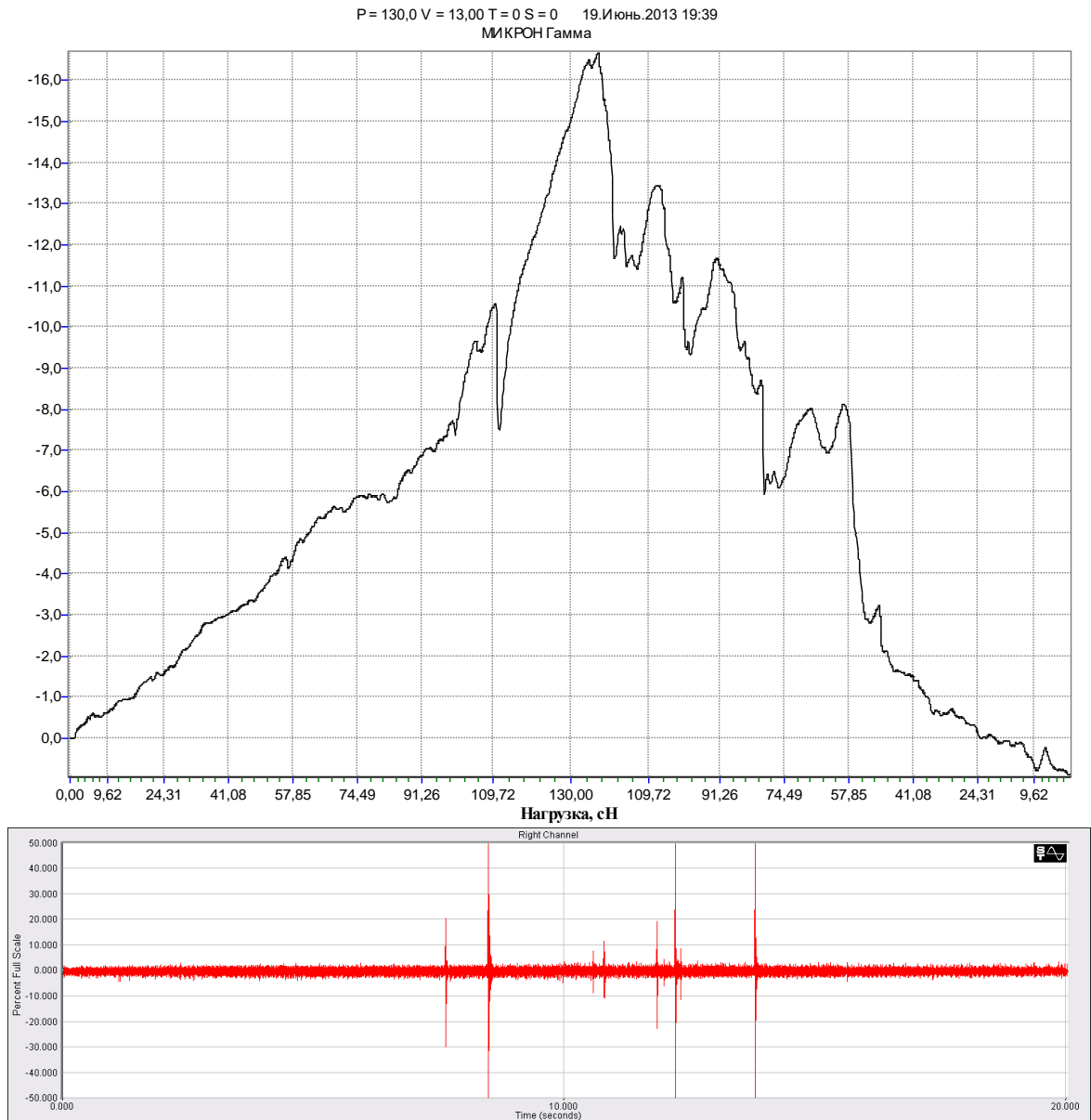


Figure 3.11 – Sample №6 (Scratch №1)

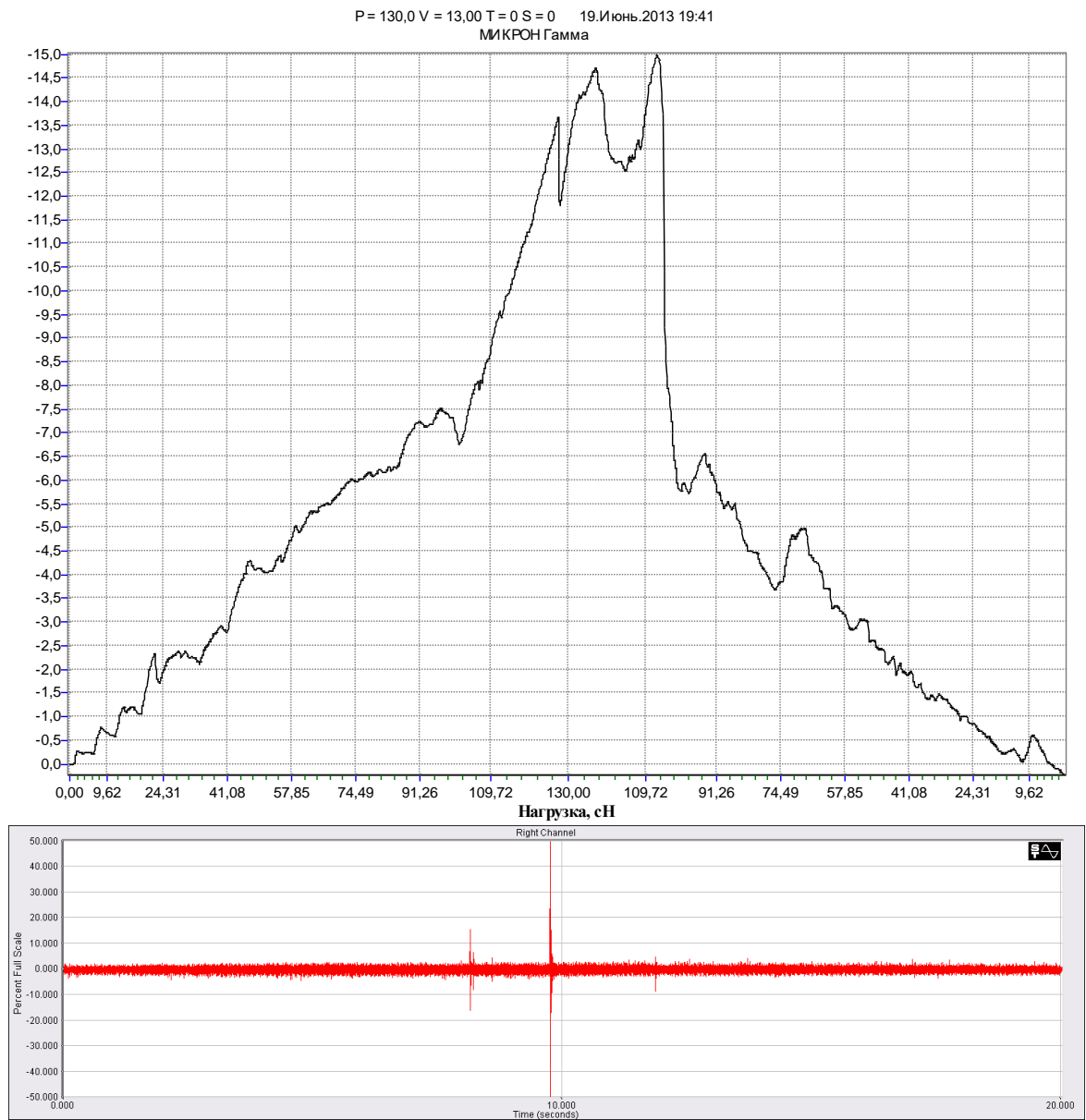


Figure 3.12 – Sample №6 (Scratch №2)

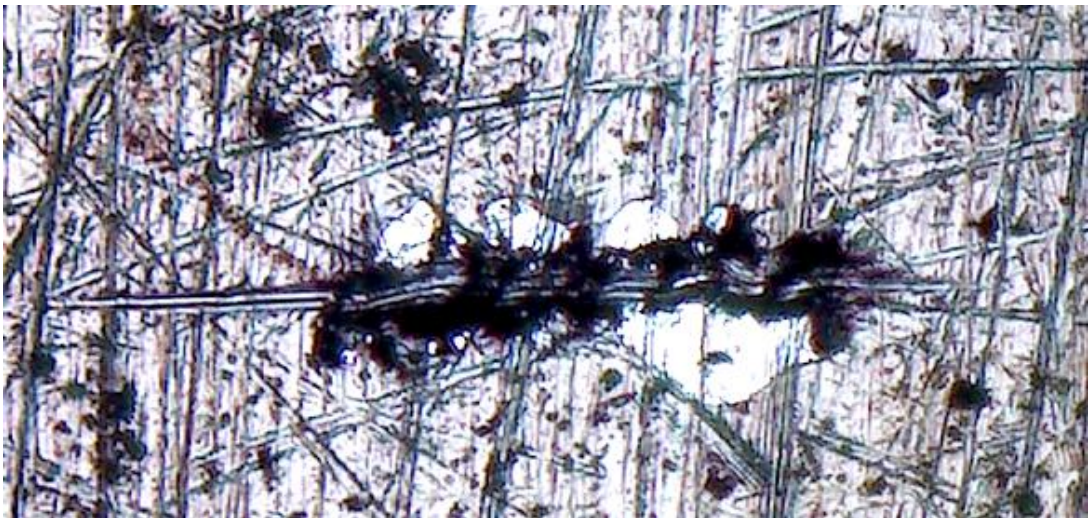
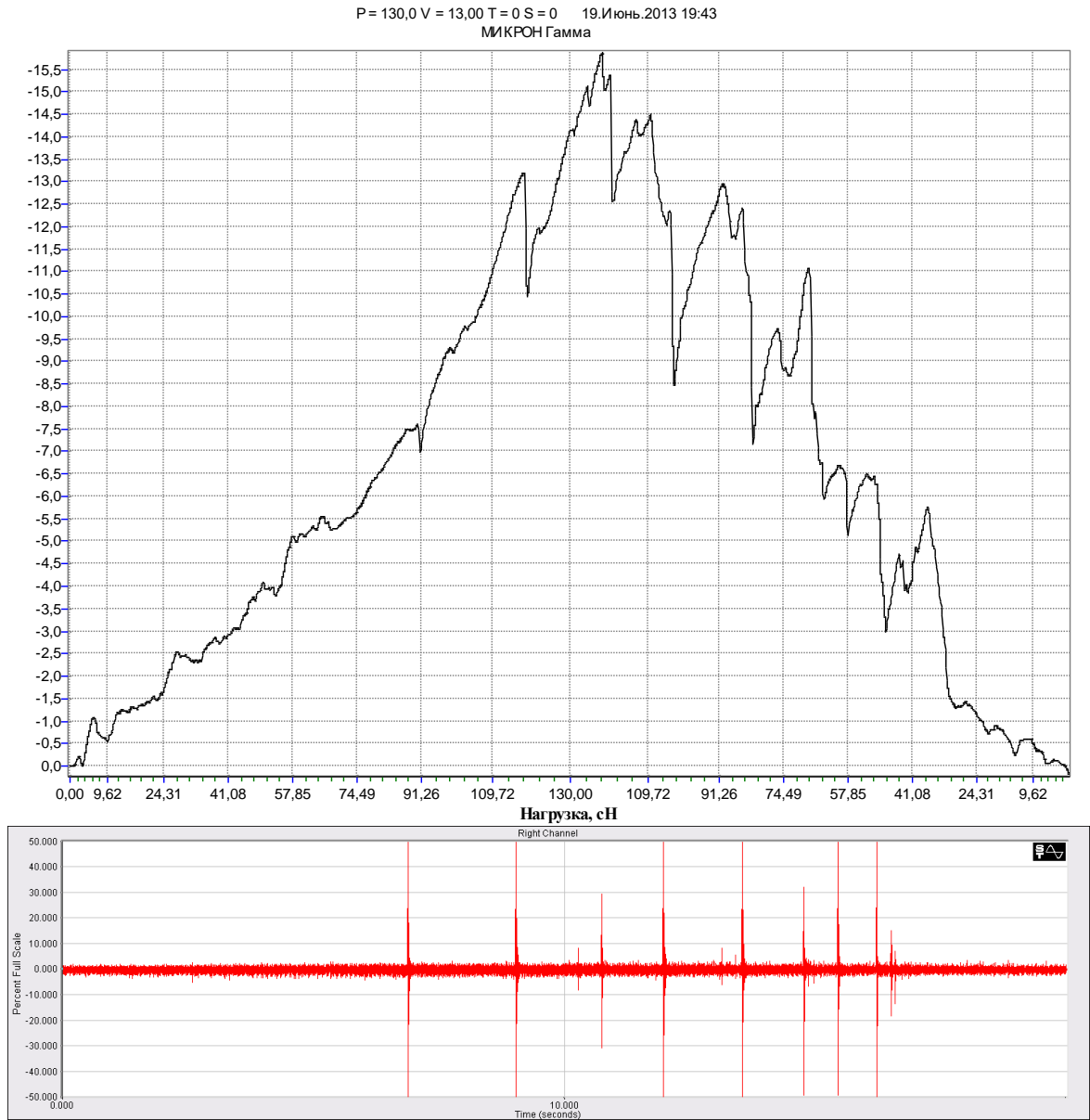


Figure 3.13 – Sample №6 (Scratch №3)

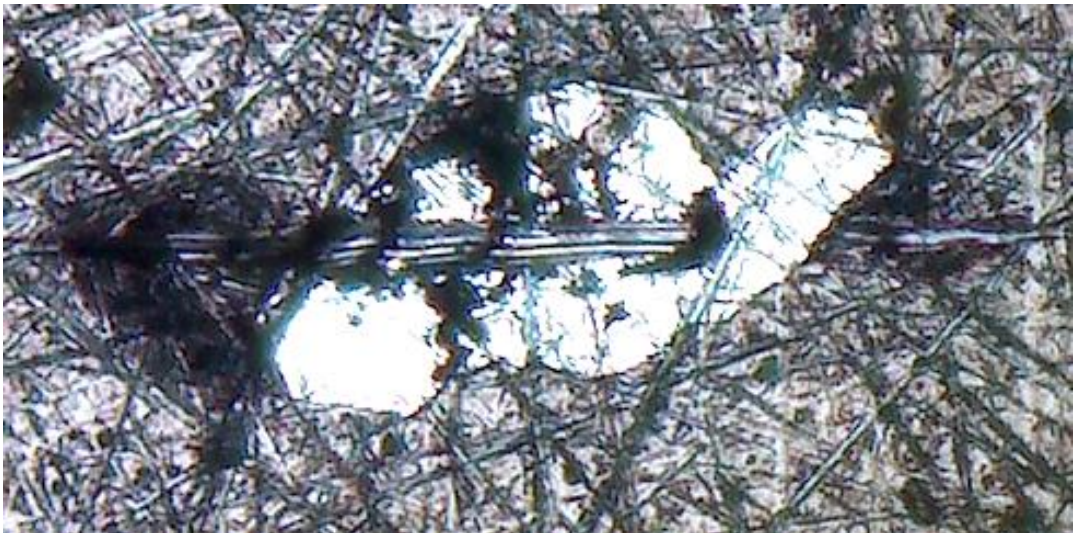
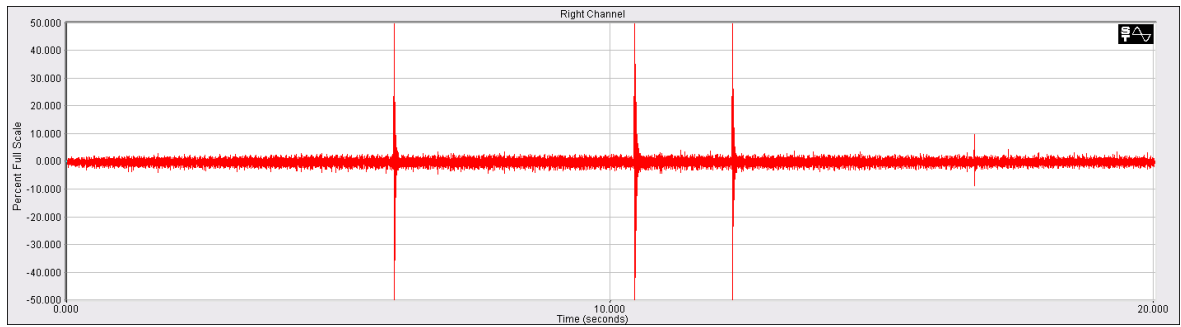
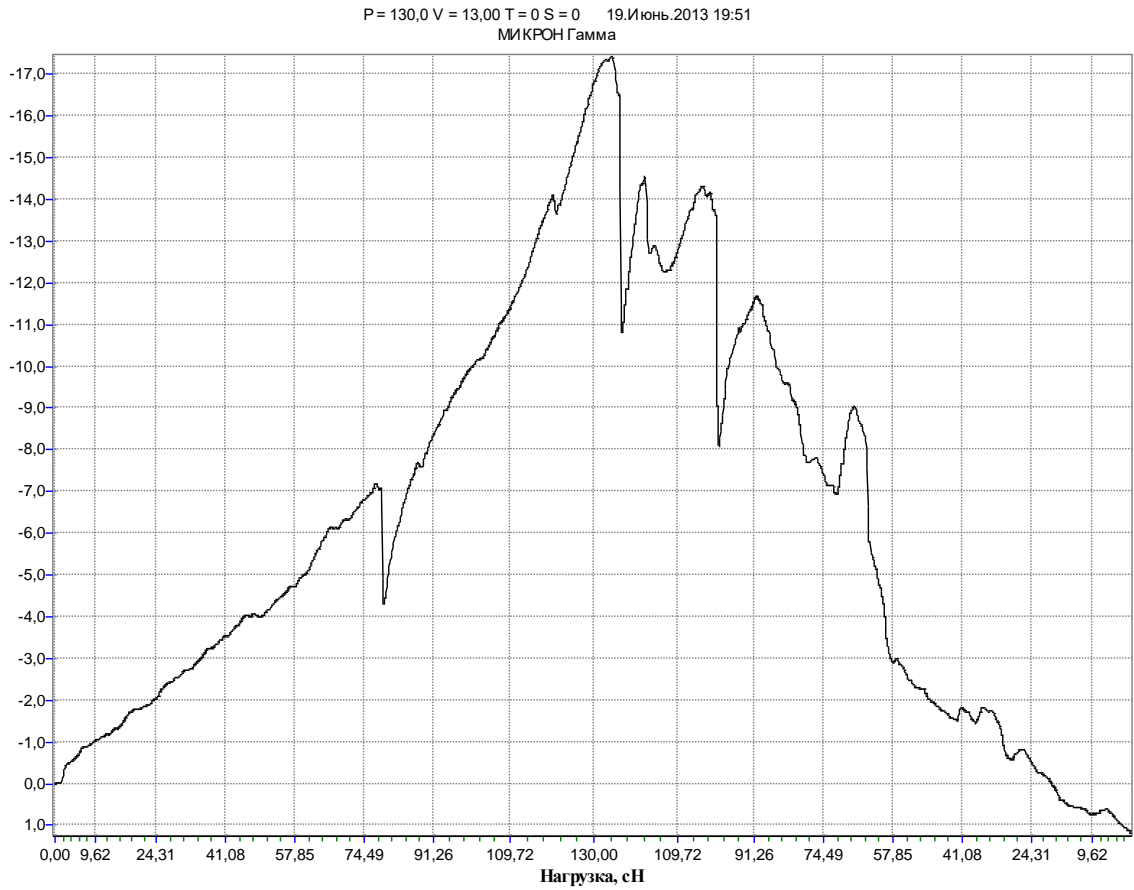


Figure 3.14 – Sample №7 (Scratch №1)

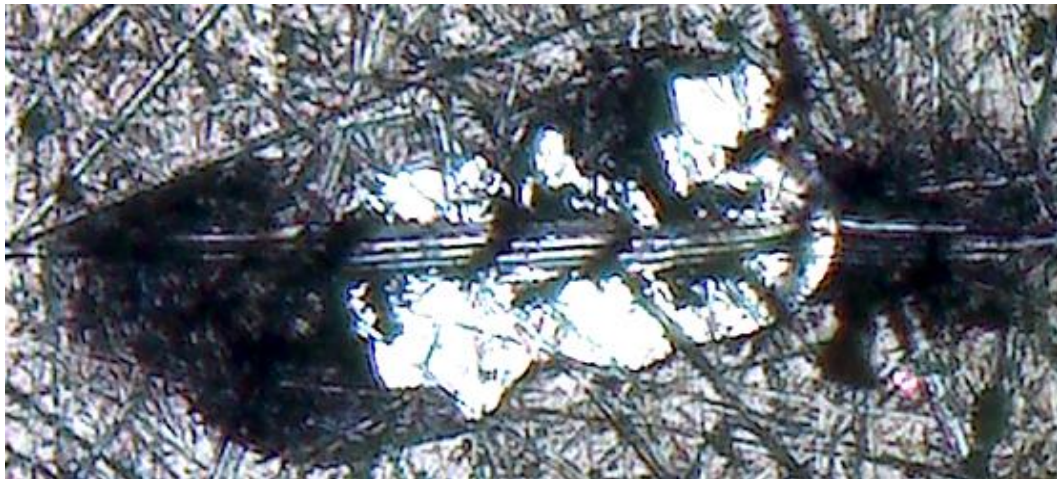
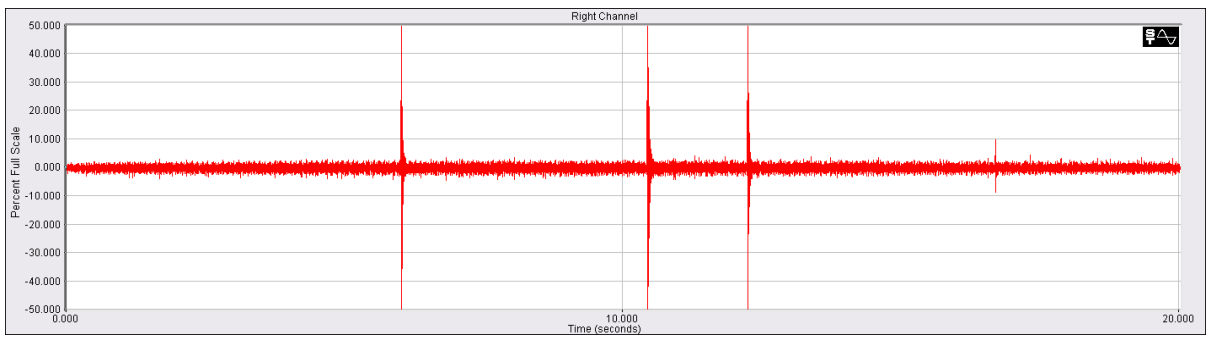
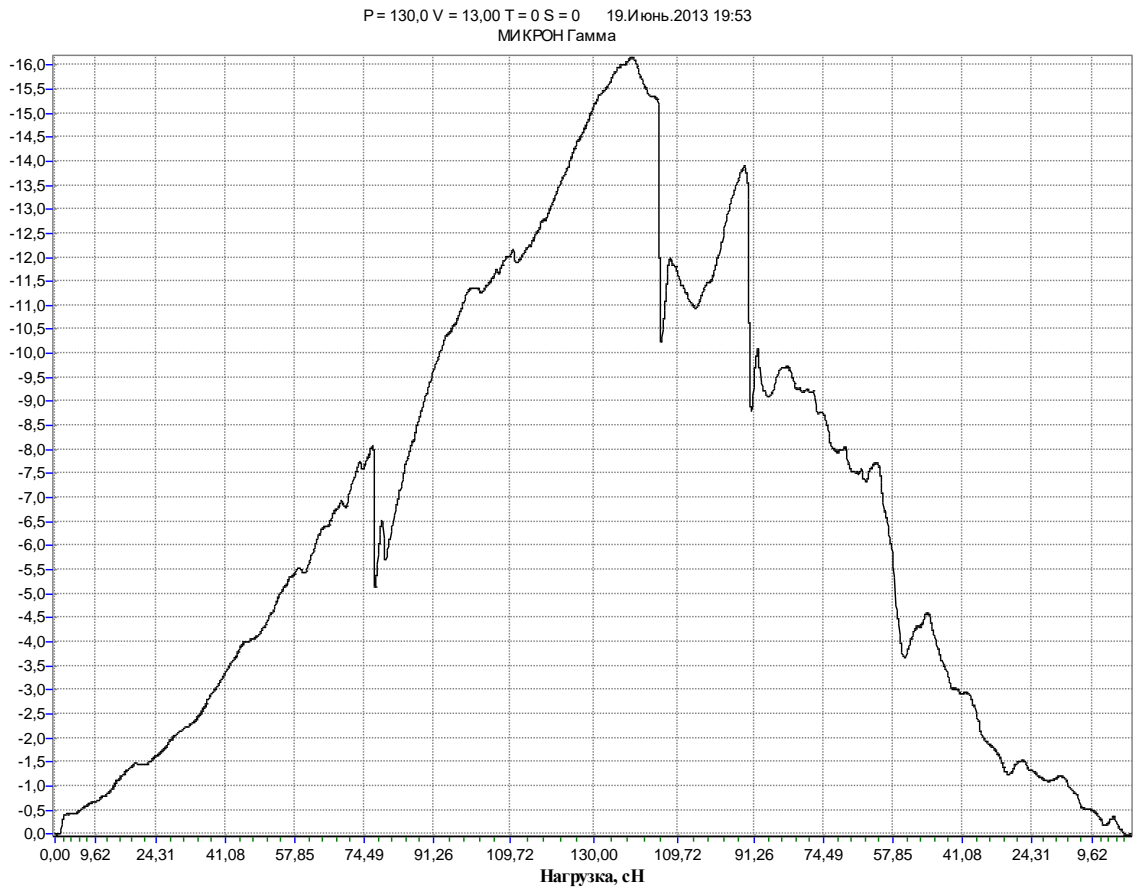


Figure 3.15 – Sample №7 (Scratch №2)

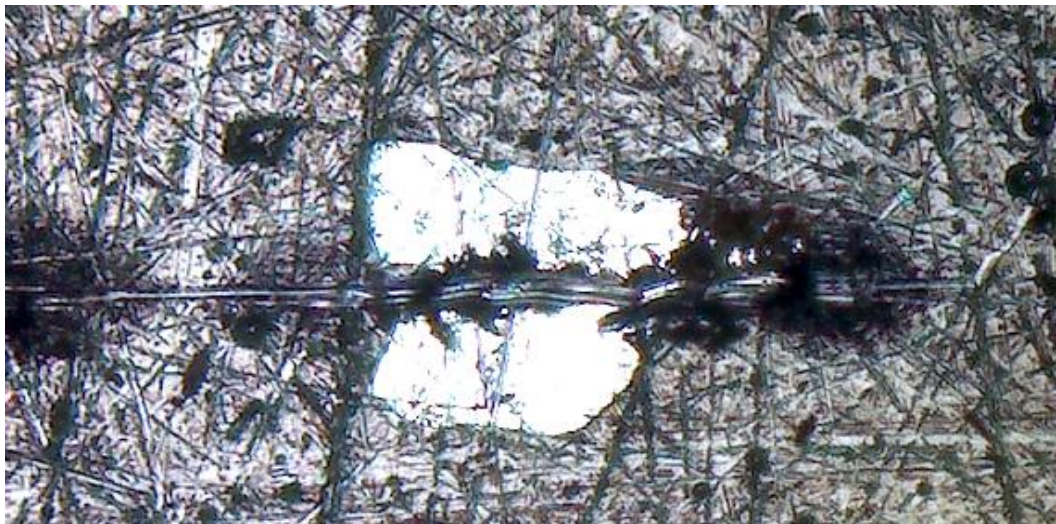
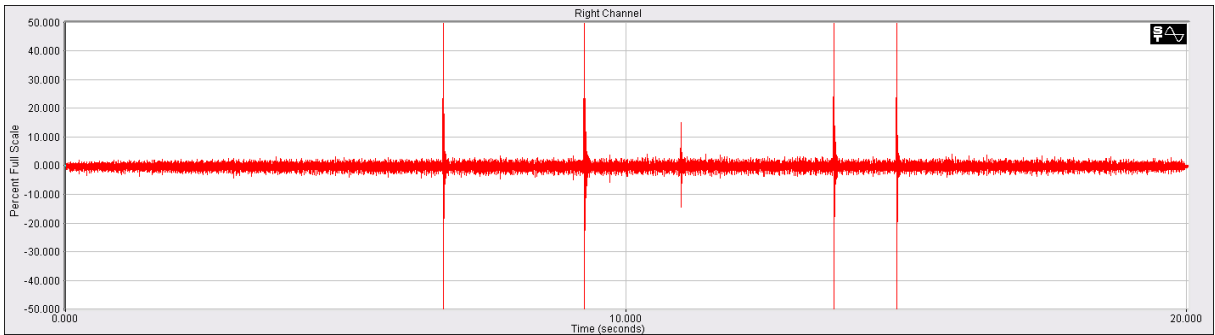
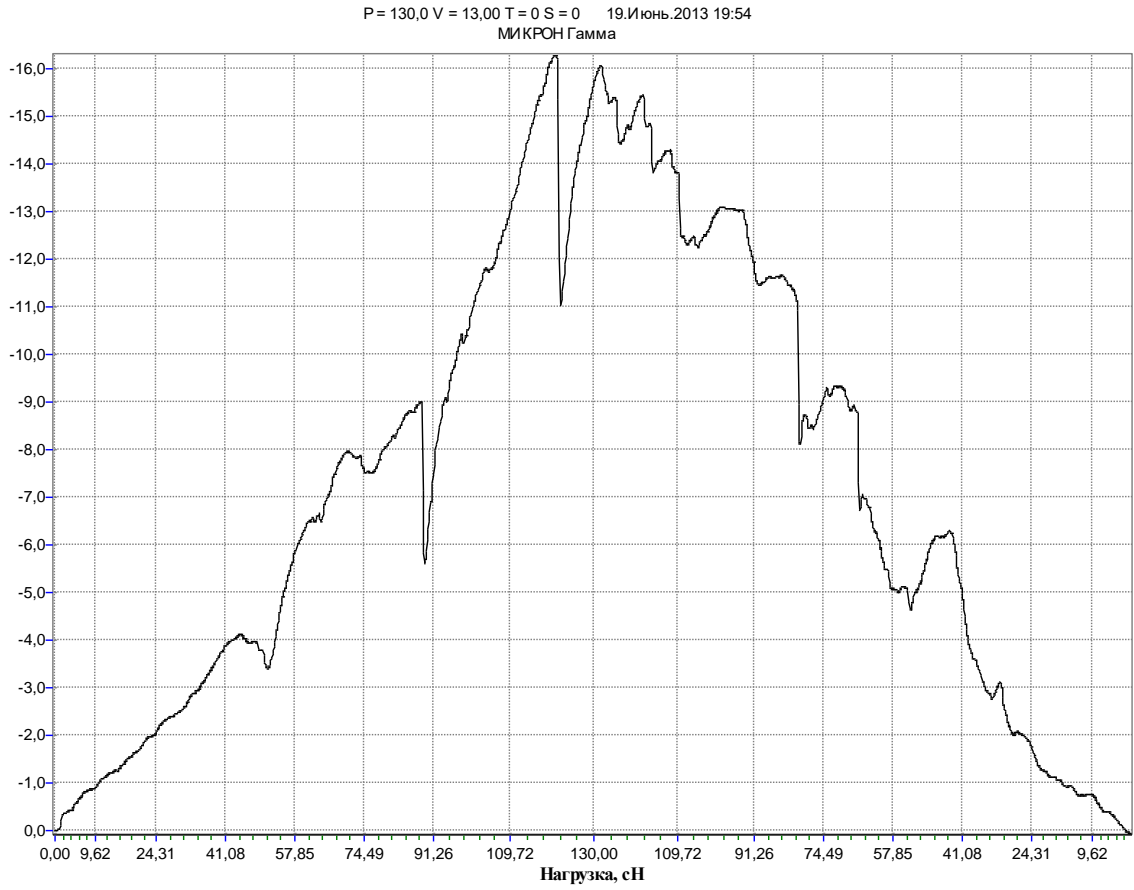


Figure 3.16 – Sample №7 (Scratch №3)

Conclusion to Part 3

1. According to the results of studies of magnetron AlN coatings on MA8 alloy substrates, it was established that sample №13 AlN has the highest adhesive strength, and №14 AlN has the lowest adhesive strength.

2. Studies of the adhesion strength of magnetron coatings n-TiC / a-C on samples of steel X12M with CrC and VC sublayers showed that sample №6 had the greatest adhesive strength and №3 had the smallest adhesion. This is also confirmed by the “ball-grinding” tests, after which the coating split off the substrate.

3. Studies of the adhesive strength of magnetron coatings of aluminum on MA8 alloy substrates showed that under these loading conditions, only plastic deformation of the coating material occurs without failure.

We experimentally show that the scratch test is a good method for quality assurance/quality control testing of the adhesion of hard coatings and is useful in the development of new coatings for process optimization.

PART 4

LABOUR PROTECTION

Introduction

To conduct the experimental investigation of this diploma work we need a scratch tester “Micron-Gamma” to test the surface layer of materials using micro-nanoindentation and sclerometry. The subject of this work is an engineer, who works with machine tool for rolling. For analyzing of the work conditions was chosen a laboratory room in one of the office buildings.

4.1 Organizing of working space:

Workplace for investigation is a small laboratory room in office that is located in the department of designing aircrafts. The room houses one machine tool and one working place.

The linear size of the room 7m×4m, height – 2.4 m, area – 23 sq. amount of space – 87.6 m³. All dimensions listed are approved by building codes Ukraine ДБН В.2.2-28-2010 “Administrative buildings”. Indoors, use mixed lighting. The walls are painted in white.

Main technical specifications:

Maximum load is.....500,

Loading resolution:

at range of 150g.....0.001;

at range of 500g.....0.01

Range of measured premises, mkm.....0.01 – 200

Indenter loading rate, gps.....0.01 – 100

Number of logged values:

in micro indention mode.....2000;

in scan mode.....unlimited

Table positioning accuracy, mkm.....10

Maximum microscope magnification.....×400

The most favorable microclimate in the workplace is the temperature no more than 24°C, relative humidity should be 40-60 % air velocity – 0.2 m/s. To maintain optimal values used microclimate heating, ventilation and air conditioning. Noise sources are machine tool for rolling, computer cooling units, laser printers, air condition. The room is a first aid kit, Carbon dioxide fire extinguisher to extinguish the fire.

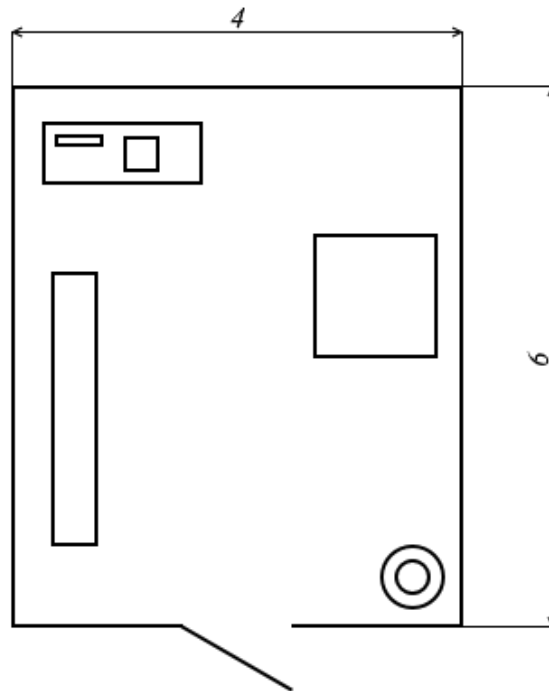


Figure 4.1 – The laboratory room

4.2 The list of harmful and hazardous factors

According to the hygienic standards ГН від 08.04.2014 №248 «Гігієнічна класифікація праці за показниками шкідливості та небезпечності факторів виробничого середовища, важкості та напруженості трудового процесу»:

- microclimate (temperature, humidity, air velocity, infrared radiation);
- barometric pressure;
- non-ionizing electromagnetic fields and radiation: electrostatic fields, permanent magnetic fields, electric and magnetic fields of industrial frequency (50 Hz), electromagnetic radiation of the radio frequency range, electromagnetic radiation of the optical range, in particular laser and ultraviolet;
- ionizing radiation;
- production noise, ultrasound, infrasound;

- vibration (local, general);
- illumination: natural (lack or insufficiency), artificial (insufficient illumination, direct and reflected dazzling glare, etc.);

- ionization of air;

2) chemical factors:

- substances of chemical origin, some substances of biological nature, which are obtained by chemical synthesis and / or for control of which are used methods of chemical analysis, aerosols of fibrogenic action (dust);

3) biological factors:

- microorganisms - producers, living cells and spores of microorganisms, contained in bacterial preparations, pathogenic microorganisms;

4) factors of the labor process:

- heaviness (severity) of labor - a characteristic of the labor process, which reflects the level of total energy consumption, the prevailing load on the support-vehicle, cardiovascular, respiratory and other systems.

4.3 To carry out methods of decreasing influence of harmful and dangerous factors

For guaranteeing of works safety in operating electro-installations the following organizational arrangements are ought to be fulfilled:

- Appointing of persons, responsible for organization and performance of works;
- Legalization of order or instructions on work performance;
- Realization of admittance on works performance;
- Supervision of works performance;
- Legalization of work finishing, interruptions in work, transposition on other work places.

4.4 Analysis of harmful and hazardous factors

The smallest illumination of working surfaces in industrial premises is regulated by DBN V.2.5-28-2006 and is mainly determined by the characteristics of visual work.

Interindustry standards. On their basis, as a rule, standards are developed for individual industries.

DBN V.2.5-28-2006 contains eight bursts of visual work, of which the first six are characterized by the size of the recognition object. The highest normalized illumination is 5000 lux (category Ia), the lowest is 30 lux (category VIIv).

There is no natural light in this laboratory room, so only artificial light is possible. In this room, LED lamps are used, providing illumination of the workplace of 400-500 lux.

In LEDs, unlike fluorescent lamps, electric current is converted directly into light, and theoretically this can be done without much energy loss. The LED does not heat well and emits a narrow spectrum, while UV and IR radiation is usually absent. The LED is mechanically strong and extremely reliable, and its service life can reach 100 thousand hours, which is almost 5-10 times longer than that of fluorescent lamps. Finally, the LED is a low voltage device, which means it is relatively safe.

An old fan is installed in this laboratory room, which does not have enough power for normal air exchange, therefore it is necessary to calculate the required fan performance and select a new one.

Sensory loading (using screen): To reduce sensory loading, the distance from the monitor to the eyes must be at least 50 centimeters. It is best if the top edge of the screen is at eye level or slightly below. Every hour you should take a short break of 5-10 minutes. To reduce the effect of screen flickering on the image, you should install LCD monitors with a refresh rate of 75 Hz. Eye exercises should be done to prevent eye fatigue.

An adjustable break should be set during the work shift to ensure optimal work for the worker. Timed breaks during a work shift should be established depending on the duration, type of work and category of employment.

4.5 Calculation of fan performance for normal ventilation

Ventilation is a controlled air exchange that removes polluted air from the room and supplies fresh air to the place. The main requirement for ventilation systems is the removal

of contaminated, humid or heated air from the room and the supply of clean air that meets sanitary and hygienic requirements to yoga.

According to the method of air movement, ventilation is natural, artificial (mechanical) and combined (natural and artificial at the same time). Depending on the purpose - for supplying or removing air, or for both at the same time - ventilation can be supply, extract or supply and exhaust. At the site of exposure, ventilation is normal and local.

Combined ventilation systems are often arranged in factories (common with local ones, etc.), and in some cases emergency ventilation, as a rule, is a projected exhaust ventilation.

Ventilation systems must be fire- and explosion-proof, simple in the device, so as not to overheat the room, not create excessive noise, be reliable in operation and economical. In addition to the passport for each ventilation unit, make an operation log.

According to the norms of ДСН 3.3.6.042-99 "Sanitary norms for microclimate of virobniks", the calculation of the required hourly performance of the fan for the laboratory room:

$$L = k \cdot V \quad (4.1)$$

where L - hourly performance of the fan, m^3/h ; k - multiplicity of air exchange (for laboratory with machine tool for rolling = 2); V - volume of the room, m^3 .

The room size is A = 6m, B = 4m, H = 3.3m.

$$V = A \cdot B \cdot H = 6 \cdot 4 \cdot 2.4 = 57.6 \, m^3 \quad (4.2)$$

Then, $L = 2 \cdot 79.2 = 115.2 \, m^3/h$ (4. 1)

So for optimal ventilation of laboratory room the performance of ventilation fan must be not less than $115 \, m^3/h$.

4.6 Fire safety

Providing of fire safety on the territory of Ukraine, regulation of relations in this sphere by state authorities, local self-government bodies and economic entities and citizens should be carried out in accordance with "Кодекс цивільного захисту", laws and other normative-legal acts.

4.6.1 Category room

The room contains non-combustible substances and materials in the cold, so meet category room for explosion and fire hazard – E.

4.6.2 The type and number of fire extinguishers

The primary means of fire extinguishing is accomplished by set of 2 Dry Chemical Powder fire extinguishers with 9 kg of agent.

4.6.3 Sensor and fire alarm system

A fire alarm system has a number of devices working together to detect and warn people through visual and audio appliances when smoke, fire, carbon monoxide or other emergencies are present. These alarms may be activated automatically from smoke detectors and heat detectors or may also be activated via manual fire alarm activation devices such as manual call points or pull stations. Alarms can be either motorized bells or wall mountable sounders or horns.

Fire safety equipment carried out in accordance with НАПБ А.01.001-2004 rules of fire safety in Ukraine. For fire alarm sensor smoke point is selected SPD-3. The sensor is designed for tracking smoke in an area 20 square meters, so with 3 sensors placed symmetrically on the ceiling.

4.6.4 Exits

In terms of evacuation figure 4.2 clearly marked evacuation routes, emergency exits, the location of fire insurance and fire alarm.

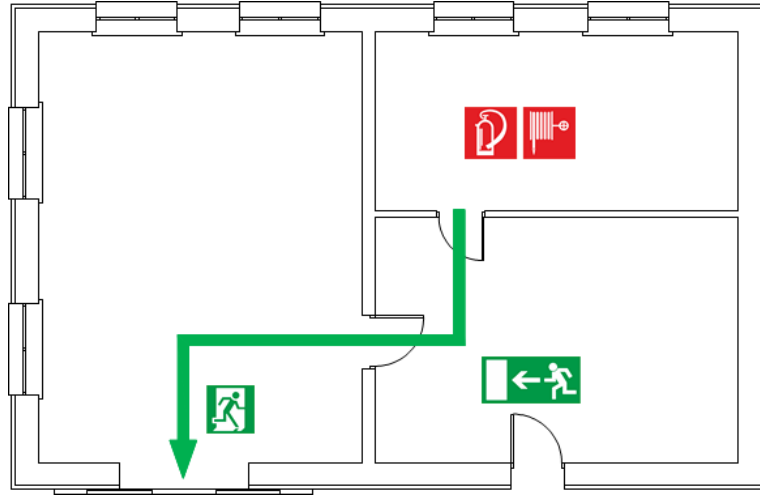


Figure 4.2 – Evacuation plan

The length of the main escape route is 30 m. For evacuation of main way to exit from your room, turn left, pass through the corridor, turn right and go through the steps to the door labeled "Exit".

Conclusion to Part 4

For normally operation of the laboratory room must be changed old ventilation fan, which can't provide enough air exchange. In the absence of a normally functioning air ventilation system in the laboratory room, the concentration of titanium nitride, titanium carbide and chemical evaporation inhaled by human, as well as many other harmful substances entering the air and adversely affecting the health of a person and significantly impairing its climate comfort, increases significantly. There are such unpleasant sensations as increased drowsiness, loss of interest in work, headache, allergic reactions. We calculate optimal performances of ventilation fan and it must be not less than 115 m³/h, so should be installed fan, which meet this parameter.

PART 5

ENVIRONMENTAL PROTECTION

Until recently, the issue of aviation's impact on the environment and human health has been marginal in the general discussions on environmental issues. But the awareness of society about the importance of environmental issues and concerns about how to address them has led governments in many countries to take appropriate policy measures to reduce the impact of aviation on nature. Recently, therefore, environmental issues in the air transport industry have attracted much more attention than it was before. There is a frank desire to preserve and enhance the level of quality achieved to date for the environment. [17]

Nowadays virtually all issues relating to global civil aviation are decided by the International Civil Aviation Organization (hereinafter referred to as ICAO). ICAO develops the basic requirements for civil aviation, including air certification requirements for environmental impact, and restricts the use of airplanes that do not meet environmental requirements. At the same time, the International Civil Aviation Organization is almost not concerned with compensating environmental damage from the impact of aircraft on the environment, placing these issues at the disposal of each individual state.

In many countries of Europe and North America there are economic mechanisms for compensating for the harmful effects of civil aviation on the environment. Unfortunately, this issue is paid little attention in Ukraine.

Almost completely there are no theoretical and methodological approaches to environmental and economic assessment of the impact of civil aviation on the environment. Further the deepening and additions to the theoretical and methodological provisions related to the creation of a mechanism for compensating environmental and economic losses from air transport processes will be required.

At the same time, according to objective estimates, in the near future, the expected increase in volumes of air transportation may amount to 30-40 % per year, and with the introduction of a new air navigation service system in Ukraine, which corresponds to the new strategy of air traffic management, the growth is expected to increase transit planes 5-

6 times! Increasing the volume of air transport in our country will usually lead to an appropriate increase in environmental impact. Thus, if even quantitative indicators of ecological and economic losses are insignificant, then their substantial growth is possible in the near future.

5.1 Evaluation of the aircraft as a source of environment pollution

Aircraft pollute the atmosphere due to the emission of harmful substances with the exhaust gases of aviation engines.

Airplanes move from one airport to another during the flight, and the atmosphere is polluted on a global scale, that is, significant pollution occurs both in airport zones and on the routes of flight. Moreover, if on the routes of flight (at an altitude of 8-12 km) the danger from this pollution is small (flights of aircraft at high altitude and at high speed cause scattering of combustion products in the upper atmosphere and in large areas, which reduces the degree of their impact on living organisms), then in the airport area, you can not count on such pollution.

Gases in the atmospheric air throw out nozzles and exhaust pipes of engines. This process is called the emission of aviation engines.

The gases generated by the operation of air transport engines account for 87 % of all emissions from civil aviation, which also include emissions from special vehicles and stationary sources.

The most unfavorable modes of operation are low speeds and "idle stroke" of the engine, when pollutants are emitted into the atmosphere in quantities that significantly exceed the discharge at loading regimes. [18]

5.2 Atmospheric emissions impact

The chemical composition of emissions due to combustion of fuels mainly depends on the type and quality of fuel, technology of production, the method of burning in the engine and the technical state of the engine of the technical condition.

The main components of the exhaust gases of modern aviation engines that pollute the atmosphere:

- SO_x sulfur oxides;
- NO_x oxides;
- carbon monoxide;
- hydrocarbons that have not been completely burned, C_xN_y (methane CH₄, acetylene C₂H₂, ethane C₂H₆, benzene C₆H₆, etc.);
- aldehydes (formaldehyde HCHO, acrolein CH₂ = CH = CHO, acetic aldehyde CH₃CHO, etc.);
- soot (fine particles of pure carbon) - stands out in the form of a loop of engine nozzles during take-off of the airplane (soot is generally released a little).

The NO_x content of the aviation engine exhaust gases depends on:

- the values of the temperature of the mixture in the combustion chamber (the higher it is, the more it forms NO_x), and it is maximum (2500...3000 K) in the takeoff mode;
- The amount of time the mixture is contained in the combustion chamber (the larger it is, the more NO_x is formed), and this occurs at low speeds of the aircraft.

That is, the maximum emission of NO_x occurs at the outburst mode of the engine and modes close to it (in case of take-off of the aircraft and when it sets the flight altitude).

Carbohydrates (SCNU) - the main component of liquid and gaseous fuels. Aviation fuels - gasoline, kerosene - vary among themselves by the content of paraffinic, petroleum and aromatic hydrocarbons, as well as sulfur compounds.

In the near-surface area during the take-off of the aircraft approximately 50% of emissions in the form of microparticles, among which - a lot of heavy metals, immediately dissipates at the airports adjacent to the territory. The other part for several hours is in the air in the form of aerosols, and then also settled on the ground.

Each engine developed (for airplanes) undergoes a series of tests (certification) before being put into serial production, including environmental safety studies, and therefore the International Civil Aviation Organization (ICAO) has developed stringent emission standards for aviation engines. [19]

Table 5.1 – Emissions from Combustion Processes

Emissions	Generation source of the product
CO ₂	Carbon dioxide is the product of complete combustion of hydrocarbon fuels like gasoline, jet fuel, and diesel. Carbon in fuel combines with oxygen in the air to produce CO ₂
H ₂ O	Water vapor is the other product of complete combustion as hydrogen in the fuel combines with oxygen in the air to produce H ₂ O
NO _x	Nitrogen oxides are produced when air passes through high temperature/high pressure combustion and nitrogen and oxygen present in the air combine to form NO _x
HC	Hydrocarbons are emitted due to incomplete fuel combustion. They are also referred to as volatile organic compounds (VOCs). Many VOCs are also hazardous air pollutants
CO	Carbon monoxide is formed due to the incomplete combustion of the carbon in the fuel
SO _x	Sulfur oxides are produced when small quantities of sulfur, present in essentially all hydrocarbon fuels, combine with oxygen from the air during combustion
Particulates	Small particles that form as a result of incomplete combustion, and are small enough to be inhaled, are referred to as particulates. Particulates can be solid or liquid
Ozone	O ₃ is not emitted directly into the air but is formed by the reaction of VOC _s and NO _x in the presence of heat and sunlight. Ozone forms readily in the atmosphere and is the primary constituent of smog.

Technological advancement has reduced aircraft fuel consumption and emissions significantly over the last 30 years and this is expected to continue in the future. The industry's historical transition from piston engines to modern high-bypass turbofans resulted in major advancements in energy efficiency and environmental performance. During this same era, the industry developed and deployed new, lightweight, high-strength

materials, automated navigational, operational, and engine control systems, and employed vast new computational capabilities to improve aerodynamic efficiency and integrate highly complex operational strategies. Changes to fleet average fuel economy progress slowly as commercial passenger service aircraft typically remain in the fleet for 35-40 years. The next figure 5.1 shows the trend and projections in aircraft fuel economy over time. Aircraft fuel efficiency has historically improved by about one percent per year. This trend is expected to continue for the foreseeable future.

As they age, existing aircraft are retired and replaced with new aircraft. New aircraft also are added to the fleet for new capacity. By 2020, 70 % of the fleet will be aircraft added since 2002, which will have advanced technology and capabilities. The figure 5.2, replicated from an International Civil Aviation Organization (ICAO) report, illustrates this transition of the international commercial aircraft fleet. Over an 18-year period, many of today's aircraft will be retired as they reach the end of their life. These aircraft will be replaced and other aircraft will be added to accommodate the growing demand for air travel. The new fleet will be much more energy efficient and have lower emissions.

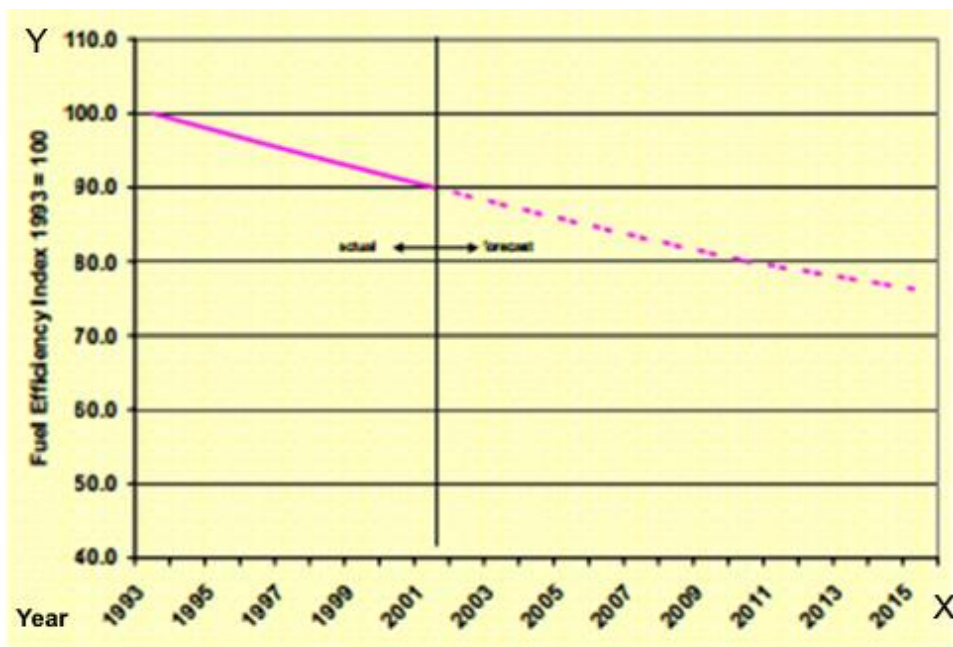


Figure 5.1 – Trend and projections in aircraft fuel economy over time

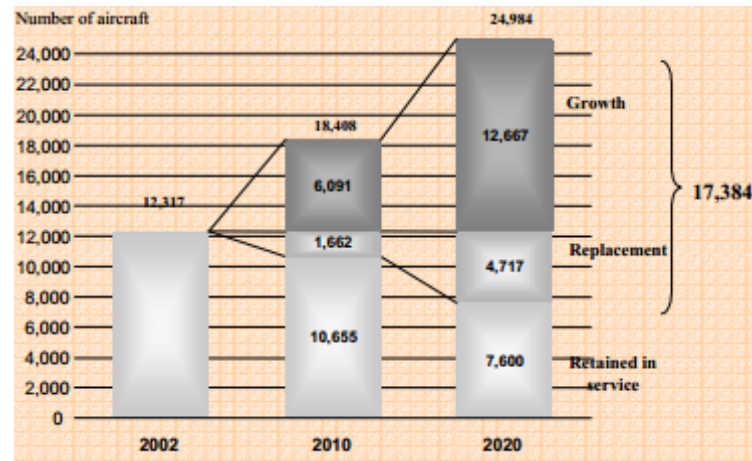


Figure 5.2 – Transition of the international commercial aircraft fleet

5.3 Recommendations to reduce environmental impact

As a result of air transport, pollution of soils, water bodies and atmosphere occurs, and the very specificity of the impact of air transport on the environment is detected in significant noise and significant emissions of various pollutants. [20]

The negative effects of various aviation sources of noise, primarily, are carried out on operators, engineers and technicians of production units. Historically, airports are located near densely populated areas of the city. Therefore, with the growth of cities and the intensification of air transport there is a serious problem of the coexistence of the city and the airport. The population of the airspace and the nearby settlements feel the noise from the flying planes. The staff of airports, air passengers and visitors are less disturbed by noise.

In addition to noise, aviation leads to electromagnetic pollution of the environment. It is caused by the radar and radio navigation equipment of the airport and aircraft. Radar equipment can create high voltage electromagnetic fields that present a real threat to people.

The effect of electromagnetic waves on living organisms is complex and insufficiently studied. When interacting with organisms, electromagnetic waves are partially reflected, but are partially absorbed and propagated in them. The degree of influence depends on the amount of energy absorbed by the tissues of the organism, the frequency of waves and the size of the biological object.

With the constant action of low-intensity electromagnetic waves, there are disorders of the nervous and cardiovascular system, endocrine organs, and others. A person feels irritation, headaches, weakening of memory, and so on. Adaptation to electromagnetic effects does not arise.

Emissions from aircraft engines and stationary sources are another aspect of the impact of air transport on the environmental situation, but aviation has a number of differences compared with other modes of transport:

- the use of gas turbine engines for the most part predetermines a different nature of the processes and the structure of emissions of exhaust gases;
- the use of kerosene as a fuel leads to a change in the components of pollutants;
- flights of aircraft at high altitude and at high speed cause scattering of combustion products in the upper atmosphere and in large areas, which reduces the degree of their impact on living organisms.

If you talk about the practice of application "Green" technologies on aviation transport Ukraine, then it should be noted that this concept of development is at an early stage. Within the framework of implementing ICAO's policy in this Direction in January 2017 by the State Aviation The Ukrainian service, together with the Ministry of Infrastructure, signed a Memorandum of Understanding with the Federal Aviation Administration (FAA) on the reduction of exposure aviation on the environment. Document provides conditions for cooperation in the field of aviation transport, in particular, research, promotion, development and use of environmentally balanced alternative types of aviation fuel.

The parties have agreed to exchange information and best practice in the following areas:

- airborne noise and their impact;
- emissions and aviation influence;
- assessment of aircraft technologies;
- environmentally and energy efficient operation of aircraft from terminal to the terminal;
- simulation and analysis of aviation;

- alternative fuels for jet fuel engines

It should be noted that in Ukraine there is none an airport that could be considered "green", and some attempts to switch to conservation natural resources and gradual transition to "Ecological" development are made at the International airport "Boryspil". So, within the framework of realization of the plan of energy independence from consumption the air company introduces innovative technologies of heating on alternative fuels. In particular, the airport was established the first in Ukraine "Economizer", which allows to receive up to 20 % heat energy from the boiler waste - smoke. However, technological solutions in other areas of reducing the negative impact on the environment remain unresolved. As for other Ukrainian airports, then there is almost no practical application of the "green" decisions in their activities, as well the ecological management system is not adequately adapted to the external and internal conditions of their functioning. The main reason such a situation is the lack of financial resources and passivity of the state to such project's direction. It should be noted that only on condition of state support, reforming the system "Environmental" taxation, the formation of "environmental" pricing policy of airlines, the availability of sources of investment "green" solutions in the aviation sector and others. possibly implemented innovative conservation projects resources and reduce the negative impact of aviation transport on the environment.

It should be added that according to the experience of the leading "green" airports in the world at the level of domestic airports for effective environmental management you need to do the following:

- 1) to form an effective system of environmental management of the airport, taking into account it external and internal operating conditions;
- 2) analyze all sources of emissions that are available at the airport and identify all possible ways reduction of greenhouse gas emissions;
- 3) to develop an effective control system and monitoring of all processes at the airport that have a negative impact on the environment and climate;
- 4) install modern energy-saving systems;
- 5) to install photovoltaic systems (autonomous solar installation with batteries);

6) to implement measures to equip production capacities with energy-saving lighting;

7) equip electric charging stations (on the territory of the airport), etc.

Conclusion to Part 5

Air transport has a great influence on the Earth's atmosphere. Aircraft gas turbine engines operate on aerosols, the chemical composition of which is somewhat different from automotive gasoline and diesel fuel of better quality with less sulfur and mechanical impurities. However, the main mass of exhaust gases is emitted by aircrafts directly in the airspace at relatively high altitudes, at high speeds and turbulent flow, and only a small proportion - in the vicinity of airports and settlements. The main components that pollute the environment are: carbon monoxide, unburnt hydrocarbons, nitrogen oxides and soot. In idle and when walking on tracks, when approaching the exhaust gases, the content of carbon monoxide and carbohydrates is significantly increased, but the amount of nitrogen oxide is reduced.

The most dangerous is the flow of these substances into the stratosphere, which may be one of the causes of the destruction of the ozone layer.

Reducing the amount of harmful emissions can be achieved by increasing engine efficiency, and hence reducing the amount of exhaust gases. The reduction of fuel consumption, and hence the emission of toxic substances, is also achieved by improving the operation of aircraft, namely: increasing the filling capacity of airplanes by useful cargo, reducing the run of airplanes on airbases under the propulsion of their own engines by towing their tractors to the runway, as well as for due to the location of airports at a considerable distance from the cities.

GENERAL CONCLUSION

1. Modern protective coatings significantly improve the performance of products, reduce their cost and provide the surface with unique properties necessary for solving a specific task. Protective coatings are used to modify the properties of the surface of the parts and improve the wear resistance, corrosion resistance, fatigue strength etc.
2. An analysis of literary sources has shown that the use of coatings in the aerospace industry is steadily increasing. So, the coatings are widely used to protect the main elements of gas turbine engines, airplane glider and helicopters, bearings, fasteners, hinged joints, and so on.
3. Properties of coatings depend on their composition and structure, the parameters of the application process, the quality of surface preparation and cleaning, as well as adhesion strength. Adhesive strength between the coating and the main material is crucial for performance and depends on many factors. Thus, the problem of assessing the adhesion strength is very relevant and represents a practical interest in controlling the quality of the coating process in the production, and in developing new coatings.
4. The paper proposes the use of a sclerometer test method to evaluate the adhesion strength of protective coatings. The method of sclerometer test is based on the continuous recording of the resistance of the displacement of the indenter over the surface with a given load law.
5. The conducted experimental studies allowed to determine the coatings with the highest adhesion strength and experimentally confirm the efficiency of the use of sclerometer test method for their evaluation.

REFERENCE

1. A.R.West, "Solid State Chemistry" John Willey & Sons, Singapore (2003)
2. B.Malliet, J.P.Celis, J.R.Roos, L.M.Stals and M.van Stappen, *Wear*, 142 (1991)
3. R.Barrell and D.S.Rickerby, *Metals and Materials* (1989)
4. S.Kadlec, J.Musil, W.D.Mfinz, G.Hakanson and J.E.Sundgren, *Surface and Coatings Technology*, 39/40 (1989)
5. K.L.Chopra, "Thin Film Phenomena", McGraw Hill, New York (1969)
6. Y.Gao, H.Niu, C.Q.Chen, *Chem. Phys. Lett.*, 367 (2003)
7. C.Weaver, *Faraday Special Disc. Chem. Soc.*, 2, 18 (1972)
8. J.Strong, *Rev. Sci. Instrum.*, 6, 97 (1935)
9. B.N.Chapman, PhD Thesis, University of London (1969)
10. J.E.E.Baglin and G.J.Clark, *Nucl. Instrum. Meth.*, B7/8, 881 (1985)
11. R.Jacobsen, *Thin Solid Films*, 34, 191 (1976)
12. A.Kikuchi, S.Baba and A.Kinbara, *J. Vat. Sci. Japan*, 26,475 (1983)
13. O.S.Heavens, *J. Phys. Radium*, 11, 355 (1950)
14. C.Weaver, *J. Vat Sci. Technol.*, 12, 18 (1975)
15. M.T.Langier, *Thin Solid Films*, 117, 243 (1984)
16. Davies.M, *Standard Handbook for Aeronautical and Astronautical Engineers* (2003)
17. І.І.Тимкович, Д.Д.Кальницька, *Захист ґрунтів та води від забруднення стоками аеропортів: Еколого – Правові вимоги* (2016)
18. Anthony C. Fischer-Cripps, *Nanoindentation* (2004)
19. О.Запорожець, *Транспортна екологія* (2017)
20. З.І.Боярська, *Екологічні аспекти безпеки цивільної авіації в Україні* (2012)